INFORMATION TO USERS

This manuscript has been reproduced from the microfilm master. UMI films the text directly from the original or copy submitted. Thus, some thesis and dissertation copies are in typewriter face, while others may be from any type of computer printer.

The quality of this reproduction is dependent upon the quality of the copy submitted. Broken or indistinct print, colored or poor quality illustrations and photographs, print bleedthrough, substandard margins, and improper alignment can adversely affect reproduction.

In the unlikely event that the author did not send UMI a complete manuscript and there are missing pages, these will be noted. Also, if unauthorized copyright material had to be removed, a note will indicate the deletion.

Oversize materials (e.g., maps, drawings, charts) are reproduced by sectioning the original, beginning at the upper left-hand corner and continuing from left to right in equal sections with small overlaps. Each original is also photographed in one exposure and is included in reduced form at the back of the book.

Photographs included in the original manuscript have been reproduced xerographically in this copy. Higher quality 6" x 9" black and white photographic prints are available for any photographs or illustrations appearing in this copy for an additional charge. Contact UMI directly to order.

UMI

A Bell & Howell Information Company
300 North Zeeb Road, Ann Arbor MI 48106-1346 USA
313/761-4700 800/521-0600

Université d'Ottawa · University of Ottawa

ACKNOWLEDGEMENTS

My sincerest thanks go out to my supervisor, Dr. Tony Durst, for his dedication and advice throughout my academic endeavor. He understood the importance of balancing school and family and I am truly grateful for his wisdom in pointing me in the right direction.

I would like to equally acknowledge the devotion of Dr. John Arnason to this project. His enthusiasm and knowledge of biology has sparked my interest of this field of study with regards to the biological applications of organic compounds.

I would also like to thank my colleagues, Terry Connolly and Yvonne Lear, for sharing with me their knowledge of organic chemistry and for encouraging me at times when I doubted my abilities.

To my parents, Fern and Sue Delorme, for only wanting me to be happy. Their unconditional love and support have been so important to me throughout my life and academic career.

To my sister and best friend, Chantal, for always knowing how to make me laugh and for her continual support.

To my brother-in-law, Sylvain, for understanding how important the bond is between sisters.

Lastly but definitely not least, to my husband Ray who has stood by me from the very beginning. He admired my work from a distance and was always ready to offer his support and encouragement. At a time when my life took a 90° turn, he was there to listen and to understand, for that I am truly grateful.

TABLE OF CONTENTS

LIST OF FIGURES

LIST OF TABLES

LIST OF ABBREVIATIONS AND SYMBOLS

ATP	adenine triphosphate
BLB	blacklight-blue
BMS	borane methyl sulfide
NBS	N-bromosuccinimide
Calc.	calculated
COL.	Coleoptera
J	coupling constant
d	days
DPM	decompositions per minute
DMSO	dimethyl sulfoxide
EI	electron impact
eq.	equivalents
Hz	Hertz
HPLC	high pressure liquid chromatography
HRMS	high resolution mass spectrum
h	hours
IR	infrared
kDa	kilodaltons
LEP.	Lepidoptera
L:D	light:dark

MS	mass spectrum
m/z	mass/charge ratio
mp	melting point
mCPBA	meta-chloroperbenzoic acid
mmol	millimoles
min	minutes
M	molar
N	normal
NMR	nuclear magnetic resonance
$M^{\cdot}$	parent molecular ion
ppb	parts per billion
ppm	parts per million
rpm	revolutions per minute
RT	room temperature
SDS-PAGE	sodium dodecyl sulfate-polyacrylamide gel electrophoresis
THF	tetrahydrofuran
TLC	thin layer chromatography
p-TSA	para-toluene sulfonic acid
UV	ultraviolet
W	watts

ABSTRACT

With the development of multidrug resistance in cancer patients undergoing chemotherapy, compounds which can enhance the intracellular accumulation and cytotoxic action of anticancer drugs are greatly needed. The present work summarizes the results of a study done by Dr Claude Bernard on the effect of the natural lignan, dillapiol, on multidrug resistance phenotypes. In a tissue culture system, dillapiol was selectively toxic to hamster drug-resistant B30 cells; this same compound was substantially less toxic to the drug-sensitive AUXB1 cell line. The so-called collateral sensitivity of drug-resistant tumor cells to an otherwise benign lignan compound makes dillapiol an ideal candidate for an adjuvant in chemotherapy. Examination of the toxicity of dillapiol revealed no negative effects with respect to weight changes or behavior of the rats, no deaths, and no abnormalities of the brain, liver, heart, kidney and lungs. Moreover, a drug-fate study using ^{14}C-radiolabeled dillapiol showed that the lignan is available to the liver, kidney and gut and is excreted almost entirely via the urine.

A novel synthesis of dillapiol which allows the incorporation of ^{14}C radioactivity in the final product is also discussed. The seven-step sequence, starting with commercially available sesamol, affords dillapiol in 21% overall yield. The difficult step is the formylation of phenol **22** with tin tetrachloride and paraformaldehyde which gives the aldehyde in 60% yield. ^{14}C-labeling of dillapiol for the drug-fate study was successfully carried out in the last step of the sequence using relatively inexpensive $^{14}CH_3I$.

The preparation of several dillapiol derivatives from either the intermediates of the dillapiol synthesis or from the modification of dillapiol itself is presented. Investigation of

the potential use of a few of these derivatives (**52-56**) as chemosensitizers revealed that alcohols **53** and **54**, as well as ester **56** display the same selective toxicity as dillapiol for drug-resistant tumor cells, the degree of activity being somewhat lower. Several of the derivatives were also shown to display significant synergistic activity towards the insecticide α-T. A relationship between polarity and α-T toxicity is established.

CHAPTER 1
INTRODUCTION

1.1 Multi-resistance to Insecticides

A major challenge of pest management is the development of multi-resistance[1]. This phenomenon occurs when a population of insects can no longer be controlled either with the usual insecticides, or with several chemically unrelated insecticides to which the insects may never have been exposed. It affects over 500 species of pest insects and mites[2], and it is estimated that 50% of all new insecticide applications for agricultural pests in the United States are made as a result of insects having become resistant to existing insecticides[3]. The origin of the problem can be traced to plant/insect co-evolution. As a means of combatting the wide spectrum of allelochemicals that are synthesized by plants, phytophagous insects have developed a number of defense mechanisms which allow them to use these plants as food resources. Some of the same mechanisms can also be used by insects to adapt to pesticides.

In contrast to the slow evolution of resistance towards natural insecticides, resistance to synthetic insecticides has developed much more rapidly perhaps because of the intense selection pressure that is created by highly toxic synthetics. According to Raffa and Priester[4], the principal mechanism involved in the multi-resistance to insecticides is the transformation of these often lipophilic compounds into more hydrophilic metabolites that can later be excreted out of the insect[5]. The principle enzymes responsible for this biotransformation are the polysubstrate monooxygenases (PSMOs), formerly called mixed function oxidases (MFOs). By converting the insecticides to

excretable metabolites, the PSMOs ensure that the levels of the insecticide within the insect are too low to have serious effects on their biological targets.

One strategy for reversing multi-resistance is to use natural or synthetic compounds which inhibit enzymes of the detoxification pathway. By reducing the activity or the level of detoxification enzymes, these inhibitors delay the rate at which insecticides are eliminated by insects and therefore increase the toxicity or lengthen the time of action of these insecticides. Compounds having this effect on insecticides are known as synergists. The most numerous and active PSMO inhibitors which are frequently used as insecticide synergists contain a methylenedioxyphenyl group as part of their chemical structure[6]. The planar methylenedioxyphenyl (MDP) group appears to bind preferentially to the heme of cytochrome P-450 in the PSMO, forming adducts that are relatively stable and not easily displaced by carbon monoxide or other lignans[7]. An important class of compounds with a high incidence of this structural feature are the lignans. Figure 1.1.

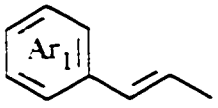

Monolignan

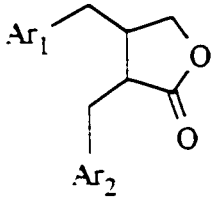

Oxodiarylbutane

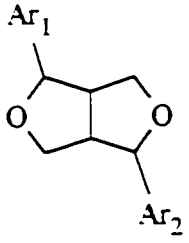

Furofuran

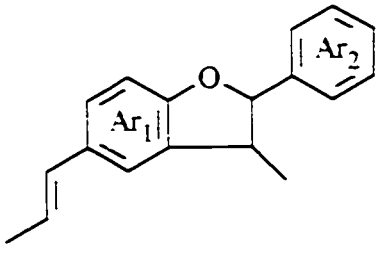

Neolignan

Figure 1.1: Classification of Lignan Structures
Reference: Ayres and Loike, 1990

Monomers of lignans (monolignans) such as apiol, dillapiol and safrol all contain an MDP structure and are potent synergists of several classes of commercial insecticides including pyrethrins, carbamates and organophosphates[8,9]. Other synergists of the lignan family include hinokinin, an oxodiarylbutane, sesamolin, a neolignan, and the furofuran (furolignan), sesamin. Table 1.1 lists some of the known synergists along with examples of insects that are affected by their activity. The structures of a number of these synergists are shown in Figure 1.2.

Table 1.1: Lignans with Synergistic Activity and the Insects which are Affected

Structural class	Insect species	Reference #
Oxodiarylbutanes		
hinokinin	three grain pests	10, 11
Furofurans		
sesamin	*Bombyx mori* (LEP.)	7
asarinin		6
savinin		6
justicidins A and B		12
Neolignans		
sesamolin	*B. mori* (LEP.)	6
Monolignans		
dillapiol	*Cylas formicarius* (COL.)	13, 14, 15, 16
myristicin	*Heliothis zea* (LEP.)	15, 17
safrol	*Heliothis zea* (LEP.)	6, 18

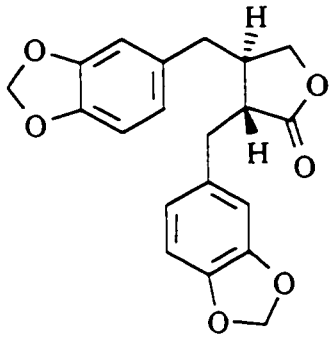

Hinokinin

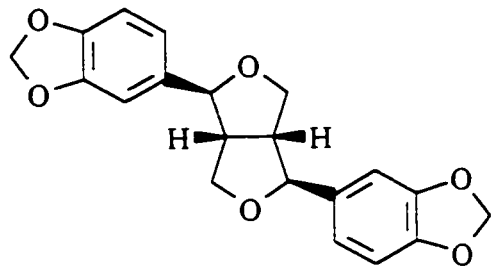

Sesamin

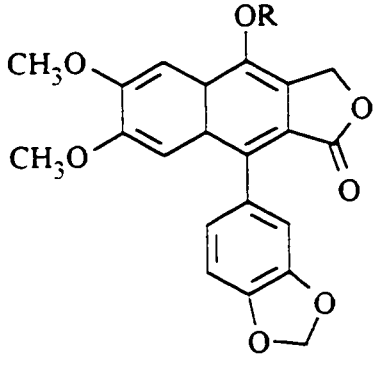

Justicidin A R = CH_3
B R = H

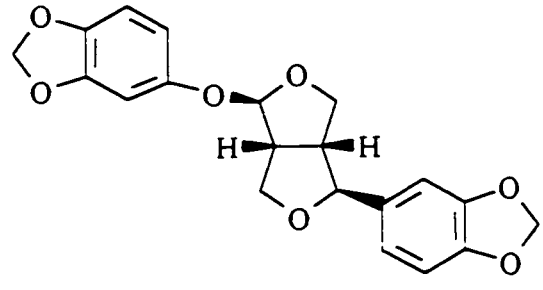

Sesamolin

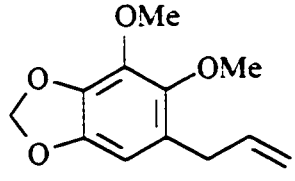

Dillapiol

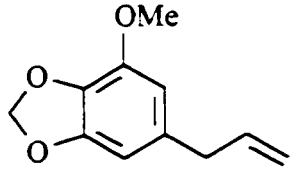

Myristicin

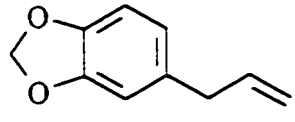

Safrol

Figure 1.2: Lignans with Synergistic Activity

Lignans are widely distributed in plants but are commonly found in the *Asteraceae* (sunflower family) and in the pepper family, *Piperaceae*, a family of vines and shrubs growing mainly in the tropics. This family of 2000 species has a long history of medicinal

and pesticidal use in Asia[19] and Africa[20] but has attracted little scientific attention in the neotropics in spite of an equally long utilization in local pharmacopoeia[21]. In addition to the lignans, several of their synthetic derivatives, for instance piperonyl butoxide, have also displayed significant synergistic activity towards several classes of insecticides.

Piperonyl butoxide, **1**, a commonly used pyrethrum synergist, is synthesized from safrol (3,4-methylenedioxyallyl benzene), a natural product. As with the lignans, this derivative inhibits the enzymes of the detoxification pathway, in particular, the PSMOs[22,23] and restores the sensitivity of insects to insecticides. This compound presently dominates the market but is under toxicological review and may be de-registered. Dillapiol, one of the main constituents (up to 35%) of Indian dill (*Anethum Sowa* Roxb.) seed oil is potentially a safe alternative to piperonyl butoxide. Another source is *Piper aduncum* L. inflorescences which yields >95% dillapiol in the steam distillate[24]. Dillapiol offers several advantages over piperonyl butoxide, the most significant being its natural origin in food plants which makes it attractive to organic growers who are in search of natural pest control agents. Moreover, the synergistic activity of dillapiol towards insecticides has been shown in many instances to surpass that of piperonyl butoxide[16,25]. This increased activity would allow lower concentrations of the active to be used thereby lowering the cost of pest management.

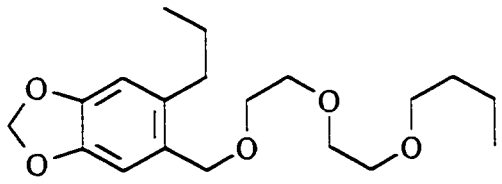

1

1.2 Multi-resistance to Drugs

The problem of multi-resistance is not restricted to insect pests. Fish, protozoa, bacterial and mammalian cancers also display the multi-resistance phenotype. However, due to the negative impact of this phenomenon in the treatment of cancer, most of the studies have been directed towards mammals[26-28]. Although chemotherapy has shown some success in the treatment of cancer often, tumors responding to a first treatment, or cells killed by a specific drug, develop a resistance to the drug being administered, even to multiple compounds that are unrelated to the selecting agent in structure, cellular target and mode of action. This resistance results in failed chemotherapy and is known as multidrug resistance.

The drugs involved in multidrug resistance include a variety of cytotoxic agents of plant origin such as vincristine, directly extracted from *Vinca major (Catharanthus major)*, etoposide (VP-16), a derivative of the lignan podophyllotoxin found in the may apple, *Podophyllum peltatum*, antibiotics of fungal origin, and a number of other molecules such as taxol which is extracted from the pacific yew tree, *Taxus brefiofolia* (Table 1.2, Figure 1.3). The mechanism of cytotoxic action of these drugs varies widely

Table 1.2: Anticancer Drugs Involved in Multidrug Resistance

Class	Anticancer drug
Antibiotics	actinomycin D
Epipodophyllotoxin	etoposide
Vinca alkaloids	vinblastine, vincristine
Antimicrotubule	colchicine, podophyllotoxin, vinblastine
Protein synthesis inhibitors	emetine, puromycin
Toxic peptides	gramicidin
Others	mitomycin C, taxol, topotecan, mithramycin

Reference: Gottesman and Pastan, 1993

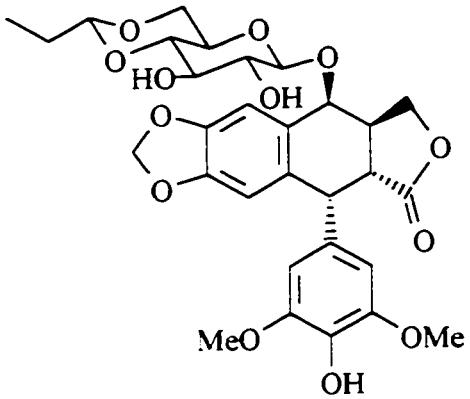

Etoposide

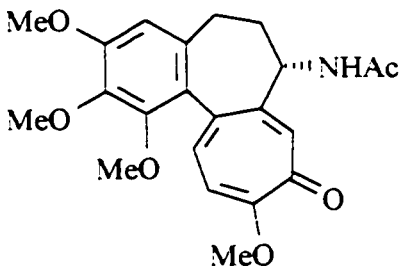

Colchicine

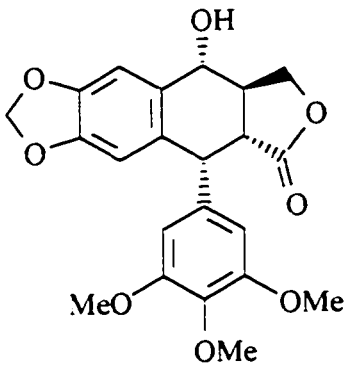

Podophyllotoxin

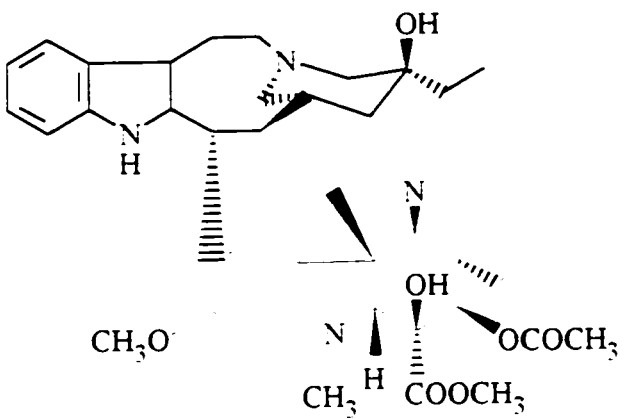

Vinblastine

Figure 1.3: Anticancer Drugs Involved in Multidrug Resistance

although at least one of the drugs, gramicidin, is thought to exert its cytotoxic action at the plasma membrane without entry into cells[26]. Despite the diversity of their modes of action, these anticancer drugs have in common their ability to be transported by a transmembrane protein termed P-glycoprotein[28]. Evidence to support a drug-binding function for P-glycoprotein was provided by a study in which a tritiated, photoactive analog of vinblastine, was found to bind to membranes prepared from Chinese hamster

lung multidrug-resistant cells[29]. SDS-PAGE fluorography revealed a prominent high molecular weight, radiolabeled doublet (150-180 kDa) in these cells which corresponded to the previously isolated P-glycoprotein[30,31]. The identification of this *Vinca* alkaloid acceptor in multidrug-resistant plasma cell membranes suggested the possibility of a direct functional role for the 150-180 kDa transmembrane protein in the development of multidrug resistance.

1.2.1 The membrane transporter, P-glycoprotein

The basis of multidrug resistance is reduced accumulation of cytotoxic drugs in cells. Pharmacological and biochemical studies have shown that drug-resistant cells can maintain a low intracellular level of drug compared to their parental sensitive cell line, and that the level of both intracellular drug and resistance are directly proportional to the extent of expression of a class of integral transport proteins called P-glycoproteins[32].

Mammalian P-glycoproteins are encoded by small gene families, with two representatives in human (MDR1 and MDR3) and three in mouse (mdr1a, mdr1b and mdr2). cDNA transfection experiments have clearly established that human MDR1[33] and mouse mdr1a and mdr1b[34] can cause multidrug resistance. Whether human MDR3 or mouse mdr2 have the same function is still a matter of debate.

Analysis of the amino acid sequences of both mouse mdr1a and human MDR1 has resulted in the following picture of P-glycoprotein[35]. The protein is about 1280 amino acids long. Its structure, shown in Figure 1.4, consists of two similar halves, each containing six alpha-helical transmembrane spanning regions (drawn as cylinders embedded in the lipid bilayer), followed by a highly conserved nucleotide binding fold. A

embedded in the lipid bilayer), followed by a highly conserved nucleotide binding fold. A poorly conserved linker region connects the two halves. The structure also includes two highly conserved ATP binding sites, one in each intracellular domain, and a site of N-linked glycosylation (chain of circles).

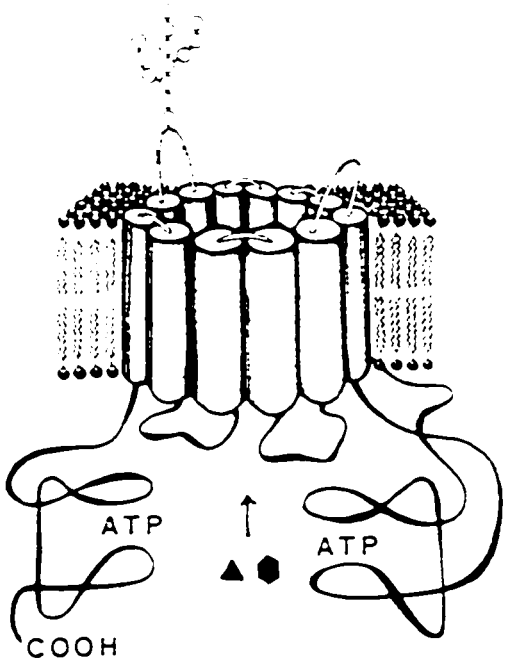

Figure 1.4: Model of P-glycoprotein
Reference: Bradley et al., 1988

The nucleotide binding folds in mammalian P-glycoproteins show significant homology to the nucleotide binding folds of a family of bacterial transport proteins, most notably to that of *E. coli* haemolysin b, a membrane protein that transports a 107 kDa haemolytic protein across the bacterial membrane. Extensive sequence homology is also

observed with many proteins in eukaryotic cells, such as the protein STE6, a transporter for the **a** peptide mating factor of yeast. Based on the similarity to many protein transporters, it is thought that P-glycoproteins confer drug resistance by actively extruding a range of different drugs (triangle and hexagon, Figure 4) from the cell through their pore using the energy derived from the hydrolysis of intracellular ATP.

Although it was originally thought that the P-glycoprotein pump was only responsible for multi-resistance in mammals, fish, protozoa and bacteria, it is now suspected that this pump also plays a role in the resistance of insects to insecticides. For instance nicotine, a major allelochemical of tobacco plants, is innocuous to the tobacco hornworm, *Manduca sexta*, which feeds on these plants, but is highly toxic to most insects and mammals. Recent studies using a mammalian P-glycoprotein antibody have shown that the tobacco hornworm possesses a P-glycoprotein-like protein in its blood-brain barrier as well as in the epithelial wall of its Malpighian tubules[36]. It is believed that the combined activity of this P-glycoprotein homolog and of detoxification enzymes accounts for the low, non toxic levels of nicotine in the sensitive sites of the tobacco hornworm. The description of a multidrug resistance-like gene in the fruit fly, *Drosophila melanogaster*[37], further suggests that a P-glycoprotein-like mechanism plays a role in insect resistance to xenobiotics.

1.2.2 Reversal of resistance

The possible involvement of a P-glycoprotein-like pump in the malaria parasite, *Plasmodium falciparum*, was indirectly suggested by the reversal of resistance to chloroquine with known inhibitors of the pump. Verapamil, a calcium channel blocker and

inhibitor of the P-glycoprotein pump in multidrug-resistant mammalian cells[38], as well as several analogs, had a remarkable capacity to reverse chloroquine resistance *in vitro*, an activity unrelated to the calcium channel[39].

Several pharmacological agents that enhance the intracellular accumulation and cytotoxic action of P-glycoprotein-transported drugs have been reported (Table 1.3, Figure 1.5). These agents are not highly cytotoxic by themselves but restore the sensitivity of multidrug-resistant cells to a drug by competing for the transport system responsible for resistance (the P-glycoprotein). For instance, verapamil, was shown to bind specifically to isolated membrane vesicles of multidrug-resistant cells and to inhibit photoaffinity labeling of P-glycoprotein by a vinblastine analog in membrane vesicles[40].

Table 1.3: Pharmacological Agents that Reverse Multidrug Resistance

Class	Agents that reverse drug resistance
Calcium channel blockers	verapamil, azidopine
Anti-arrhythmics	quinidine, amiodarone
Antihypertensives	reserpine
Antibiotics	hydrophobic cephalosporins
Antihistamines	terfenadine
Immunosuppressants	cyclosporine A
Steroid hormones	progesterone
Calmodulin antagonists	chlorpromazine
Detergents	Tween-80
Antidepressants	tioperidone

Reference: Gottesman and Pastan, 1993

Although these drugs are effective in reversing multidrug resistance, they possess major and potentially dangerous side effects such as cardiac toxicity (verapamil) or

immunosuppression (cyclosporin A) that limit their clinically achievable concentrations. Therefore, new, better, and less toxic chemosensitizers need to be developed.

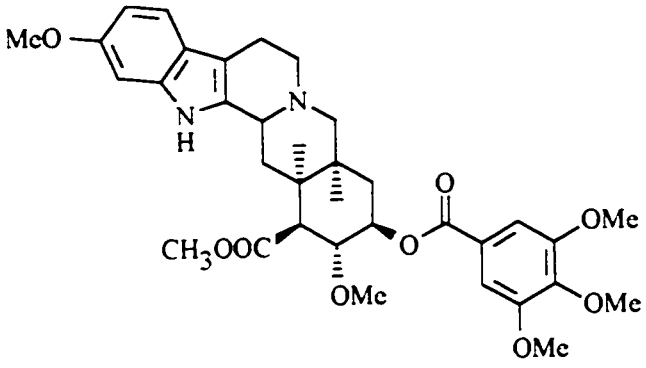

Reserpine

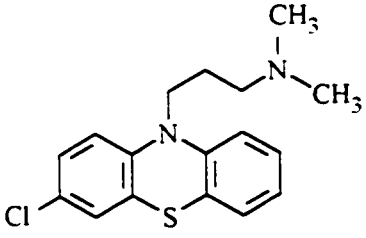

Chlorpromazine

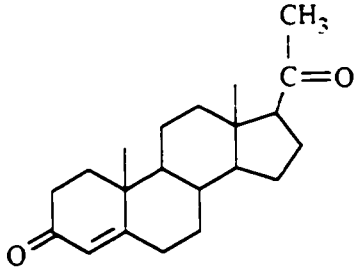

Progesterone

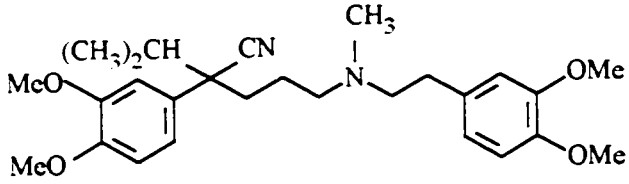

Verapamil

Figure 1.5: Modulators of Multidrug Resistance

The objective of this study is to synthesize dillapiol and a variety of derivatives and to investigate their activity as 1) chemosensitizers and 2) insecticide synergists.

1.3 Sources of Dillapiol

1.3.1 Natural sources

1.3.1.1 Dill seed oil

Previous publications on the extraction and purification of dillapiol from Indian dill seed have reported yields ranging from 27 to 35%[16,41]. Our investigation of the content of dillapiol in this plant showed that 10 g of Indian dill seed, when crushed and steam distilled, affords approximately 200 mg of an oil which, according to ^{1}H NMR, is a mixture of mainly carvone and dillapiol in a 7:1 ratio. Subsequent analysis of this mixture by GC revealed that the oil was comprised of approximately 2% dillapiol. In contrast with Indian dill, Canadian dill seed showed no trace of dillapiol.

1.3.1.2 *Piper aduncum*

Piper aduncum is a good source of dillapiol. In 1994, professor Tony Durst from the University of Ottawa collected 100g of leaves, fruit, and wood chips/sawdust from this plant in Costa Rica which was then steam distilled. Each distillate was extracted with hexane and ethyl acetate and then analyzed for dillapiol by ^{1}H NMR. Among the three parts of the plant, the seeds of the fruit were found to contain the most dillapiol (~300 mg in the hexane extract and ~30 mg in the ethyl acetate extract). This corresponds to approximately 0.3% dillapiol based on freshly picked fruit. A significantly smaller amount (~30 mg) of dillapiol was found in the hexane extract of the wood chips/sawdust and only a trace was detected in the leaves.

1.3.2 Synthetic sources

Efforts aimed at the synthesis of dillapiol have been scarce. In fact, only three have been published up to date[42-44]. This may be attributed in part to the popularity of piperonyl butoxide as a potent synergist of pyrethrins and to the availability of dillapiol from natural sources. Also, dillapiol is a rather simple looking compound and thus not a particularly worthy challenge to many synthetic chemists. The major challenge in the synthesis is to assemble efficiently the pentasubstituted benzene ring system. None of the three syntheses thus far described have met this criterion. The first synthesis of dillapiol dates as far back as 1934[42], the most recent having been published in 1980[44]. All three syntheses make use of the Dakin reaction to introduce the second hydroxyl group needed for formation of the methylenedioxy ring in dillapiol.

1.3.2.1 Baker's synthesis

The first total synthesis of dillapiol was reported by Baker and coworkers in 1934[42]. The 5-step synthesis started with now commercially available gallacetophenone **2** (25g, US $75), which was converted to the dimethyl ether **3** in 50% yield by treatment with dimethyl sulfate and potassium carbonate. The hydroxyl group at C-2 is less reactive than those at C-3 and C-4 due to hydrogen bonding. Subsequent oxidation of this dimethyl ether under Dakin conditions afforded **4** in moderate (59%) yield. The Dakin reaction involves the initial attack of a hydroperoxide anion on the carbonyl carbon. Formation of an ester intermediate by phenyl migration is then followed by hydrolysis to give the desired catechol. Treatment of **4** with allyl bromide under basic conditions afforded ether **5** which was not characterized but was subjected to Claisen rearrangement

conditions. The desired product **6** was obtained in only 27% yield. The structure of **5** was based on the knowledge that migration of an allyl group in a Claisen rearrangement yields either an ortho or para hydroxyallylbenzene[45]. Finally, treatment of **6** with diiodomethane and potassium carbonate afforded dillapiol **7** in 24% yield.

Although at first glance this synthesis seems to provide a straightforward route to dillapiol, the low overall yield of 2% greatly limits its usefulness as a large-scale source of dillapiol.

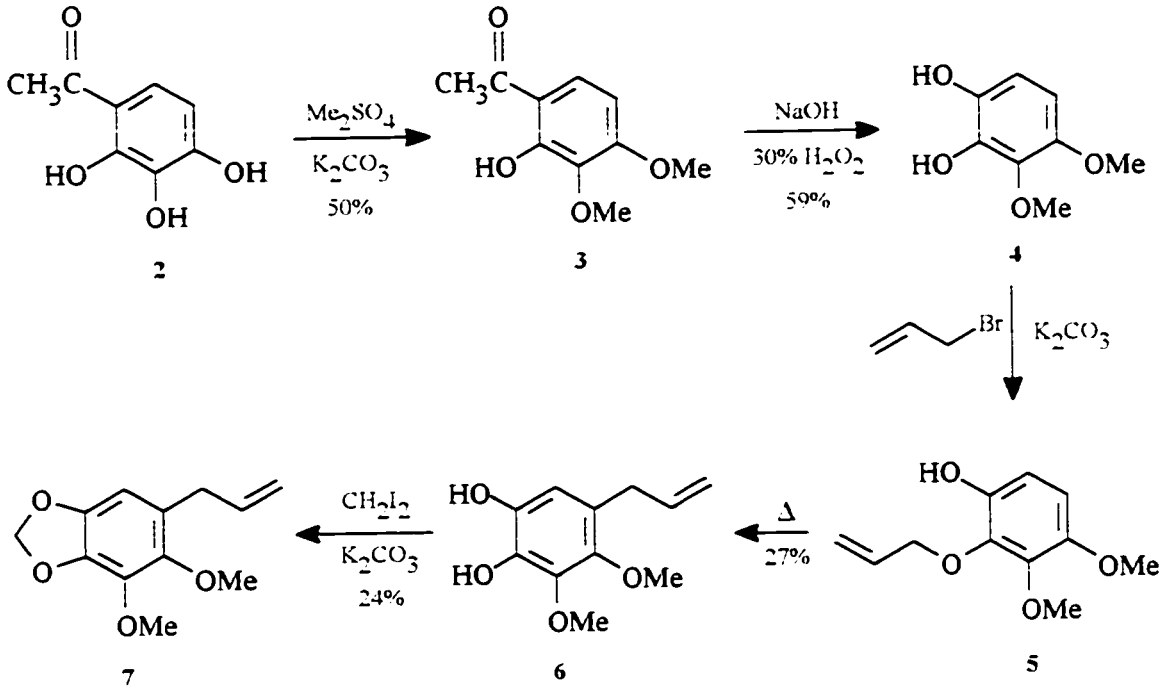

Scheme 1.1 - Baker's Synthesis of Dillapiol 7

1.3.2.2 Dallacker's synthesis

Dallacker's synthesis[43] differs from Baker's synthesis in that the starting material was a trisubstituted benzene, the fourth substituent being introduced only later in the synthesis by means of a formylation reaction. The synthesis started with inexpensive 2-hydroxy-3-methoxy-benzaldehyde (o-vanillin, current price 100g, US $50) **8** which was converted in 88% yield to the catechol **9** via a Dakin oxidation. Treatment of **9** with bromochloromethane under basic conditions afforded **10** in 56% yield. Subsequent formylation of **10** with N-methylformamide and phosphorus oxychloride gave a 1:1 mixture of **10** and 4-methoxy-2,3-methylenedioxybenzaldehyde. Separation of the two aldehydes gave the desired compound **11** in 44% yield. Oxidation of **11** under Dakin conditions gave the phenol **12** in 64% yield. Conversion of **12** to the allyl ether **13** by treatment with allyl bromide and potassium carbonate followed by an ortho Claisen rearrangement afforded **14** in 72% overall yield from **12**. The final step, a simple methylation reaction with dimethyl sulfate, proceeded quantitatively giving dillapiol **7** in 10% overall yield.

The Dallacker synthesis affords a slightly higher overall yield than the Baker route despite being two steps longer. A significant drawback of this sequence is the generation of a 1:1 mixture of compounds in the third step which requires a careful separation and ultimately lowers the overall yield of dillapiol. As in Baker's synthesis, the formation of the methylenedioxy group occurs in rather low yield. A synthesis which avoids this ring closure could significantly improve the overall yield of dillapiol.

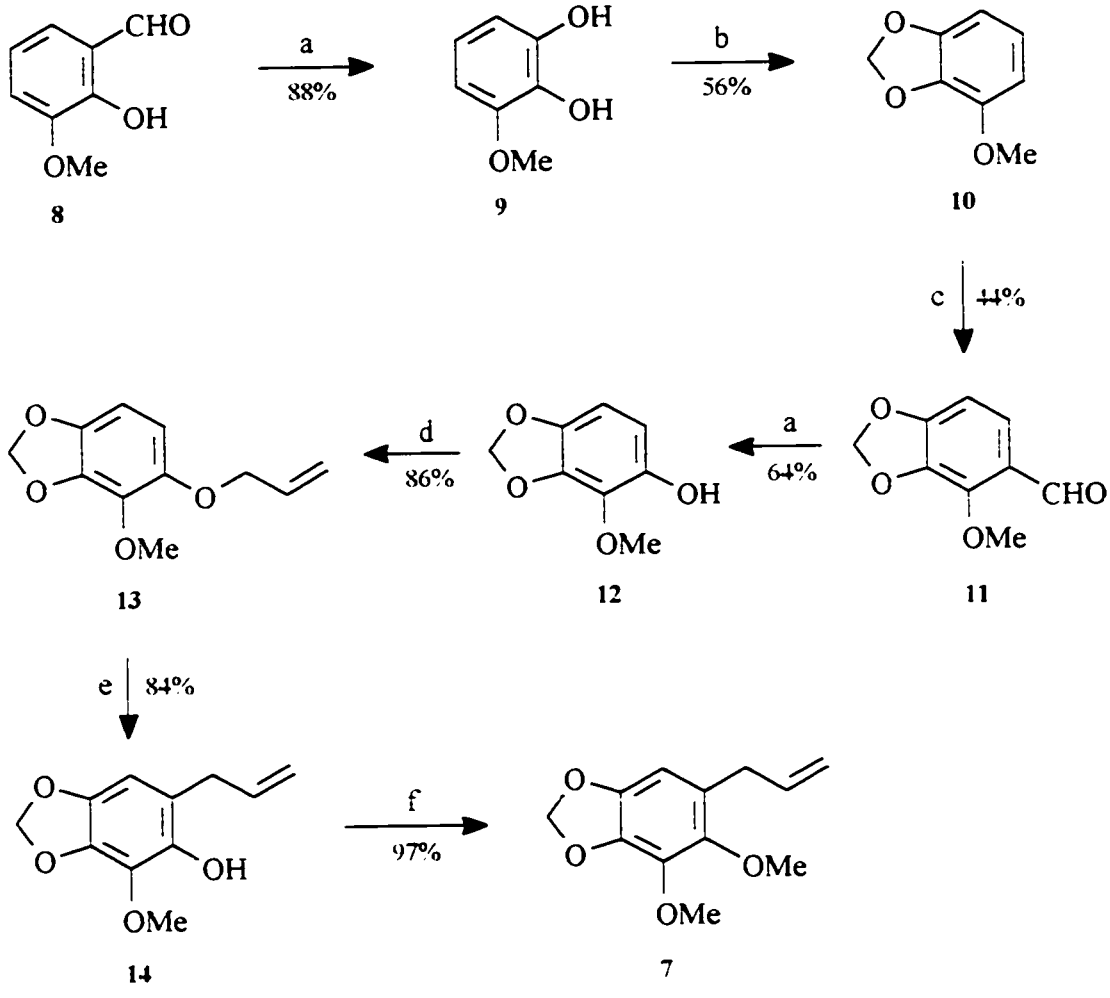

Reagents: (a) NaOH, 30% H_2O_2; (b) CH_2ClBr, Na_2CO_3; (c) $POCl_3$, $HCON(CH_3)_2$; (d) allyl bromide, K_2CO_3; (e) 190 °C; (f) Me_2SO_4, K_2CO_3

Scheme 1.2 - Dallacker's Synthesis of Dillapiol 7

1.3.2.3 Cannon's synthesis

The most recent synthesis of dillapiol was reported by Cannon,[44] who synthesized the monolignan from 1,2,3-trimethoxybenzene **15**. Treatment of **15** with acetyl chloride/$AlCl_3$ led to the introduction of the acetyl group and concomitant demethylation of the adjacent methoxy group affording **16** in 54% yield. Conversion of **16** to the allyl

ether **17** by treatment with allyl bromide and potassium carbonate, followed by a para Claisen rearrangement gave the phenolic ketone **18** in 53% overall yield from **16**. When **18** was subjected to a Dakin oxidation, a mixture of the desired dihydroxy compound **19** and unreacted starting material were obtained. Attempts to separate this mixture were unsuccessful, therefore the reaction mixture was treated directly with dibromomethane and potassium fluoride giving dillapiol **7** in 38% yield from **19** and 6% overall. This low overall yield can be attributed in part to the inefficiency of the final step, the formation of the methylenedioxy group.

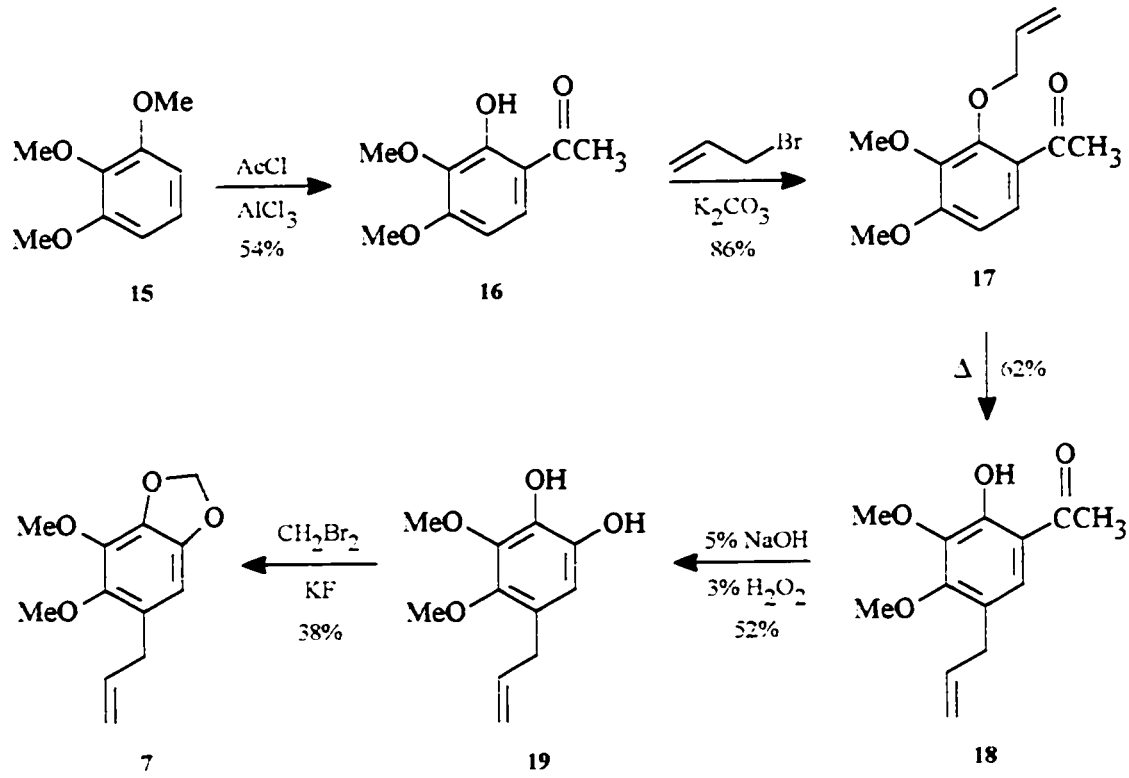

15 16 17 18 19 7

Scheme 1.3 - Cannon's Synthesis of Dillapiol 7

CHAPTER 2

A NOVEL SYNTHESIS OF DILLAPIOL AND ITS DERIVATIVES

2.1 Introduction

The potential use of dillapiol in the field of cancer chemotherapy has increased the need for a reasonably efficient synthesis which allows the incorporation of ^{14}C in its structure. By radiolabeling dillapiol, it would be possible to determine its distribution among various key organs as well as its metabolic fate in the body.

Due to the cost of ^{14}C-radiolabeled reagents and the safety problems associated with handling such compounds in typical laboratory situations, it is preferable to introduce the radioactivity in the last step of the synthesis. Although this could be accomplished via any of the before mentioned syntheses, only the Dallacker synthesis would be viable. Both Baker's and Canon's synthesis create the methylenedioxy ring in the last step of the sequence and thus would require the use of ^{14}C-radiolabeled diiodomethane or dibromomethane to introduce the radioactivity. These are not available commercially. On the other hand, dimethyl sulfate or methyl iodide represent available, relatively cheap sources of ^{14}C radioactivity. As discussed earlier, Dallacker's synthesis has the disadvantage of a low overall yield and a difficult separation and is therefore unattractive. As a result, a new synthetic pathway to dillapiol has been developed.

2.2 A Novel Synthesis of Dillapiol

It was decided to use sesamol, **20**, as the starting material for our synthesis (Scheme 2.1). The use of this compound, which is commercially available from Aldrich

(25g, US $37), has the decided advantage of avoiding the low yield associated with the formation of the methylenedioxy ring. When sesamol was treated with allyl bromide and potassium carbonate, allyl ether **21** formed in quantitative yield. The product, an orange liquid, did not require any purification and the spectroscopic data matched those described in the literature[46]. As expected, the allyl group migrated under Claisen rearrangement conditions with high regioselectivity to the less hindered ortho position to afford, in 81% yield, the o-allyl phenol **22**. Spectroscopic data were in accordance with those cited in the literature[46].

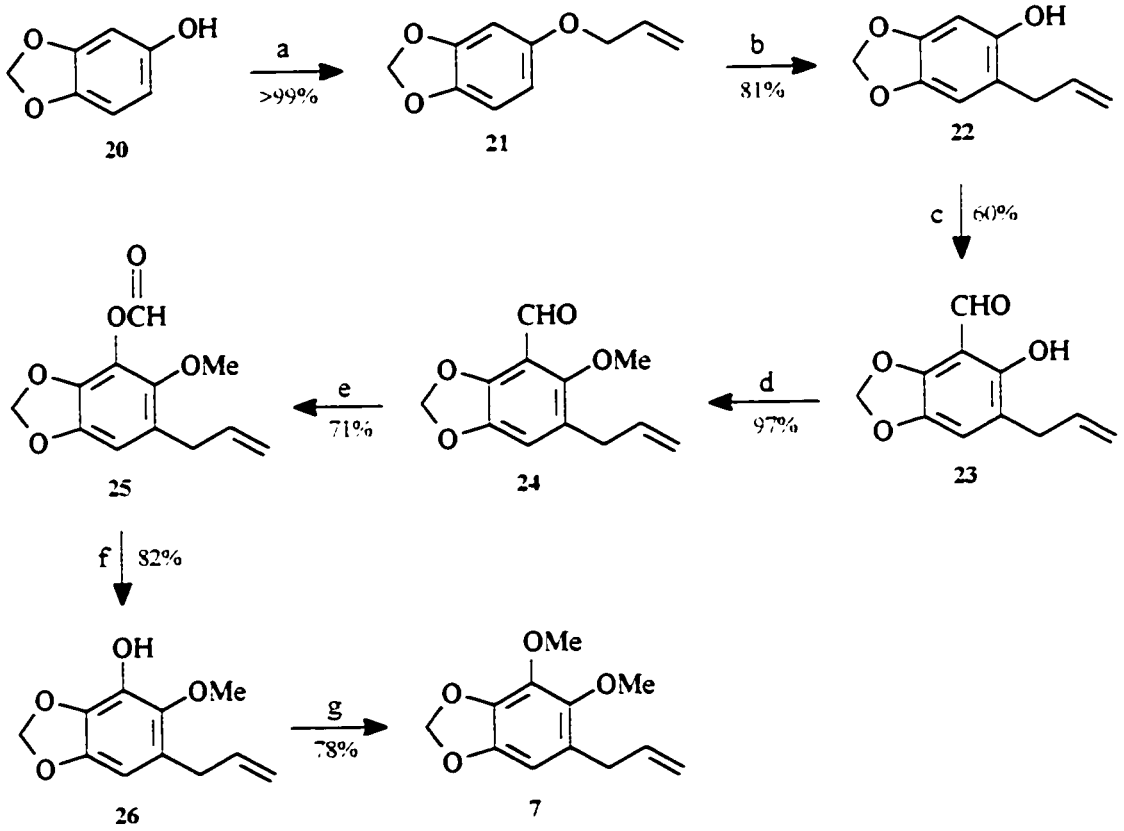

Reagents: (a) allyl bromide, K_2CO_3; (b) 190 °C; (c) $SnCl_4$, Bu_3N, paraformaldehyde; (d) MeI, K_2CO_3; (e) mCPBA; (f) 3N NaOH; (g) MeI, K_2CO_3

Scheme 2.1 - A Novel Synthesis of Dillapiol 7

Formylation of phenol **22** with tin tetrachloride, tri-n-butylamine and paraformaldehyde yielded at best 60% of **23**. Confirmation of this tranformation was obtained from both the ^{1}H and ^{13}C NMR spectra, Figures 2.1 and 2.2, respectively. The disappearance of the peak at 6.41 ppm and the appearance of a singlet at 10.65 ppm in the ^{1}H NMR spectrum confirmed that the aromatic hydrogen had been replaced by an aldehyde functionality. The aldehyde function also accounted for the signal at 191.3 ppm in the ^{13}C NMR and the 1658 cm^{-1} stretching vibration in the infrared spectrum.

The experimental procedure used for this transformation was developed by Casiraghi and coworkers to prepare salicylaldehydes[47]. It was postulated that in the first stage of the reaction, the phenol **27** reacts with tin tetrachloride to give the intermediate **28**. This intermediate is then believed to interact with paraformaldehyde giving a complex, **29**, in which the metal atom serves as a link between the two reacting species. The high selectivity that is observed for the formation of 2-hydroxybenzaldehyde rather than p-hydroxybenzaldehyde results from the orientation and close contact of the two reaction partners in this complex which enables the formaldehyde to enter easily into the ortho position. The efficient formation of this complex is the key to this reaction. Agents which could compete with paraformaldehyde for coordination with the metal atom would significantly reduce the concentration of the complex **29** and ultimately lower the yield of product.

A base, such as an amine, is needed to trap the hydrogen chloride generated in the first stage of the proposed catalytic cycle. However, as noted above, the base must have a poor affinity for coordination with the metal atom. These two requirements are met by tributylamine. The steric bulk of the base apparently renders the tributylamine-**28**

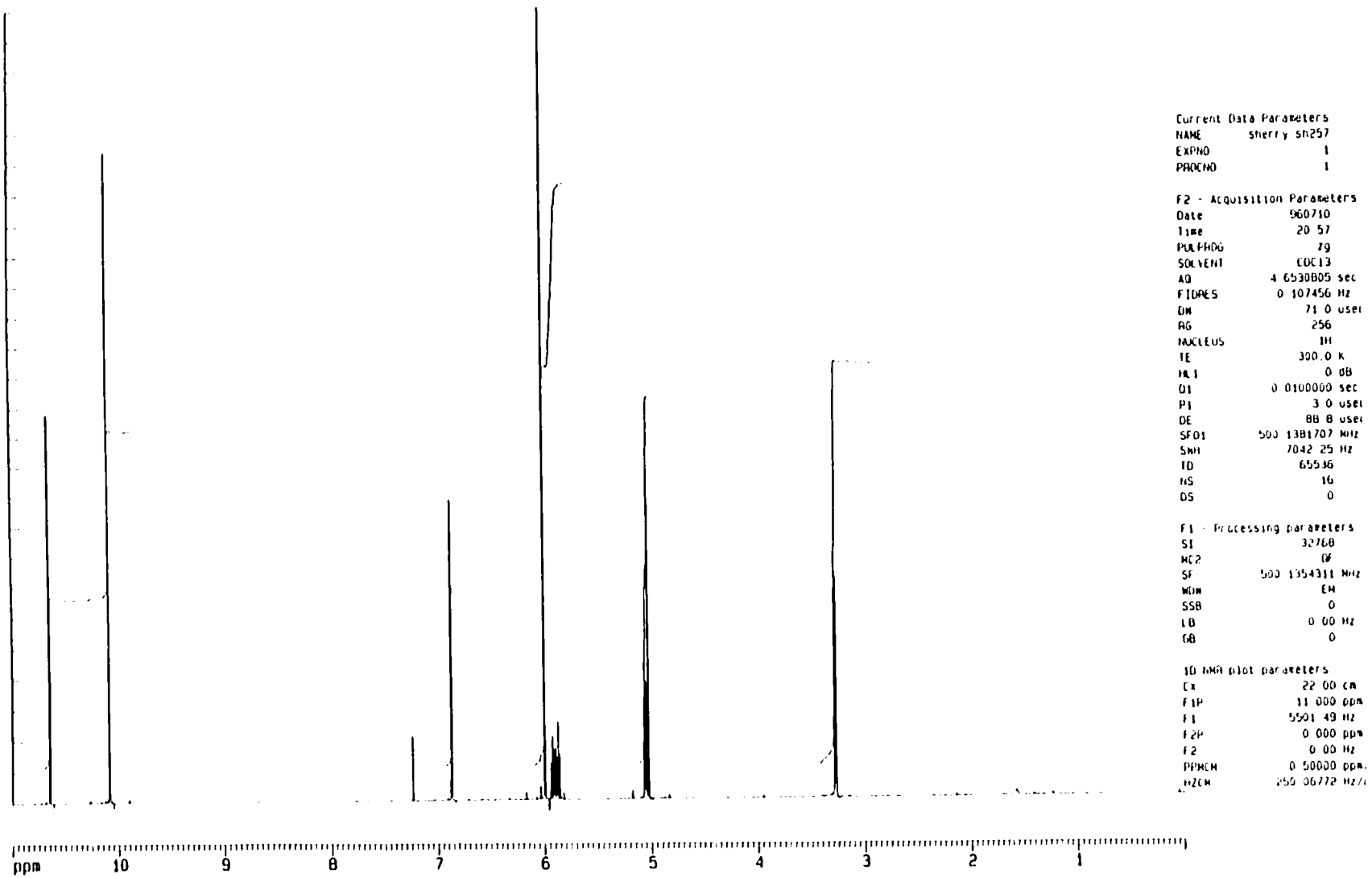

Figure 2.1 500 MHz ^{1}H-NMR Spectrum of Aldehyde **23** in $CDCl_3$

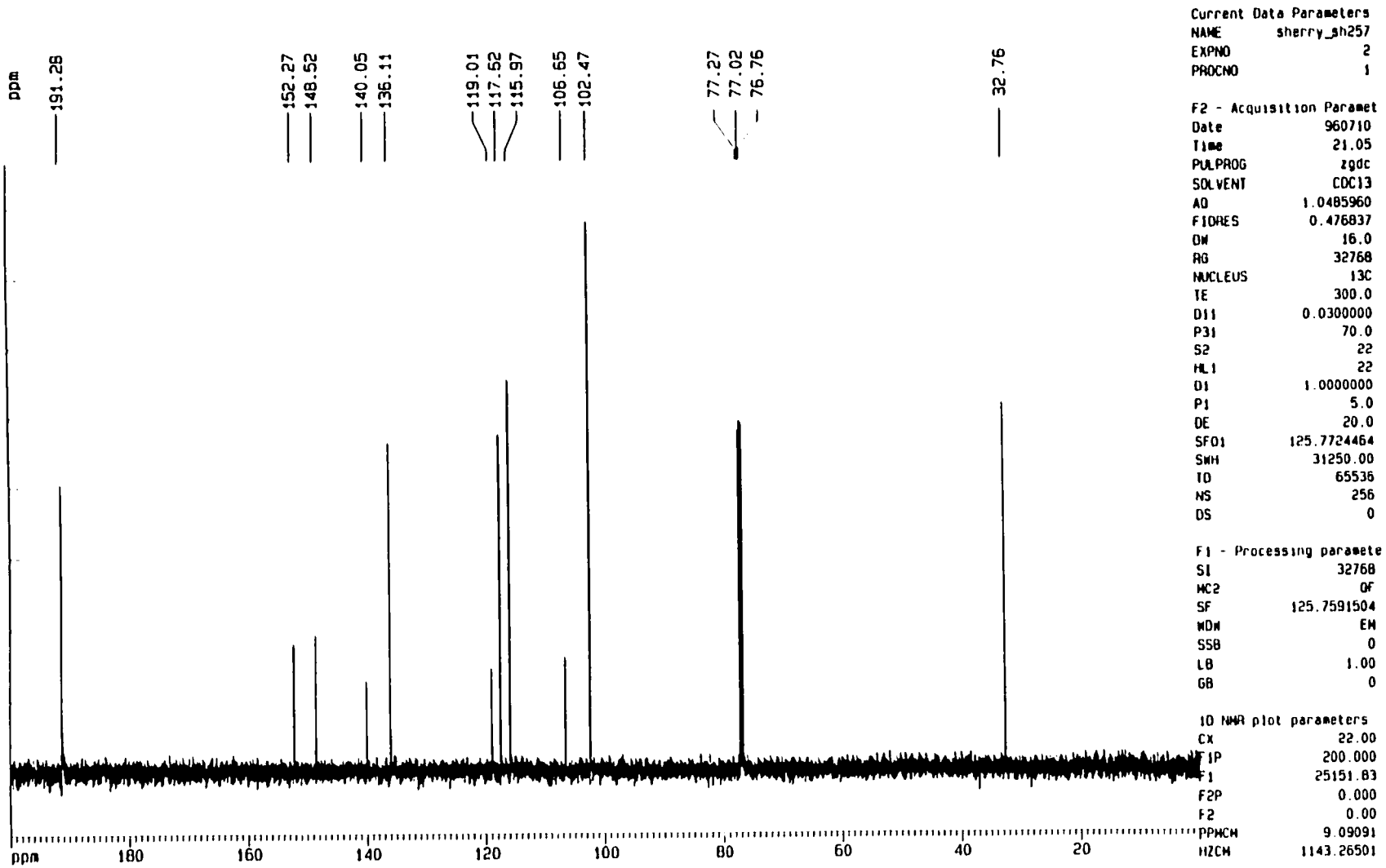

Figure 2.2 125 MHz ^{13}C-NMR Spectrum of Aldehyde **23** in $CDCl_3$

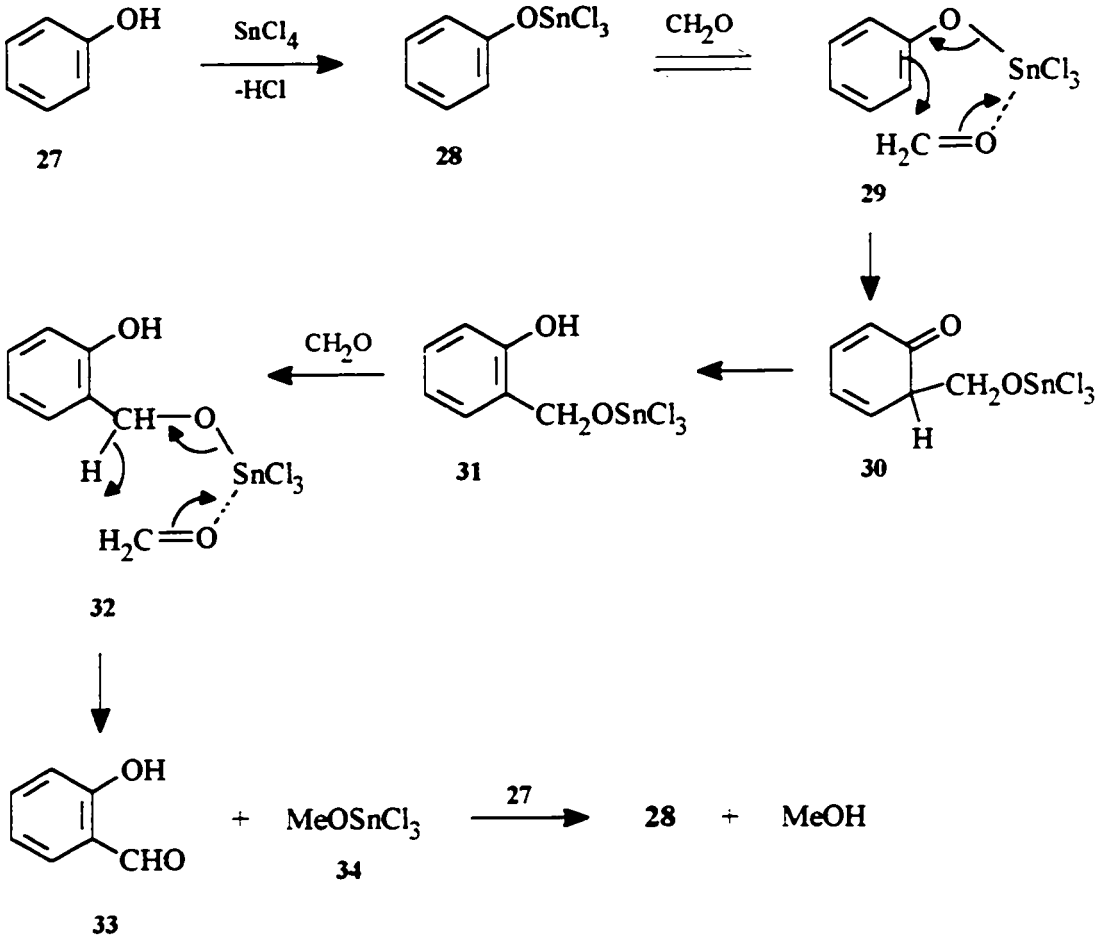

Scheme 2.2 - Mechanistic Pathway for the Tin Tetrachloride + Tertiary Amine-catalysed Condensation of Phenol with Paraformaldehyde

complex relatively unstable and therefore able to dissociate to form the transient metal phenolate-formaldehyde complex **29** via amine exchange.

The donating ability of the solvent also plays an important role in the formation of the active complex **29**. While solvents such as DMF and dimethoxyethane which can strongly solvate the phenolate metal counter-ion retard the process, those which are poor

donors such as benzene or toluene are favorable. Therefore care must be taken to choose the appropriate base and solvent.

The subsequent step is the intramolecular collapse of **29** giving the saligenol derivative **31** probably via the dienone. Reaction with a second eq. of paraformaldehyde ultimately affords the salicylaldehyde **33** following a concerted hydride transfer from the alkoxide group of the phenol to the coordinated carbonyl compound as shown in **32**. The final stage involves the alcoholysis of **34** with **27** leading to methanol with reformation of the active species **28**.

Attempts were made to increase the yield of the formylation of **22** above 60% by varying the reaction conditions. The first variation was the replacement of tributylamine with trioctylamine. It was rationalized that this somewhat bulkier base would have even less affinity than tributylamine for complexation with tin in **28**. Consequently, the formation of the active species **29** would be even more favored and a higher yield of the product would be obtained. The results, however, did not support this. In the presence of trioctylamine, the % yield dropped from 60% to 22%. Variations in the temperature and reaction time did not have any effect on the % yield.

Methylation of **23** with methyl iodide in the presence of a base proceeded at room temperature to give **24** in 97% yield as a pale yellow solid following purification by flash chromatography. Its ^{1}H NMR spectrum contains characteristic peaks at 3.77 ppm corresponding to the methoxy group and at 10.23 ppm for the aldehyde functionality. An aldehydic carbonyl signal is also present in the ^{13}C NMR spectrum at 188.1 ppm.

The following step is known as a Baeyer-Villiger oxidation. The mechanism is essentially the same as for the Dakin reaction (Scheme 2.3). It first involves the addition

of the peracid to the carbonyl carbon. The collapse of intermediate **35** subsequently leads to the formation of ester **25**. This reaction, which was carried out at 0°C, afforded the product as a colorless oil in 71% yield. Isolation of the product was complicated by the fact that it easily hydrolyzes on the column. The presence of the formyl group was identified by the appearance of a singlet at 8.26 ppm in the ^{1}H NMR spectrum and by the signal at 157.9 ppm in the ^{13}C spectrum. The carbonyl group also had a characteristic peak in the infrared spectrum at 1759 cm^{-1}.

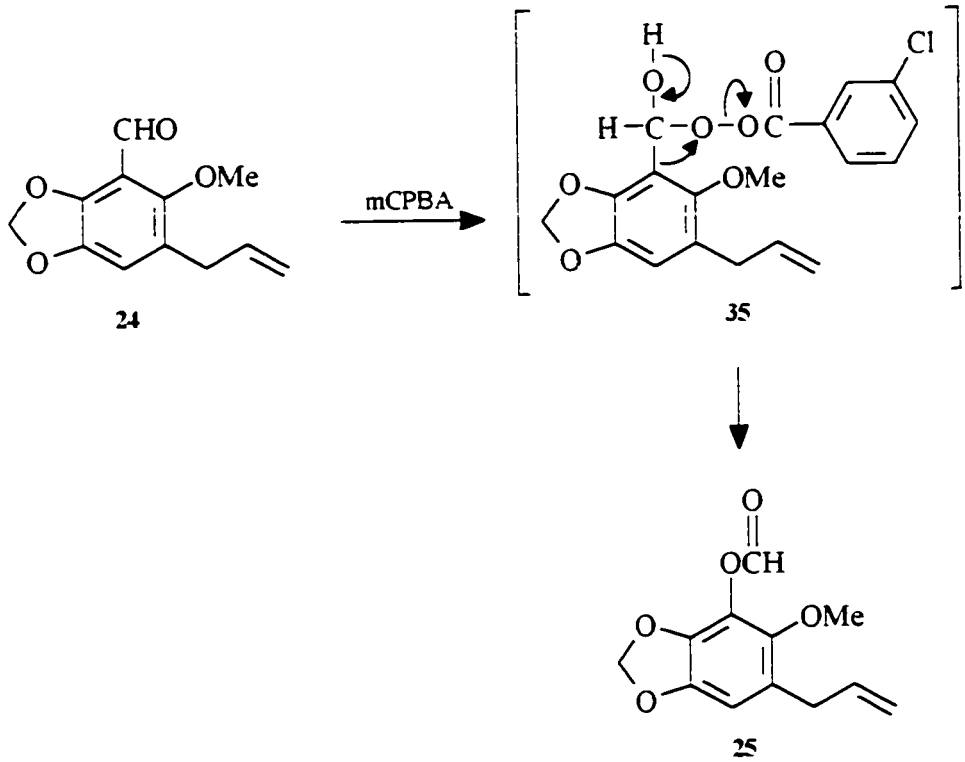

Scheme 2.3 - Mechanism of the Baeyer-Villiger Oxidation

Hydrolysis of the ester **25** was carried out with a 3N aqueous solution of sodium hydroxide for 1 h at RT, affording the phenol **26** in 82% yield. The compound was easily

identified by the singlet at 3.73 ppm due the methoxy group, the singlet at 5.50 ppm for the resonance of the phenolic hydrogen, along with the usual resonances for the allylic side chain, the aromatic hydrogen and the CH_2 group in the methylenedioxy ring (Figure 2.3). The absence of an aldehydic carbon signal in the ^{13}C spectrum confirmed the transformation (Figure 2.4).

The final transformation involved the methylation of phenol **26** with MeI and K_2CO_3 in acetone at RT to give the desired product, dillapiol. After 1 d at RT, GC analysis of the crude mixture displayed two peaks in a ratio of 2:1 corresponding to the product and starting material, respectively. The ratio increased to 10:1 after 2 d of exposure to MeI and K_2CO_3. Work-up and purification of the reaction mixture after 3 d afforded dillapiol **7** in 78% yield as a colorless oil.

The spectroscopic properties of the synthetic material are identical to those of dillapiol obtained from the natural sources. The ^1H NMR spectrum, Figure 2.5, displays two singlets at 3.74 ppm and 3.99 ppm for the two methoxy groups, a singlet at 5.86 ppm which integrates to two hydrogens for the CH_2 group in the methylenedioxy ring, a singlet at 6.33 ppm for the aromatic hydrogen and 3 additional resonances for the hydrogens in the allylic side chain. The ^{13}C spectrum of dillapiol, Figure 2.6, displays a total of twelve resonances. The benzylic carbon resonates at 33.9 ppm, the two methoxy groups, at 60.0 and 61.3 ppm, the 1° carbon in the methylenedioxy ring resonates at 101.1 ppm, and the unsubstituted aromatic carbon, at 102.8 ppm. The signals at 115.5 and 137.4 ppm are due to the doubly bonded carbons, with the terminal carbon resonating at higher field. The ^{13}C spectrum also contains 5 signals for the quaternary carbons. In order of increasing

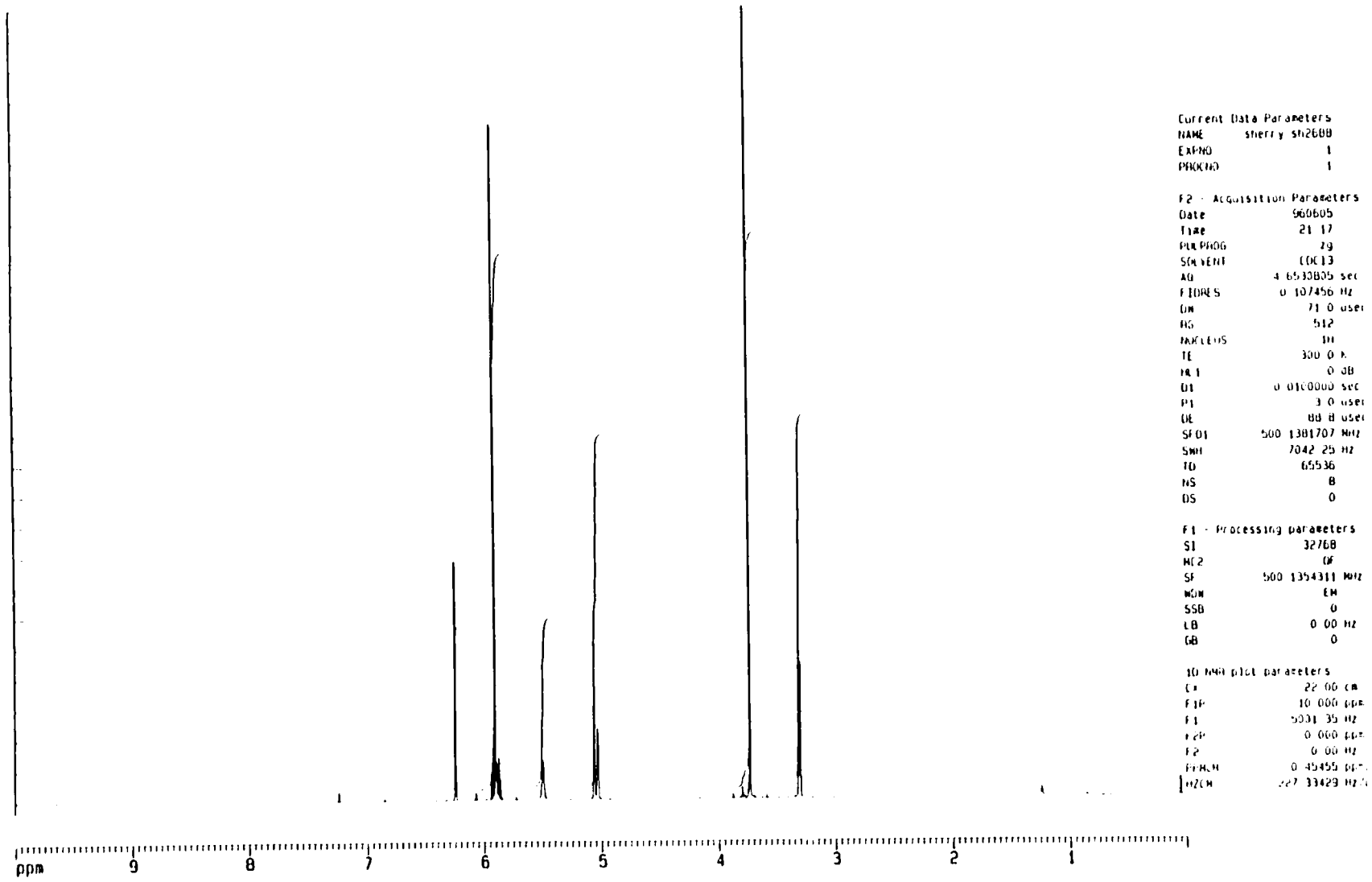

Figure 2.3 500 MHz ^{1}H-NMR Spectrum of Phenol **26** in $CDCl_3$

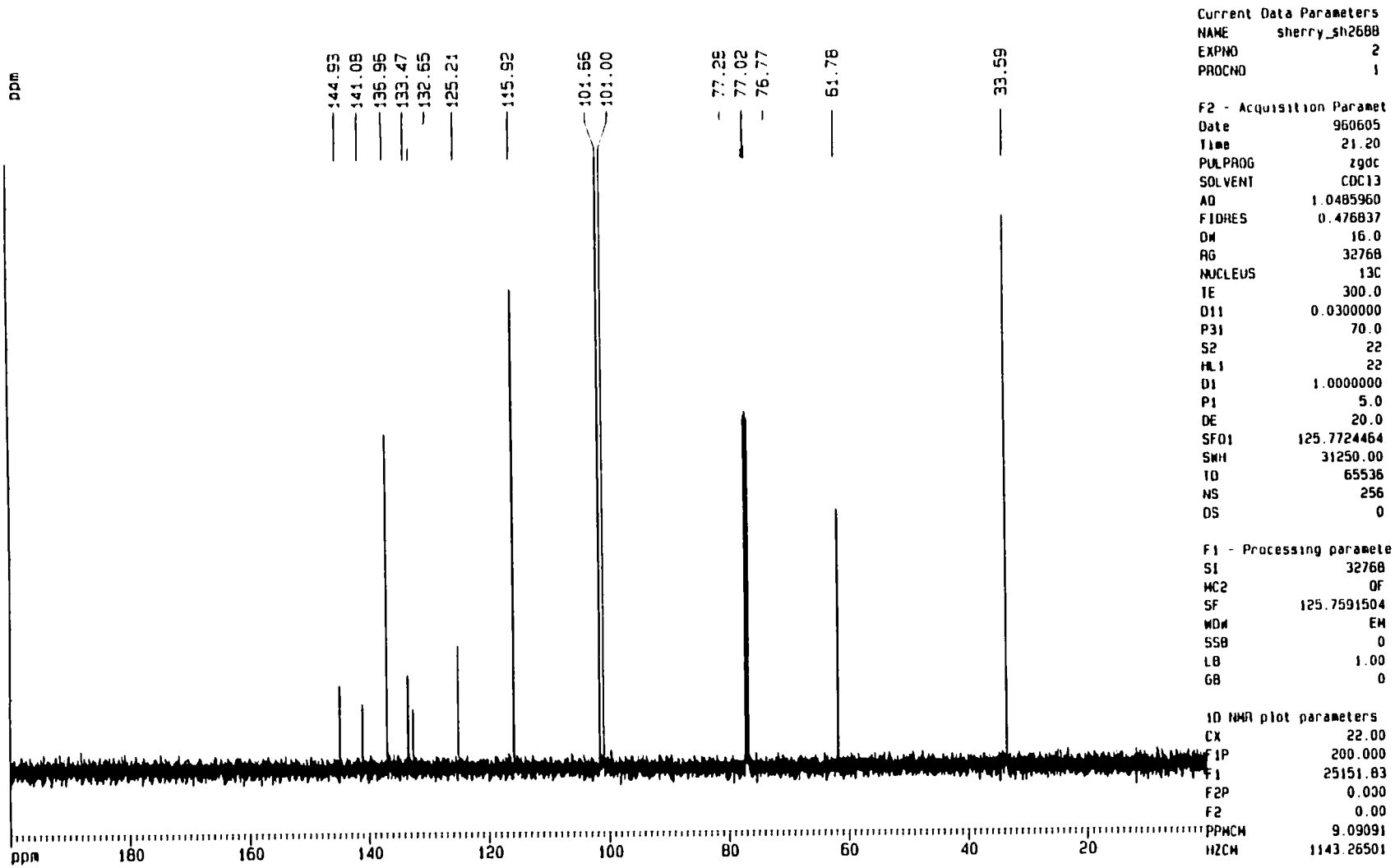

Figure 2.4 125 MHz ^{13}C-NMR Spectrum of Phenol **26** in $CDCl_3$

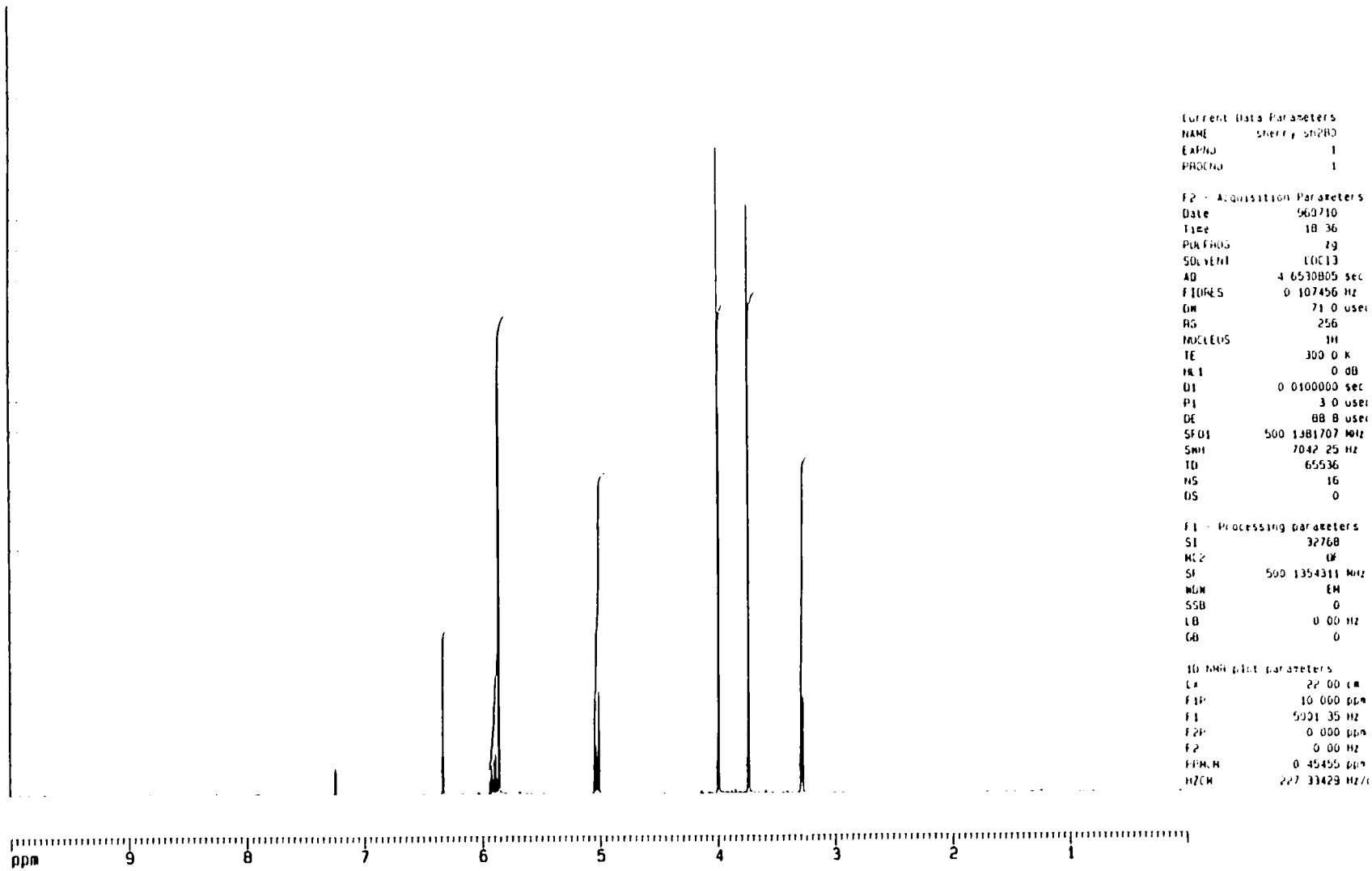

Figure 2.5 500 MHz ^{1}H-NMR Spectrum of Dillapiol 7 in $CDCl_3$

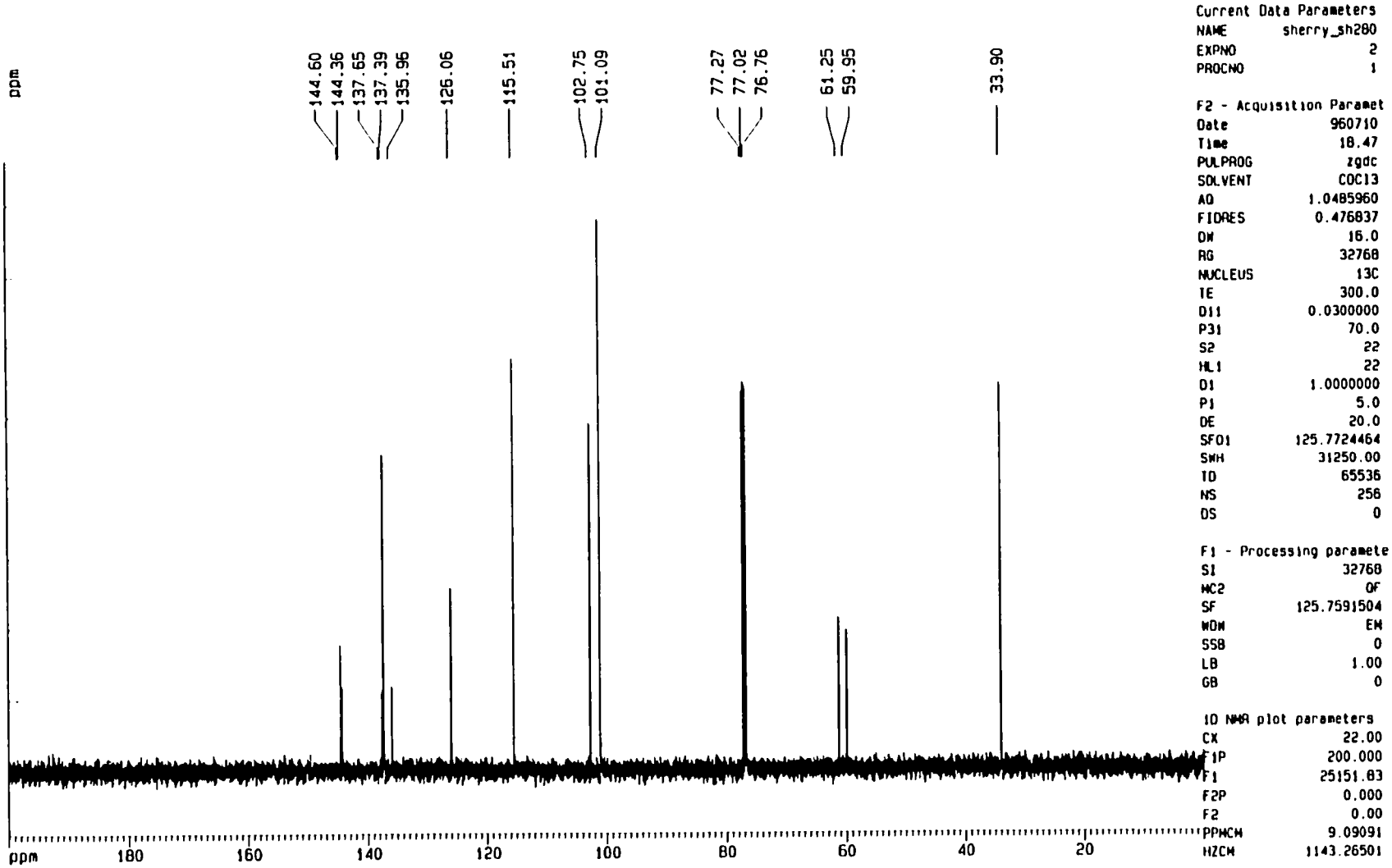

Figure 2.6 125 MHz ^{13}C-NMR Spectrum of Dillapiol 7 in $CDCl_3$

chemical shifts, the resonances can be assigned to C-1 (the carbon bearing the allylic side chain), C-4, C-3, C-5, and C-2.

This total synthesis of dillapiol offers several advantages over the previously reported syntheses, the most attractive features being its higher overall yield and the avoidance of mixtures. The present synthesis has one rather low yielding reaction, the introduction of the formyl group with tin tetrachloride and paraformaldehyde and one which is quite tricky, the Baeyer-Villiger oxidation of the benzaldehyde **24**. This reaction needs to be done carefully to avoid possible epoxidation of the allyl group. This undesired reaction was indeed observed when excess mCPBA was used or when the reaction was carried out at room temperature.

Whether this sequence would constitute a more reliable route to large amounts of dillapiol compared to the natural sources is still open to debate. Nevertheless, the new sequence was judged sufficiently reliable to allow us to prepare quantities of the various intermediates for the preparation of dillapiol analogs (See Section 2.4) and the preparation of radiolabeled dillapiol by replacing the CH_3I used in the final methylation step with commercially available $^{14}CH_3I$.

2.3 Attempted Synthesis of Dillapiol via Alternate Routes

The greatest obstacle in the synthesis of dillapiol is the incorporation of a fifth substituent between the methylenedioxy and hydroxyl groups of phenol **22**. Before attempting Casiraghi's ortho-formylation reaction, several different approaches for introducing this fifth substituent were investigated. These included the aromatic hydroxylation of **22** and its methyl ether with hydrogen peroxide-aluminum chloride, ortho

hydroxylation of **22** via the copper-catalyzed activation of molecular oxygen, ortho bromination, Friedel-Crafts acylation, and Fries and photo Fries rearrangements of the phenyl acetate derived from **22**.

2.3.1 Aromatic hydroxylations

The most direct route to dillapiol from **22** seemed to be ortho hydroxylation to give a catechol followed by dimethylation with potassium carbonate and methyl iodide. In many cases, only low yields of ortho-hydroxylated product are obtained as a result of competitive para hydroxylation. However, since the para position in **22** is blocked, it seemed reasonable to assume that a moderate yield of the 1,2-diol could be obtained.

2.3.1.1 Ortho hydroxylation with hydrogen peroxide-aluminum chloride

In 1971, Kurz and Johnson reported the synthesis of phenols from such simple aromatics as anisole, toluene and o-xylene using a hydrogen peroxide-aluminum chloride system[48]. In comparison with Vesely and Schmerling's HF-H_2O_2 system[49] and other systems[50-52] which produced rather large amounts of polyhydroxylated products, Kurz and Johnson obtained moderate yields of phenolic products with less than 3% of higher boiling phenols with their hydrogen peroxide-aluminum chloride system. They attributed this selectivity to the heterogeneity of the reaction and to the deactivation of the monophenol by coordination of the aluminum salt with oxygen. According to Kurz and Johnson, the species involved in the reaction is a hydroxyl cation which could be formed as shown below.

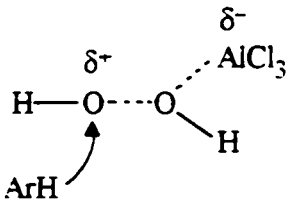

Hydrogen peroxide and aluminum chloride react to form a highly polarized peroxide-catalyst complex which subsequently undergoes nucleophilic attack by the aromatic. The formation of this type of complex seemed more reasonable than the intermediacy of the energetically, less favorable free hydroxyl cation.

When a solution of aluminum chloride and phenol **22** was treated with 30% hydrogen peroxide at 0°C, no reaction took place. A second attempt with the methyl ether of **22** also resulted in the recovery of starting material. The problem may lie in the accessibility of the ortho position. Due to the two flanking groups, the ortho position may not be exposed sufficiently to be able to attack the peroxide-catalyst complex.

2.3.1.2 Ortho hydroxylation via the copper-catalyzed activation of molecular oxygen

An ortho hydroxylation method was developed by Capdevielle and Maumy to mimic the oxidation of phenols by tyrosinases[53]. Tyrosinases are metallo-enzymes with an active site consisting of two neighboring copper atoms. These enzymes act as catalysts for the conversion of phenols into ortho quinones, via the formation of catechols, by activating molecular oxygen. Early attempts to hydroxylate phenols with oxygen and complexes of Cu^{I} or Cu^{II} [54-56] were faced with the tendancy of ortho quinones to undergo further reaction under the specified experimental conditions. The method developed by

Capdevielle and Maumy consists of the activation of molecular oxygen with cuprous salts and leads to the exclusive formation of catechols.

The oxidation of phenols is carried out in acetonitrile in the presence of a catalytic amount of cuprous chloride and consumes oxygen and elemental copper as follows:

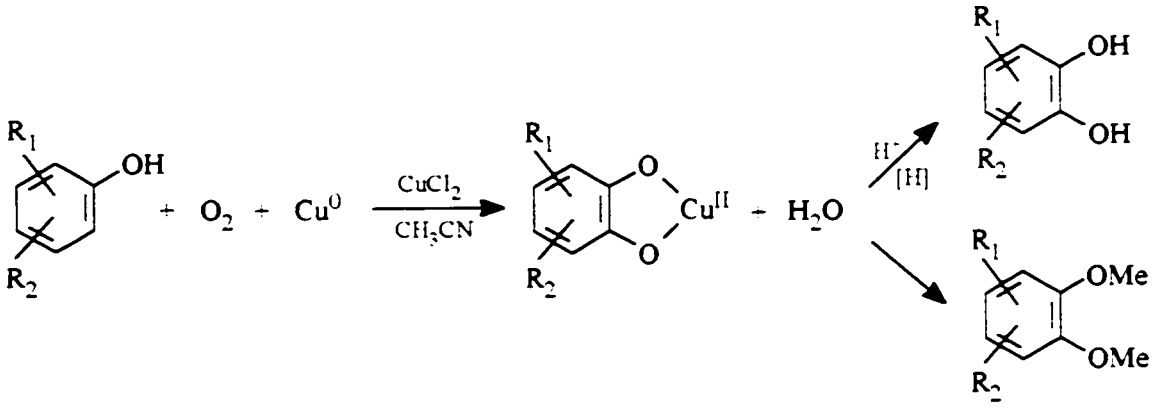

Scheme 2.4 - Ortho hydroxylation of Phenols via the Copper-catalyzed Activation of Molecular Oxygen

Phenols are converted directly to the cuprous salts of the corresponding catechols. These cuprous salts can be easily isolated and subsequently decomposed to give catechols either by acidification or by reduction. The most striking feature of this method is its total selectivity; it does not produce any ortho quinones. The selectivity is due to the stability of the copper(II) catecholates under the reaction conditions, conditions under which the free catechols would normally undergo further oxidation. In addition to forming catechols, this method also allows the conversion of phenols to 1,2-dimethoxybenzenes by treatment, *in situ*, of the copper(II) catecholates with a methylating agent. As such, this seemed an ideal sequence for converting **22** into dillapiol in a one-pot procedure.

Phenols which have been successfully oxidized by Capdevielle and Maumy vary greatly in their substituents R_1 and R_2. Yields in the order of 70 to 90% have been achieved with alkyl (R_1 and/or $R_2 = CH_3$) or alkoxy (R_1 = H, R_2 = para-OCH_3) phenols, phenol itself ($R_1 = R_2$ = H), and with phenols bearing an electron withdrawing group (R_1 = H, R_2 = para or meta-CHO, -COR, -COOR...). Attempts to hydroxylate phenol **22** were, however, unsuccessful. As with the hydrogen peroxide-aluminum chloride method of aromatic hydroxylation, the reaction returned mostly starting material but also some unidentifiable product(s).

2.3.2 Ortho bromination

As a result of the poor reactivity of phenol **22** towards direct hydroxylation, we had hoped that ortho bromination followed by copper-catalyzed displacement of bromine by hydroxide would afford the desired 1,2-diol. The first attempt at ortho bromination followed a procedure described by Weller and Stirchak in their synthesis of quassinoids[57]. This simple reaction consisted of treating a solution of the phenol, in DMF, with NBS and then stirring the reaction mixture at room temperature for an appropriate amount of time. Unfortunately, neither treatment with NBS nor a mixture of bromine and acetic acid afforded the desired ortho-brominated product. Surprisingly, only starting material was recovered.

In 1967, Pearson and coworkers described a simple and efficient process for exclusive ortho substitution[58] (Scheme 2.5). The first step involves the addition of bromine to a cold (-20°C) solution of t-butylamine. The mixture is then cooled to -70°C at which time the phenol is added. Although halogenation only takes place at a slightly

higher temperature, this temperature must be reached slowly in order to prevent the occurrence of para substitution. Low temperature also favors the precipitation of the amine hydrobromide. According to an experiment that was done in the absence of an amine, removal of the acid by precipitation is essential for the reaction to be efficient. When the acid is not quenched throughout the reaction, exclusive formation (>99%) of p-bromophenol is observed. Therefore, a strong basic aliphatic amine is required.

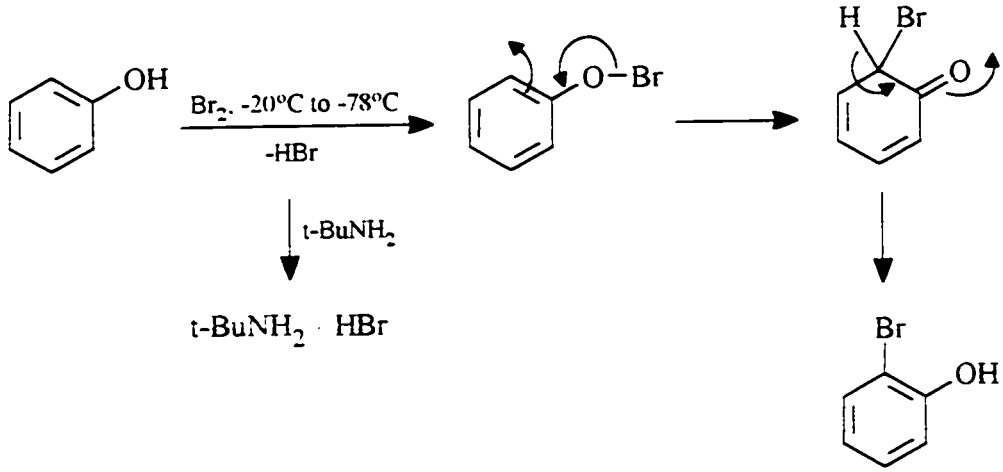

Scheme 2.5 - Possible Mechanism for Pearson's Ortho Bromination Reaction

Although the mechanism of the reaction is not known, the authors favor the phenyl hypobromite mechanism originally proposed by Dukker[59]. The mechanism first involves the formation of phenyl hypobromite through the nucleophilic attack of oxygen onto bromine. The hypobromite then undergoes rearrangement to give the 2-bromo dienone via an ortho-quinoid structure. Finally, tautomerization of the dienone leads to 2-bromophenol.

This method of preparing ortho bromophenols has been very successful for phenols containing an ortho and/or para substituent; the yields ranged from 60% in the

case of phenol itself to 92% in the case of 8-hydroxyquinoline. A surprisingly high yield (80%) of ortho bromophenol was also obtained with 2-isopropyl-5-methyl-phenol. The successful incorporation of a bromine atom between two substituents suggested that the bromination of phenol **22** may be feasible. Unfortunately, treatment of the phenol with bromine and t-butylamine did not afford the desired product. Instead, analysis of the crude mixture by ^{1}H NMR revealed a trace of starting material and one major compound. Analysis of this compound by ^{13}C NMR and EI-MS identified it as furan **36**. Evidently, bromonium ion formation and trapping of this by the phenolate is more rapid than aromatic bromination under these reaction conditions.

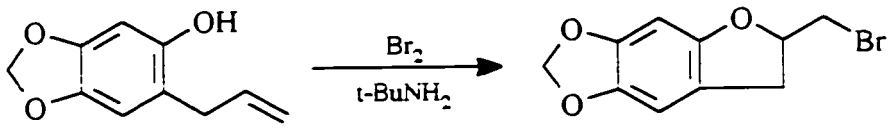

22 **36**

2.3.3 Friedel-Crafts acylation

The introduction of a hydroxyl group at position 6 could also be accomplished by treating the methyl ether of **22** with a Lewis acid and acetic anhydride, and then oxidizing the ketone under Dakin conditions. Despite numerous attempts to acylate with a variety of Lewis acids ($AlCl_3$, $BF_3{\cdot}OEt_2$, $SnCl_4$), the ketone could not be synthesized. Instead, either starting material was recovered or a mixture of compounds was generated.

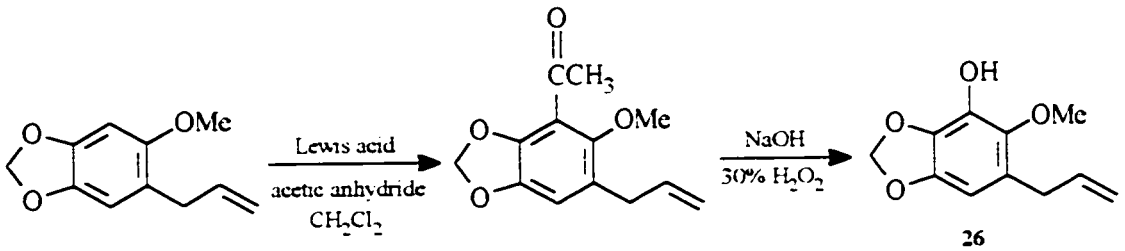

Scheme 2.6 - Alternate Synthesis of Phenol **26**

2.3.4 Fries and photo Fries rearrangements

An alternative to Friedel-Crafts acylation for introducing the acetyl group is the Fries rearrangement. It is known that when esters of phenols are heated with aluminum chloride, the acyl group migrates from the phenolic oxygen to an ortho or para position of the ring[60]. Since one of the ortho positions and the para position in **22** are blocked, acylation of **22** with acetic anhydride followed by aluminum chloride-catalyzed rearrangement should result in the formation of the desired ketone (Scheme 2.7). Acylation of **22** occurred in 86% yield but treatment of the product with $AlCl_3$ failed to give the Fries rearrangement; starting material was reisolated.

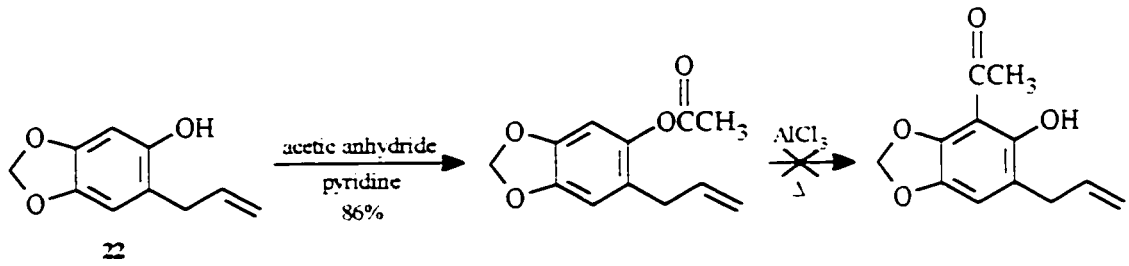

Scheme 2.7 - The Fries Rearrangement of the Acetoxy Derivative

A variation of the Fries reaction is the photo Fries rearrangement[61]. If irradiated at the proper wavelength, the phenyl acetate should rearrange to give the desired ketone. The mechanism of the light-catalyzed rearrangement, shown below for p-t-butylphenyl benzoate, first involves the dissociation of the ester molecule into a pair of radicals (II).

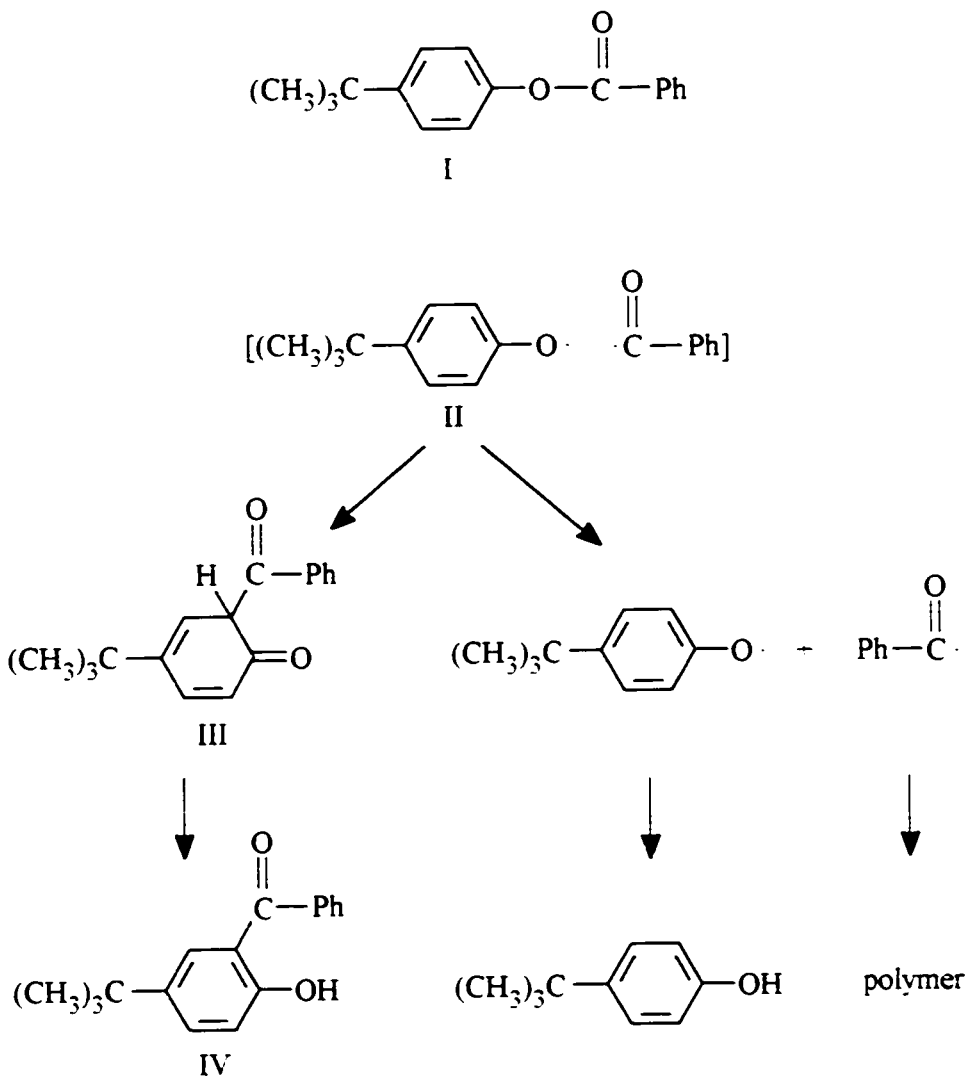

Scheme 2.8 - Mechanism of the Photo Fries Rearrangement

These two radicals are formed in a solvent cage and will tend to remain in close proximity for a sufficient amount of time to allow a large number of collisions between them. In these collisions, the two radicals can either recombine to regenerate starting material or react in such a way as the aroyl radical adds to one of the ortho positions of the phenoxy radical to afford the cyclohexadienone (III) which will eventually rearrange to the o-hydroxybenzophenone (IV). Alternatively, the two radicals may escape from the solvent cage and give separate products.

Irradiation of an ethanolic solution of the acetoxy derivative of **22** with a Hanovia medium pressure mercury lamp repeatedly afforded a complex mixture of compounds. Analysis of the crude mixture by ^{1}H NMR revealed two singlets with chemical shifts corresponding to the aromatic protons of the starting material which indicated that migration of the acetyl group to either the ortho or meta position did not occur.

2.4 Synthesis of Dillapiol Derivatives

It is known that dillapiol exhibits significant synergistic activity towards several classes of insecticides[8,9]. Presumably, this activity is due to the methylenedioxy ring which preferentially binds to the heme of the PSMOs to form adducts which are relatively stable and not easily displaced by carbon monoxide or other lignans[7]. Piperonyl butoxide, a routinely used synthetic synergist, also contains a methylenedioxy ring. However when compared, dillapiol has often been found to have a higher activity. Thus dillapiol must have a structural advantage over piperonyl butoxide. By synthesizing derivatives of dillapiol and examining their synergistic activity, it should be possible to determine the required structural elements and to possibly enhance its synergistic activity.

Examination of the behavior of various dillapiol derivatives may also be important in cancer research. Recently, dillapiol has been found to reverse multidrug resistance in tumor cells[62]. Should the analogs display similar activity, it may be possible to improve its effectiveness.

The basic concept was to prepare analogs with different substitution patterns and polarities and then examine their activity as insecticide synergists and as multidrug reversing agents. Most of the analogs described below were prepared from the intermediates found along the synthetic pathway. A small number of these, however, were obtained directly by structural modification of dillapiol itself. All of the derivatives prepared from the intermediates represent new compounds as are most of those obtained from dillapiol. In the synthesis of these compounds, relatively little attempt was made to optimize reaction yields. The major goal, as indicated above, was to prepare a small library of derivatives for evaluation of biological activity. Improvements in the yields for the preparation of particular compounds would be sought once interesting activity had been uncovered.

The first set of derivatives was obtained from phenol **22**. Reaction of this phenol with allyl bromide and K_2CO_3 afforded the allyl ether **37** as a yellow liquid in 90% yield. Spectroscopic data confirmed the presence of a second allyl group. Analysis of the ether by ^1H NMR spectrum revealed two doublet of triplets at 3.31 ppm and 4.44 ppm arising from the resonance of the allylic hydrogens in the two allyl groups. The chemical shifts of the vinylic hydrogens were, in contrast, only slightly different. The appearance of extra signals in the ^{13}C spectrum, including two vinylic methylene resonances at 117.1 ppm and 121.5 ppm, confirmed the structural modification.

As expected, exposure of **37** to a high temperature (190°C) reflux in N,N-dimethylaniline resulted in the exclusive migration of the allyl group to the open ortho position. Analysis of the crude mixture by ^{1}H NMR revealed a mixture of starting material and the desired product. Separation of the two compounds by base extraction afforded the phenol **38** in 40% yield as a yellow liquid. As expected, only one aromatic hydrogen signal, at 6.64 ppm, remained (Figure 2.7). The ^{13}C spectrum accounted for all the carbons in the molecule with 13 resonances (Figure 2.8).

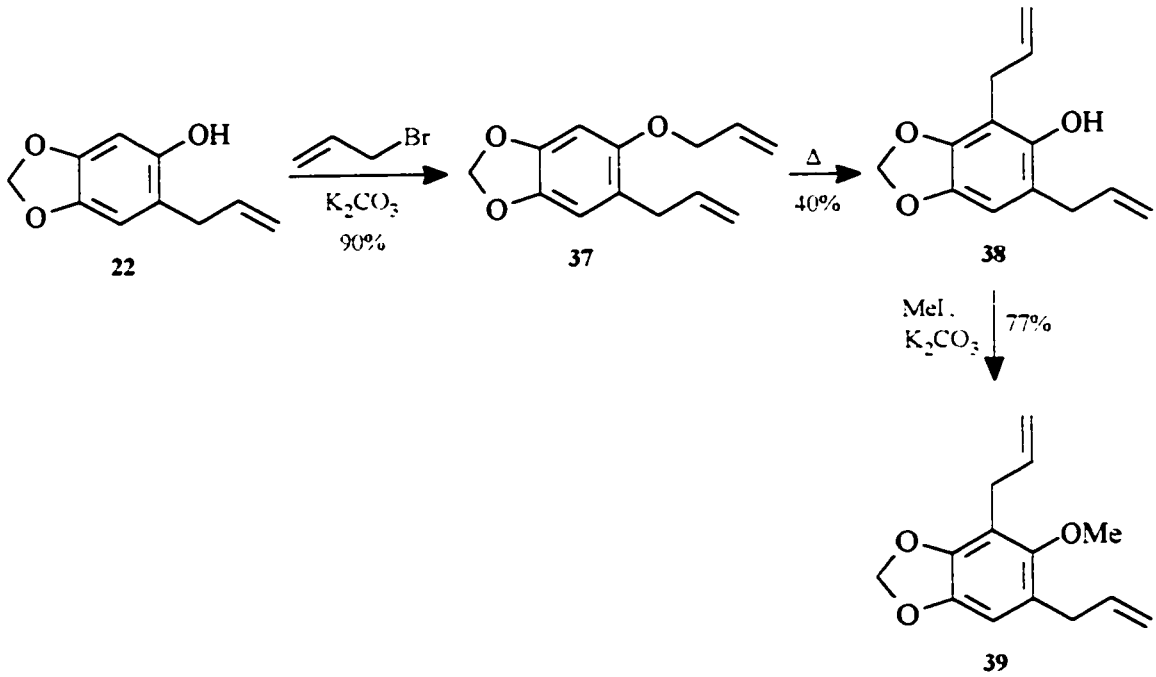

22 **37** **38** **39**

Scheme 2.4 - Synthesis of Dillapiol Derivatives **37**, **38** and **39**

Finally, methylation of phenol **38** with MeI and K_2CO_3 afforded ether **39** in 77% yield after purification of the crude mixture by flash chromatography. The ^{1}H and ^{13}C NMR spectra closely resemble those of phenol **38** but have an additional methoxy singlet at 3.66 ppm and a peak at 62.0 ppm, respectively.

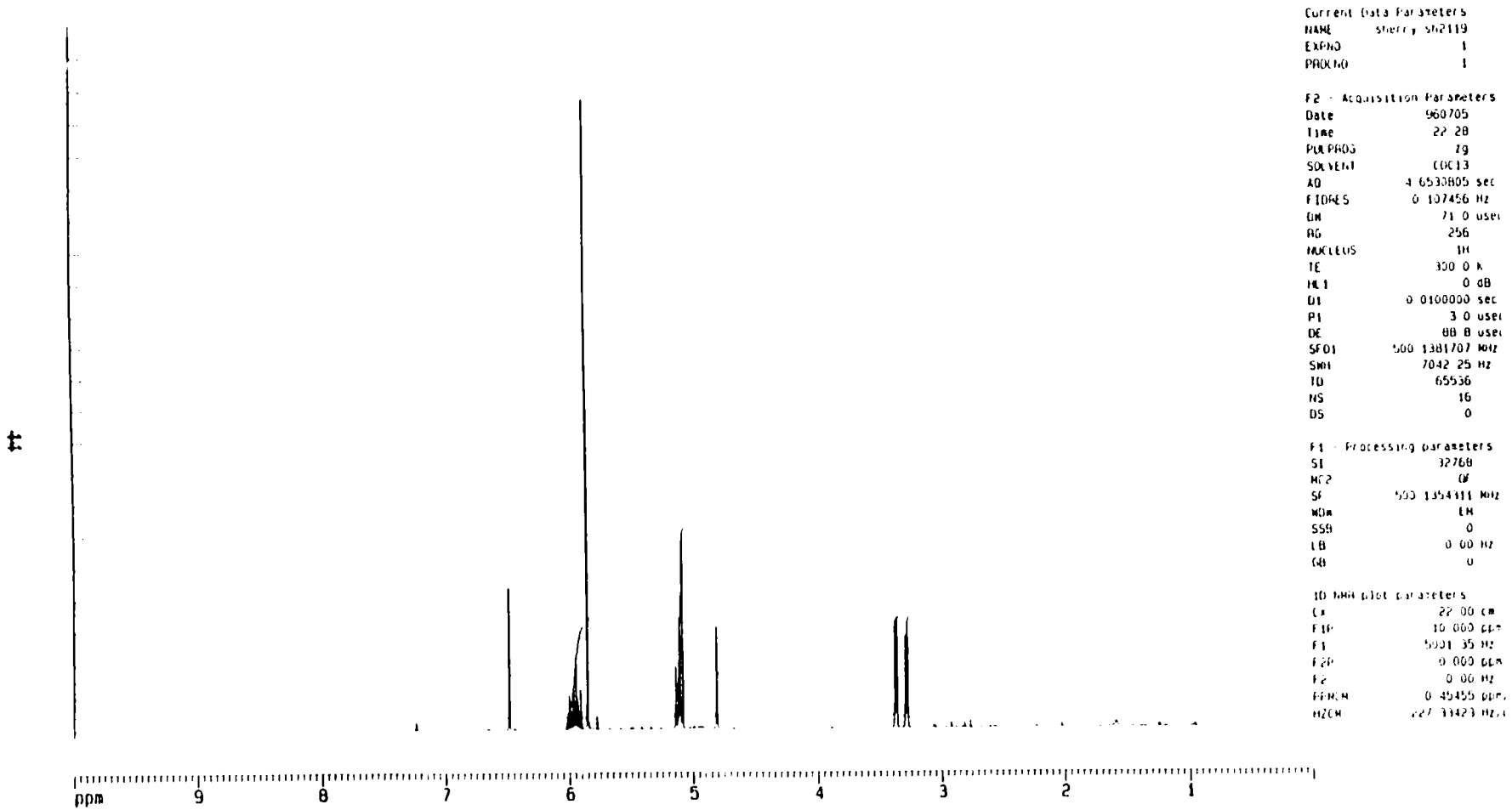

Figure 2.7 500 MHz ^{1}H-NMR Spectrum of Phenol **38** in $CDCl_3$

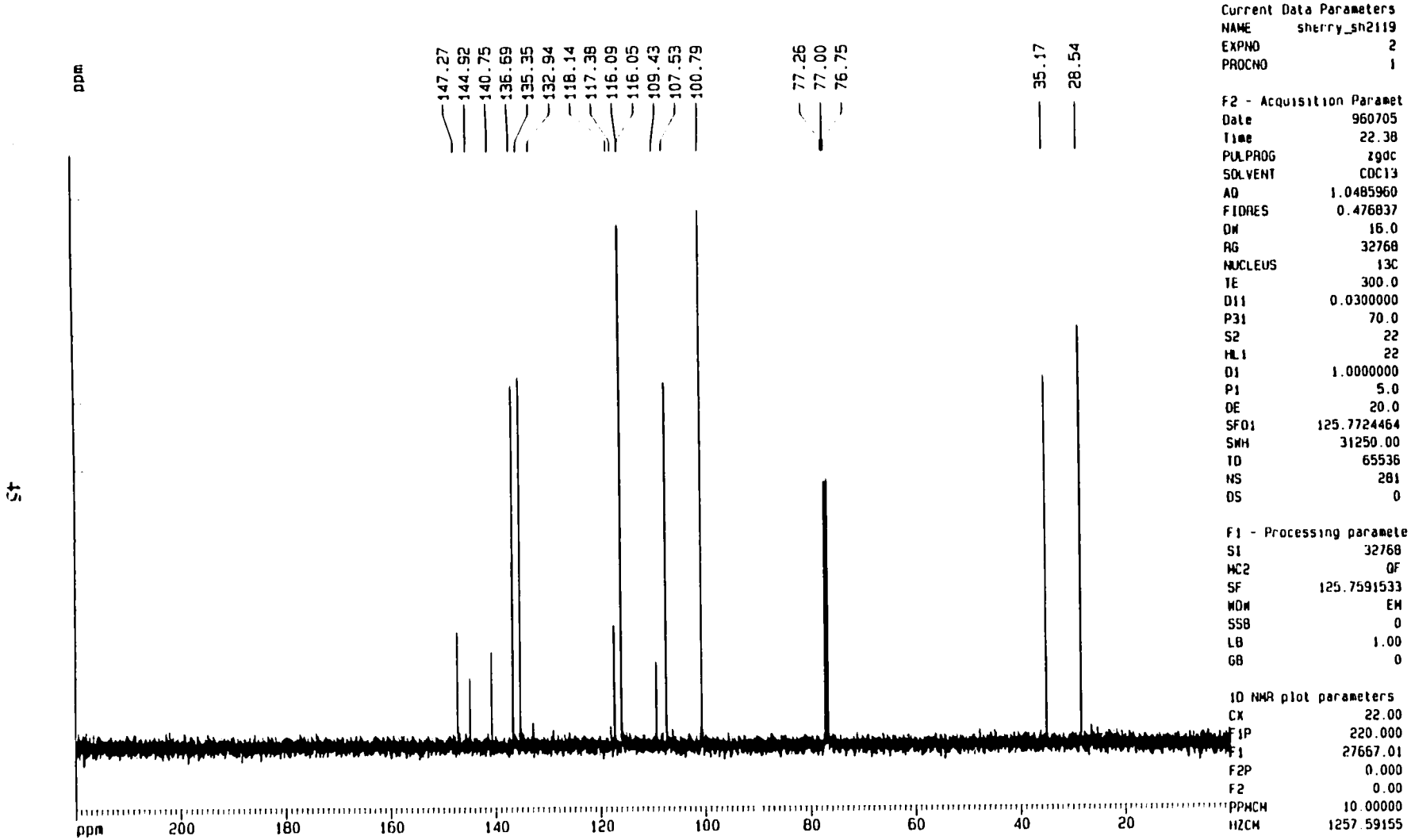

Figure 2.8 125 MHz ^{13}C-NMR Spectrum of Phenol **38** in $CDCl_3$

Phenol **22** also served as the precursor for the furan derivative **36**. Formation of this product stemmed from an attempt to introduce a bromine substituent ortho to the hydroxyl group in **22** using the procedure of Pearson and coworkers[44]. Instead, treatment of the phenol with a cooled toluene solution of bromine and t-butylamine resulted in ring closure and the addition of a bromine atom to the terminal carbon of the double bond to give **36** in 95% yield as a yellow oil. Analysis of bromide **36** by ^{1}H NMR revealed four doublet of doublets at 3.00 ppm, 3.27 ppm, 3.47 ppm and 3.56 ppm corresponding to the two methylene groups adjacent to the chiral center (Figure 2.9). The set at lower field can be attributed to the hydrogens adjacent to the bromine atom. The 10 resonances in the ^{13}C spectrum (Figure 2.10) and the appearance of an M+2 peak at 258 in the EI-MS confirmed the structural assignment.

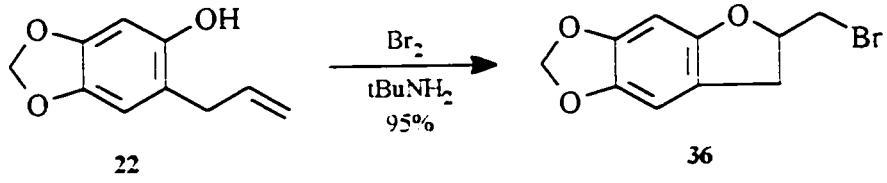

22 **36**

Scheme 2.5 - Synthesis of Dillapiol Derivative **36**

The intermediate **23** in our dillapiol synthesis was converted to three new derivatives. The first reaction consisted of reducing the aldehyde to a primary alcohol. The bright yellow color of the aldehyde disappeared seconds after it had been treated with $NaBH_4$ in ethanol. After 40 min at RT, analysis of the colorless solution revealed almost pure diol, **40**. Purification of the diol by flash chromatography afforded 83% of a white crystalline solid with ^{1}H signals at 4.81 ppm, and two singlets at 2.55 ppm and 6.85 ppm

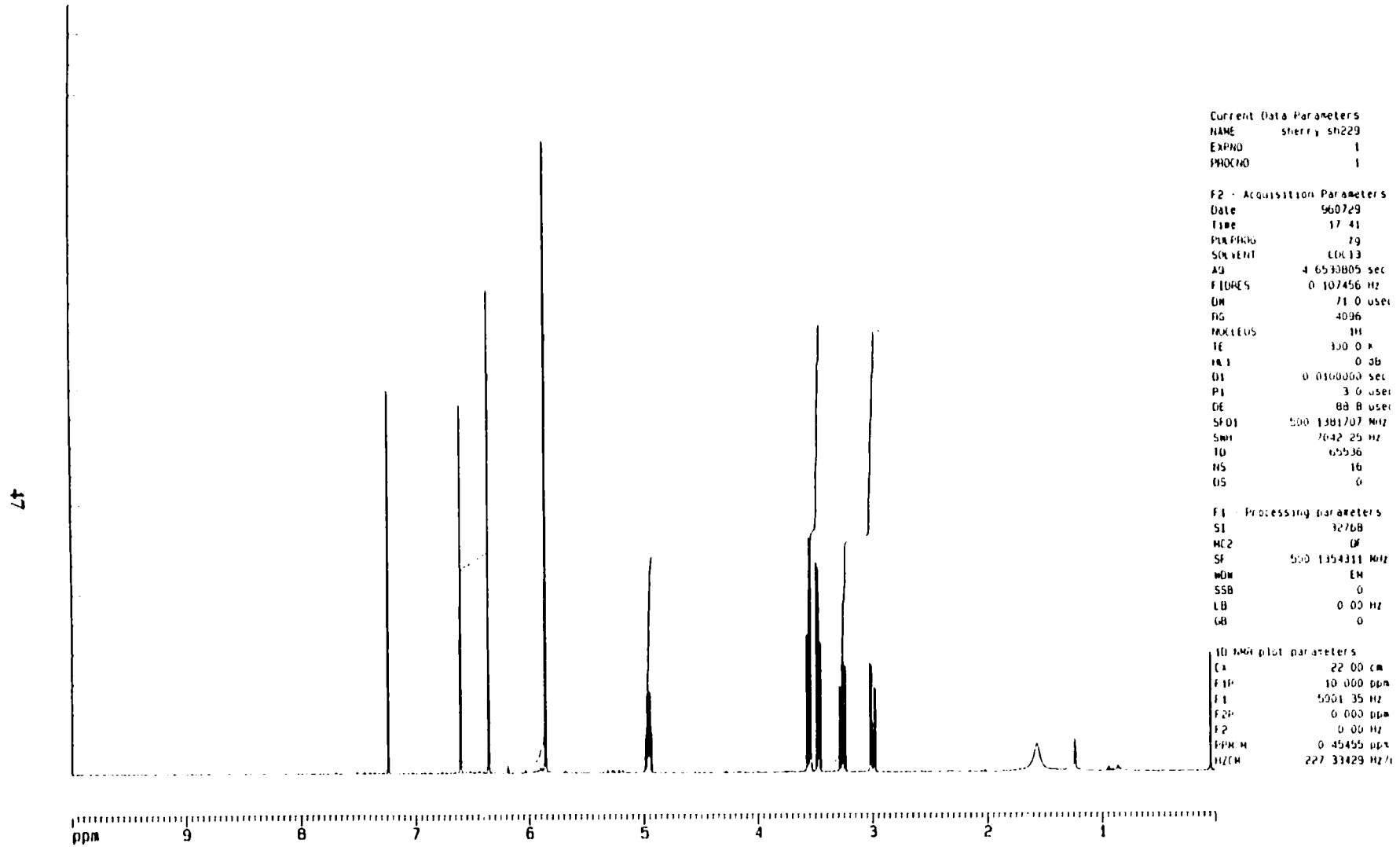

Figure 2.9 500 MHz ^{1}H-NMR Spectrum of Bromide **36** in $CDCl_3$

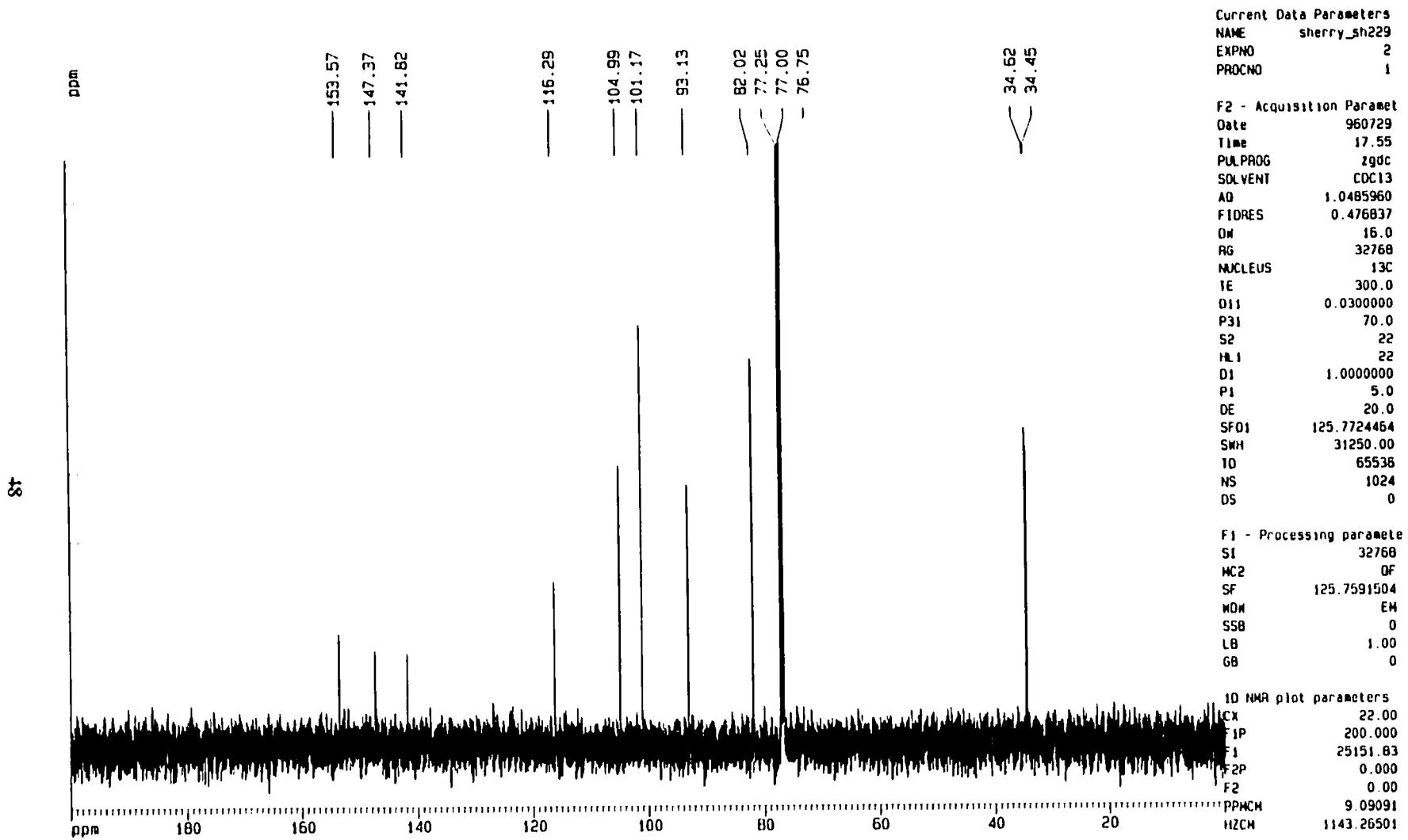

Figure 2.10 125 MHz ^{13}C-NMR Spectrum of Bromide **36** in $CDCl_3$

corresponding to the new methylene group, the primary alcohol and the phenol, respectively. The absence of an aldehyde signal at 191.3 ppm in the ^{13}C spectrum and a total of 11 peaks, including the resonance at 57.8 ppm confirmed the transformation.

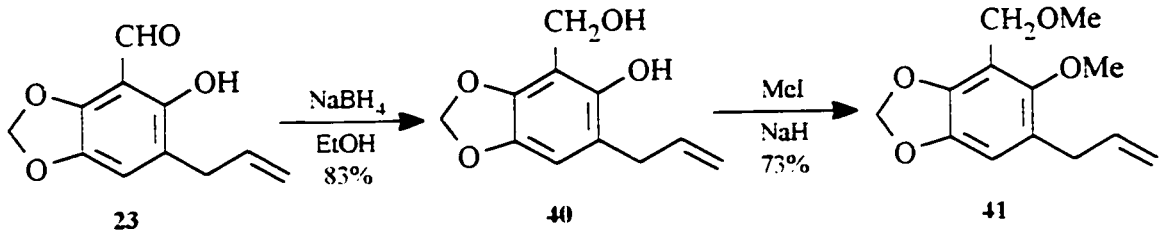

23 40 41

Scheme 2.6 - Synthesis of Dillapiol Derivatives **40** and **41**

The methoxy derivative **41** was easily obtained from **40** by methylation under strongly basic conditions. Double methylation occurred only after refluxing with MeI and NaH. The product, a yellow oil, was easily identified by its two prominent methoxy singlets at 3.40 ppm and 3.72 ppm in the ^{1}H NMR spectrum, and by the two corresponding carbon resonances at 62.8 ppm and 64.3 ppm.

Conversion of the phenolic aldehyde **23** to an alcohol such as **42** can be accomplished with the use of a Grignard reagent. Two eq. of the reagent are required. The first eq. removes the acidic phenolic proton in **23**. The second eq. adds to the carbonyl carbon to give the desired product. Reaction of **23** with the Grignard reagent prepared from 2 eq. of 1-bromooctane and magnesium afforded the diol **42** in 23% yield as a white solid after purification by flash chromatography. The ^{1}H NMR spectrum of this diol is quite interesting and somewhat surprising (Figure 2.11). The hydrogens β and γ to the OH functionality each show nonequivalence. The slightly different chemical shifts of the protons in either of these positions reflect the presence of a neighboring chiral center.

The resonances due to the β-hydrogens are seen as two distinct multiplets at 1.75-1.81 ppm and 1.85-1.91 ppm. The third multiplet at 1.41-1.46 ppm can be assigned to one of the γ-hydrogens. The other γ-hydrogen resonates at the same chemical shift as the 5 remaining aliphatic methylenes according to an HMBC experiment on pure **42** which shows a ^{1}J coupling between the carbon resonating at 25.5 ppm and the hydrogen resonances at 1.24-1.33 ppm and 1.41-1.46 ppm. The α-hydrogen resonates at higher field than the β and γ hydrogens with a chemical shift of 5.02-5.07 ppm. This signal also includes the resonance of the vinylic methylene group. The ^{13}C spectrum of **42**, Figure 2.12, identifies 19 signals, 7 of which are aliphatic methylenes. As expected, the EI-MS of **42** did not include the molecular ion, but rather the M^{+}-H_2O peak. Due to the eventual conjugation of the double bond with the aromatic ring, it is not surprising that the molecule easily loses water under electron impact.

The surprising nonequivalence of the γ-hydrogens may be due to crowding and hydrogen bonding between the alcohol and the phenol to give a six-membered ring which undoubtedly contributes to the rigidity of the system.

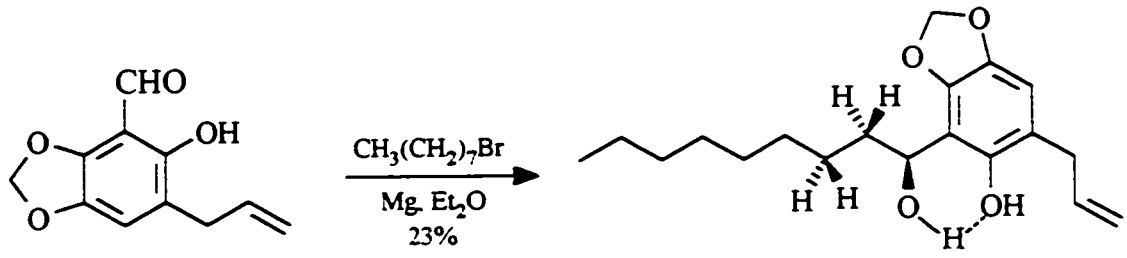

23 **42**

Scheme 2.7 - Synthesis of Dillapiol Derivative **42**

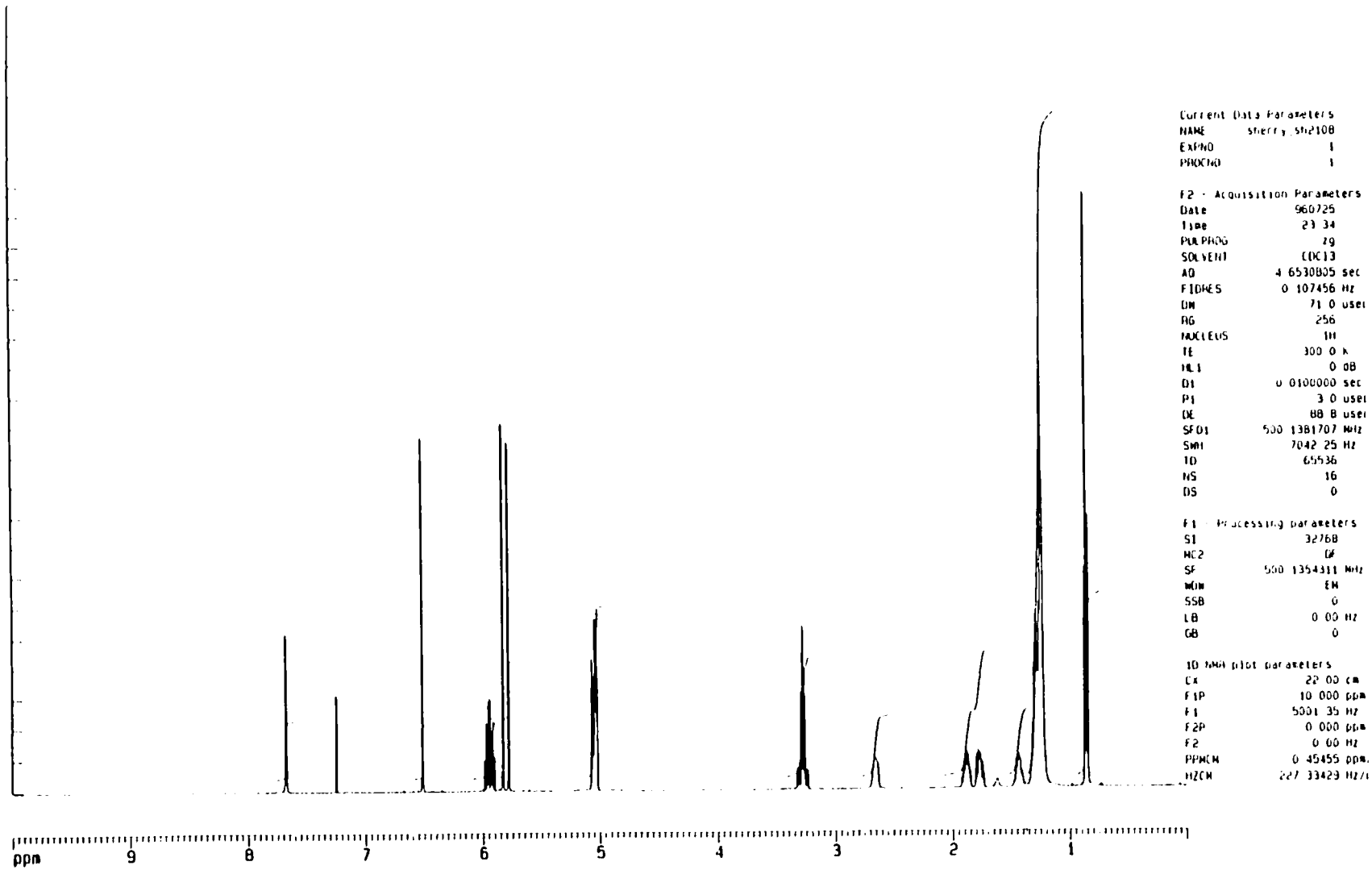

Figure 2.11 500 MHz ^{1}H-NMR Spectrum of Diol **42** in $CDCl_3$

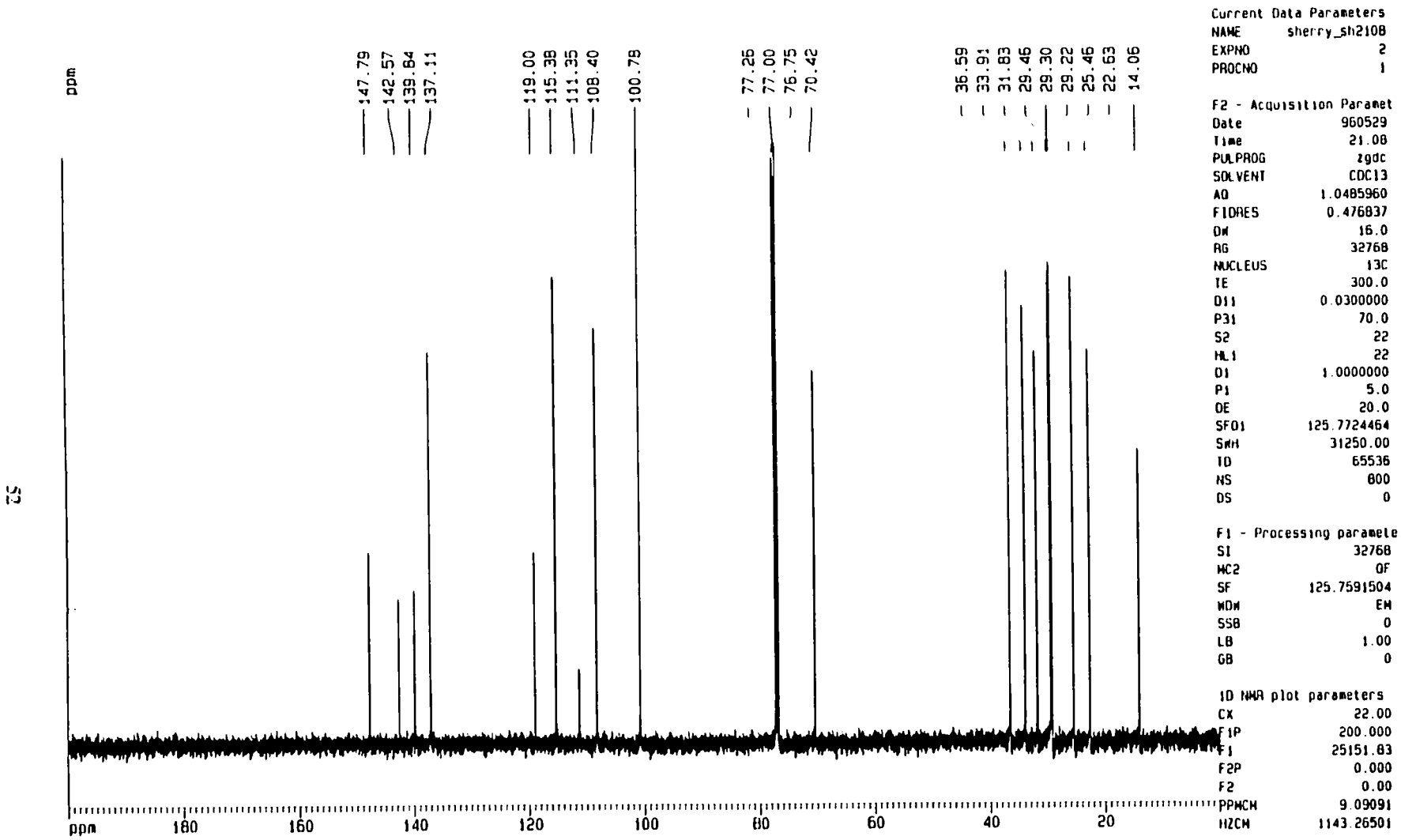

Figure 2.12 125 MHz ^{13}C-NMR Spectrum of Diol **42** in $CDCl_3$

The use of the methoxy aldehyde **24** led to the synthesis of three additional dillapiol derivatives. The first two were obtained in essentially the same way as **40** and **42**. The reduction of **24** with $NaBH_4$ resulted in the formation of the primary alcohol **43** in 75% yield. Resonances in the ^1H NMR spectrum include a broad singlet at 2.45 ppm due to the hydroxyl group, a methoxy singlet at 3.72 ppm and a new methylene singlet at 4.68 ppm. The ^{13}C resonances at 62.5 ppm and 55.7 ppm of the methoxy and new methylene groups, respectively, confirmed the transformation.

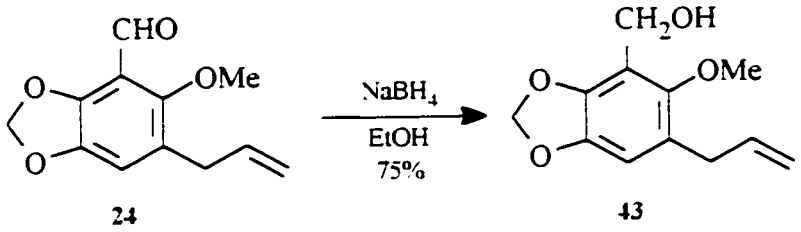

24 **43**

Scheme 2.8 - Synthesis of Dillapiol Derivative **43**

In comparison with aldehyde **23**, addition of 1 eq. of octyl magnesium bromide to an ether solution of **24** proceeded in much higher yield, affording the alcohol **44** in 65% yield after purification of the crude mixture by flash chromatography. The ^1H and ^{13}C NMR spectra closely resemble those of diol **42**. The same nonequivalence is observed for the protons β and γ to the OH functionality. The only differences are the signal at 3.70 ppm arising from the resonance of the methoxy group and the additional ^{13}C resonance at 62.5 ppm.

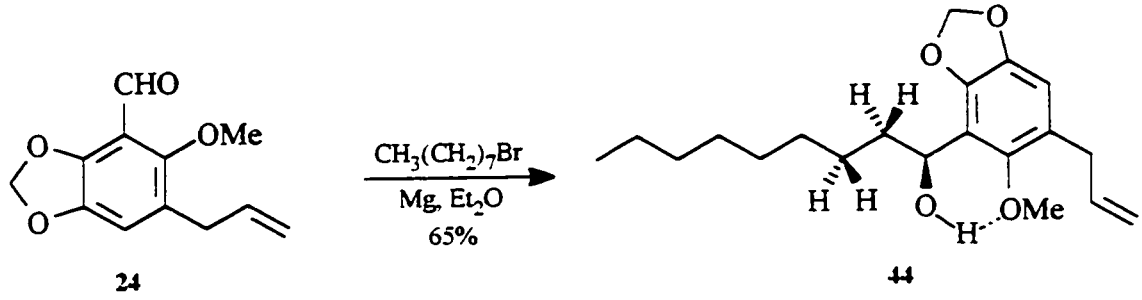

24 44

Scheme 2.9 - Synthesis of Dillapiol Derivative **44**

The reaction of **24** or **23** with Wittig reagents should lead to a variety of alkenes. Only one example was carried out, namely involving the commercially available methyl(triphenylphosphoranylidene)acetate. Reaction of this stabilized ylide with a toluene solution of aldehyde **24** for 22 h at reflux resulted in a spot to spot conversion by TLC to give, after purification by flash chromatography, 91% of the desired product **45** as a pale yellow solid.

Assignment of the trans configuration to the double bond was based on the large coupling constant (J = 16.3 Hz) observed in the ^1H NMR spectrum for the resonances of the two vinylic hydrogens. Apart from the two doublets at 6.78 ppm and 7.81 ppm for the two vinylic hydrogens, ^1H signals include the two prominent methoxy singlets at 3.69 ppm and 3.79 ppm. The carbonyl resonance at 167.9 ppm in the ^{13}C spectrum and a band at 1713 cm^{-1} in the infrared spectrum confirm the structural modification.

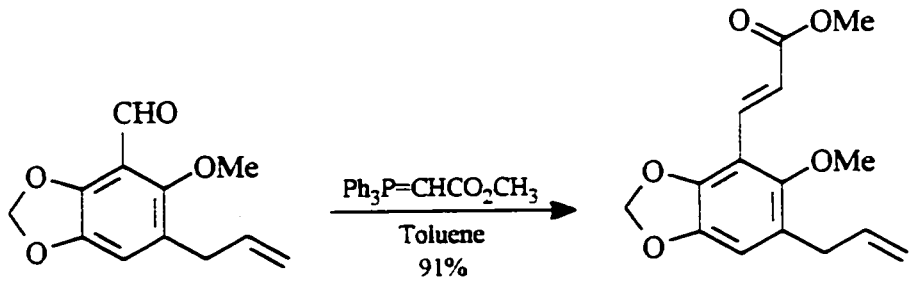

24 45

Scheme 2.10 - Synthesis of Dillapiol Derivative **45**

Reaction of the benzylic alcohol **43** with ethyl bromoacetate in the presence of a strong base should give compounds intermediate in polarity between the phenol-alcohol **42** and dillapiol itself. We anticipated formation of only the ether **46**. However, reaction of **43** with NaH followed by ethyl bromoacetate afforded an almost equal mixture of **46** and the bromoester **47**. Apparently, the rate of acyl transfer from ethyl bromoacetate to the alkoxide of **43** is competitive with S_N2 reaction. A third product resulting from the coupling of **47** with **43** also formed in the reaction but was not fully characterized. The two major products were separated and fully characterized. Key resonances in the ^1H NMR spectrum of **46** include a triplet at 1.25 ppm, a quartet at 4.19 ppm , and two singlets at 4.11 and 4.63 ppm (Figure 2.13). The chemical shift of the protons resonating at 1.25 and 4.19 ppm and their splitting pattern indicate the presence of an ethyl acetate group. The singlets at 4.11 and 4.63 ppm both integrate to two hydrogens and are assigned to the methylene groups on either side of the ether linkage, the protons at lower field being attributed to the benzylic hydrogens. The presence of a carbonyl group is also indicated by the stretching vibration at 1746 cm^{-1} in the infrared spectrum and the carbonyl signal at 170.4 ppm in the ^{13}C spectrum (Figure 2.14).

The mass spectrum of **47** (M^+ = 342, M+2 = 344, 1:1 ratio) showed the presence of one bromine in the product. The singlet at 3.71 ppm ($-OCH_3$) and the two methylene singlets at 3.84 ppm ($BrCH_2$-) and 5.23 ppm (Ar-CH_2O-) in the ^1H NMR spectrum (Figure 2.15), and the corresponding ^{13}C resonances at 62.9 ppm, 58.4 ppm and 25.8 ppm, respectively (Figure 2.16), are in accord with structure **47**.

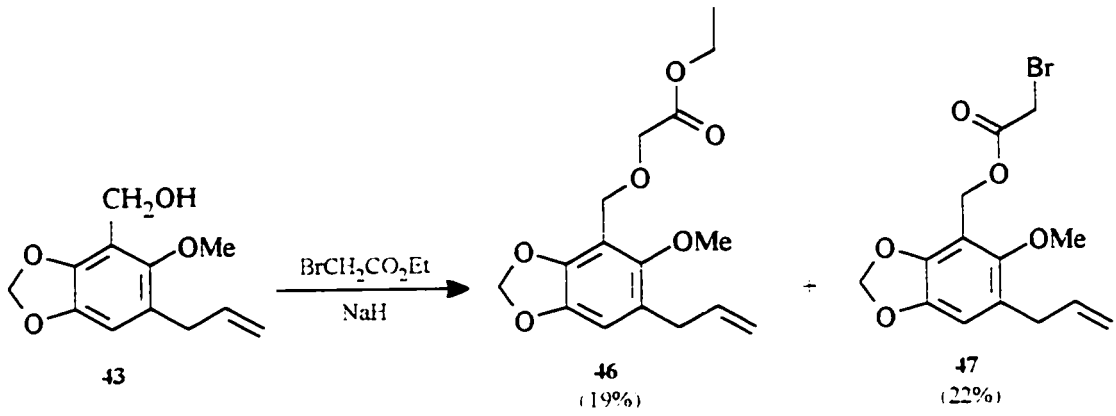

43 46 (19%) 47 (22%)

Scheme 2.11 - Synthesis of Dillapiol Derivatives **46** and **47**

The ready formation of the acyl derivative **47** suggests an easy synthesis of the diazo ester from the alkoxide of **43** and ethyldiazoacetate. Such a compound could be useful as a biological probe since irradiation should generate a reactive carbene which should react with an available nucleophile from the surrounding medium such as the NH group of an amino acid or amide and attach itself via a covalent bond. Dillapiol and its derivatives fluoresce strongly and thus it might be possible to isolate the unit trapped by the carbene and thus obtain information on the active site.

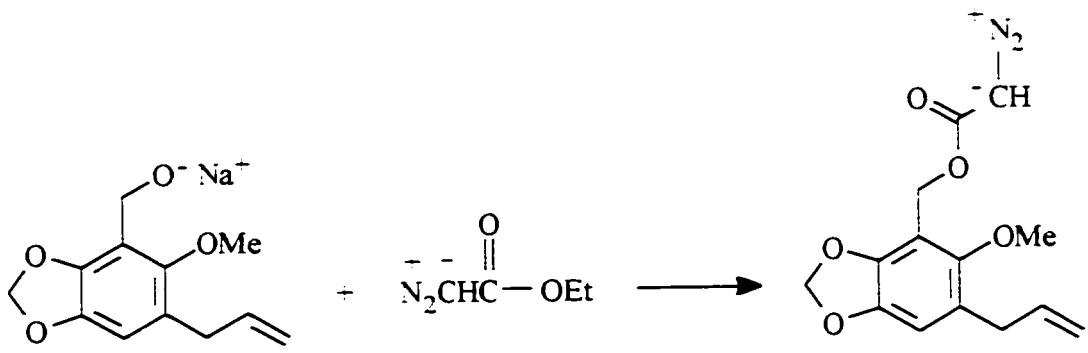

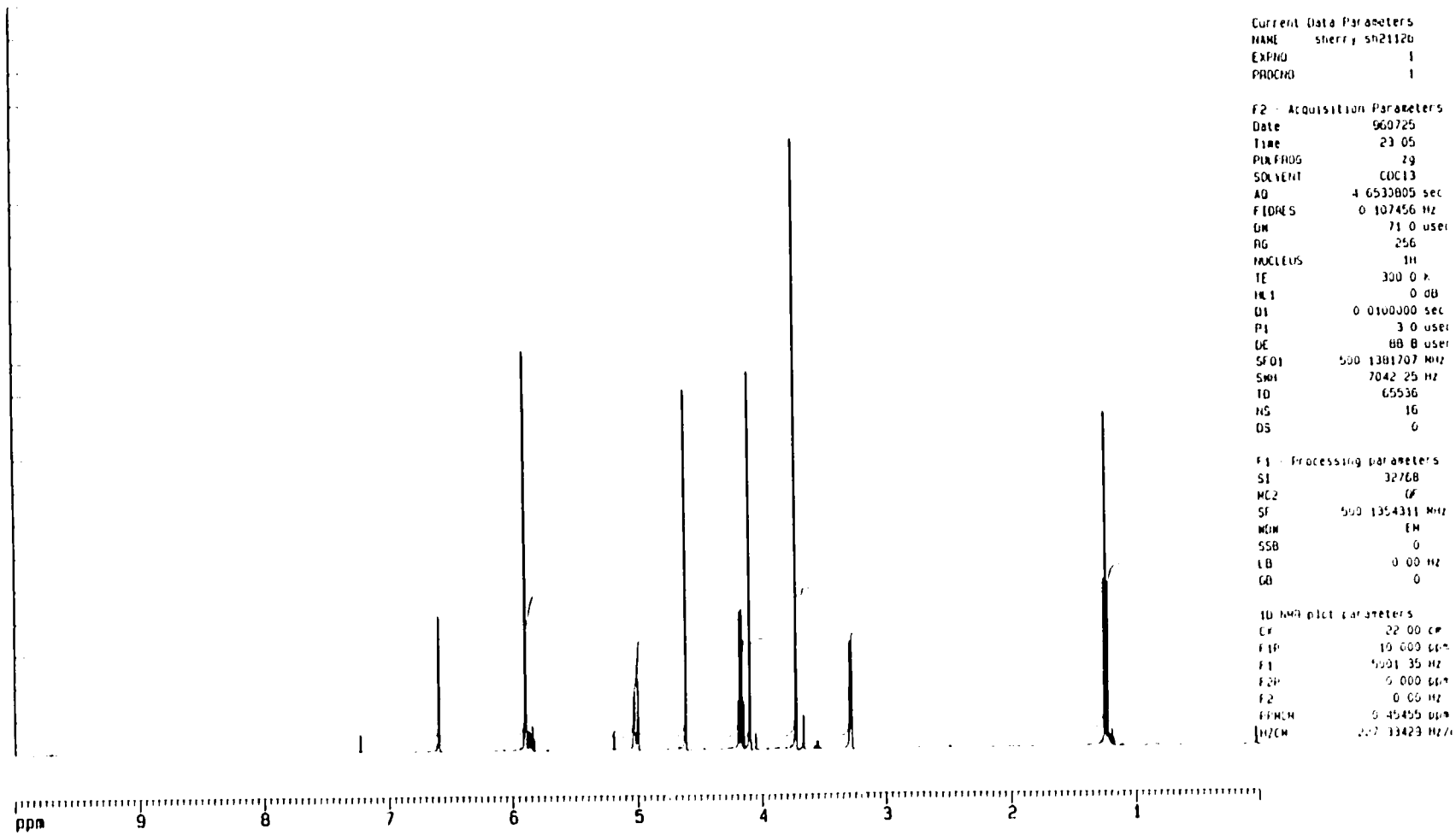

Figure 2.13 500 MHz ^{1}H-NMR Spectrum of Ether **46** in $CDCl_3$

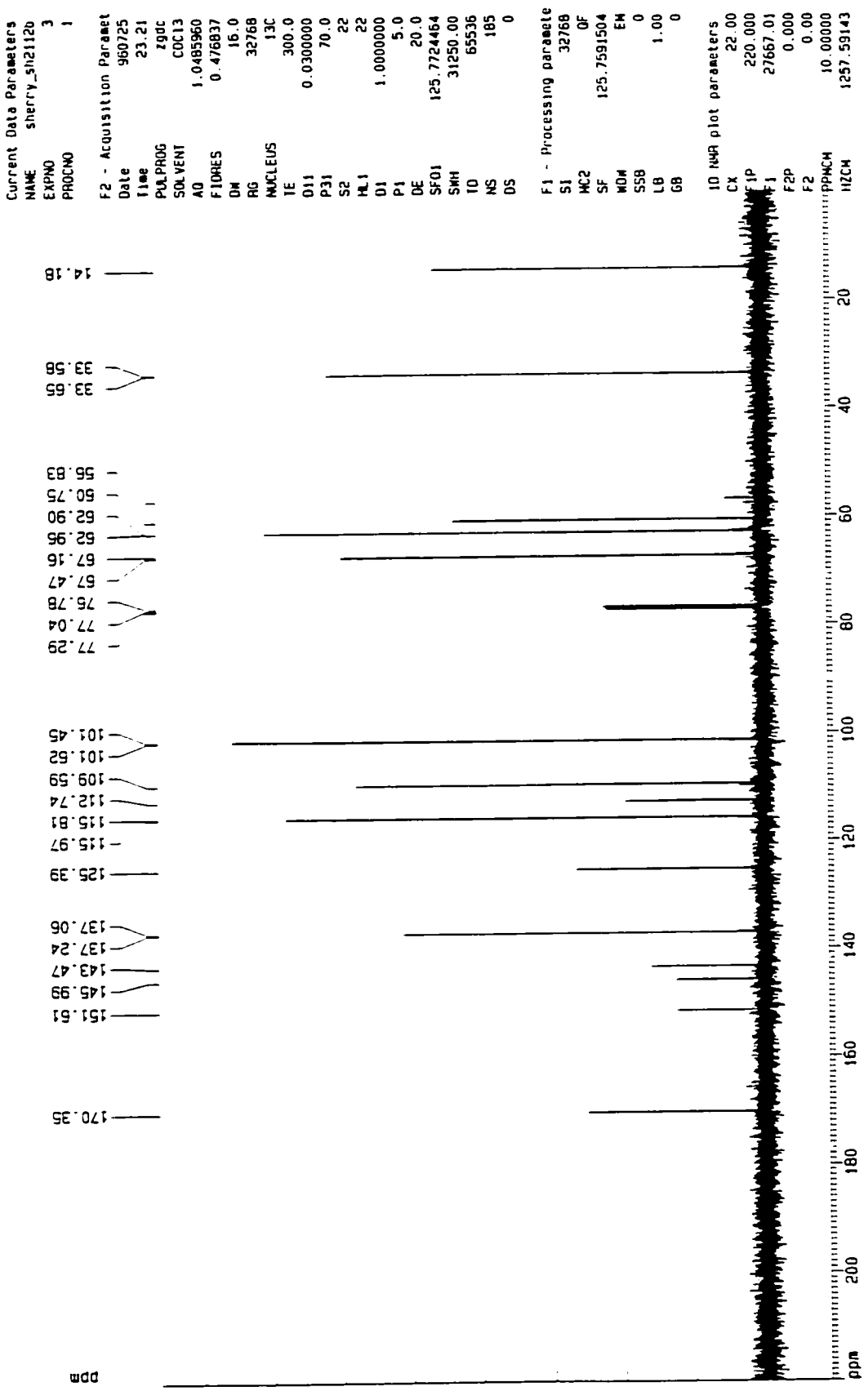

Figure 2.14 125 MHz ^{13}C-NMR Spectrum of Ether **46** in $CDCl_3$

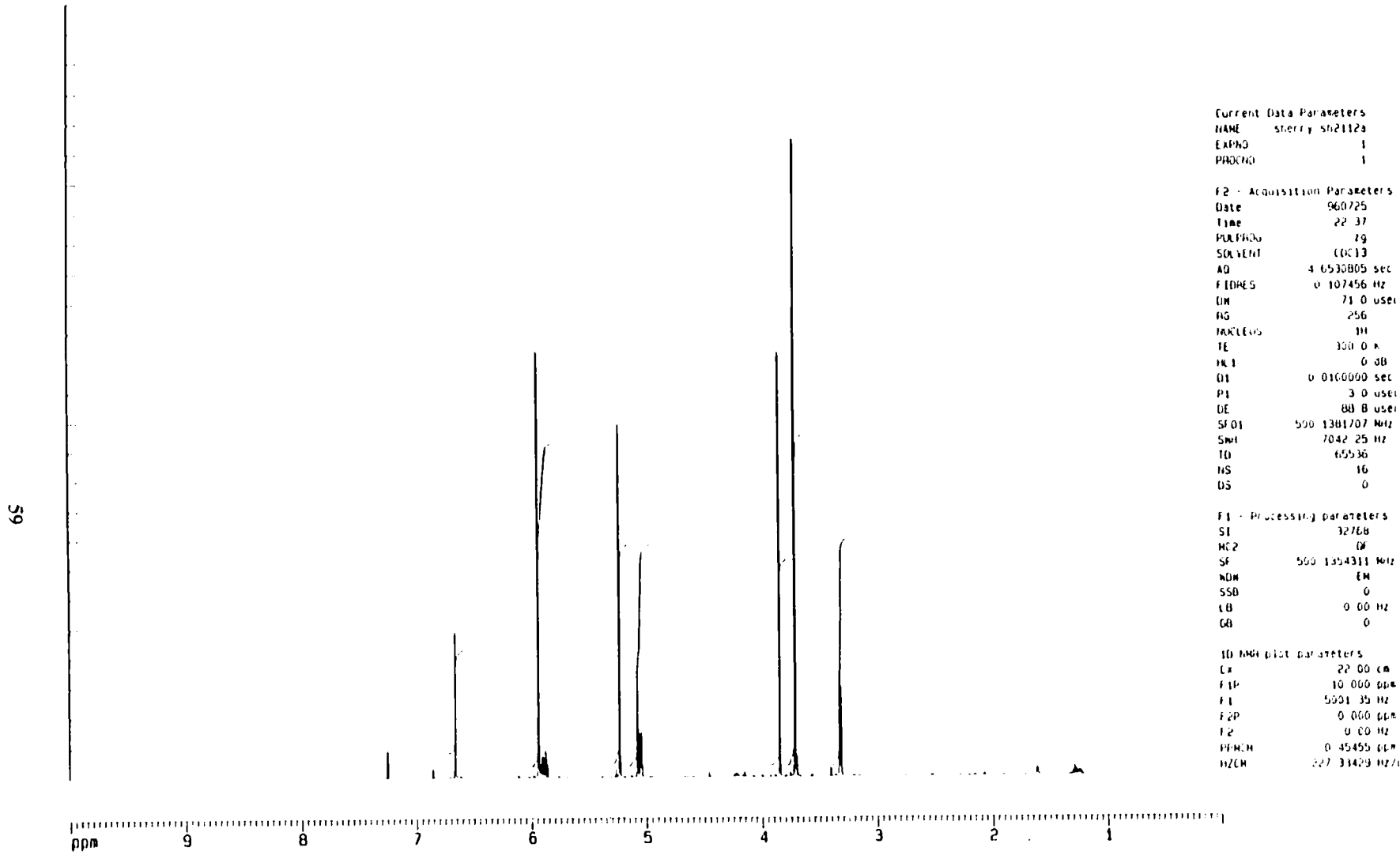

Figure 2.15 500 MHz ^{1}H-NMR Spectrum of Ester 47 in $CDCl_3$

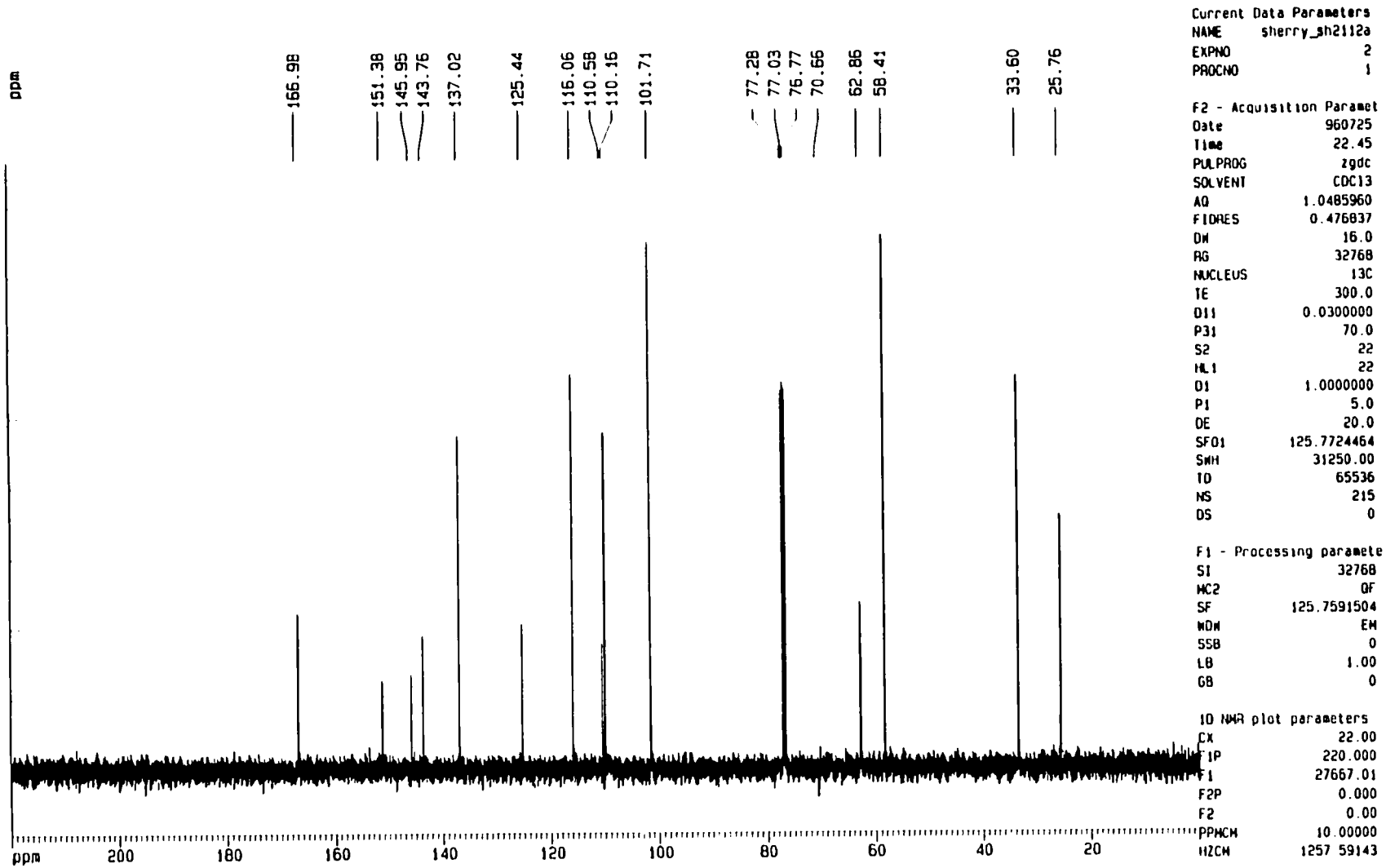

Figure 2.16 125 MHz ^{13}C-NMR Spectrum of Ester 47 in $CDCl_3$

The availability of phenol **26** from the synthesis of dillapiol facilitated the formation of ether **48**, a compound more lipophilic than dillapiol. Any difference in activity between **48** and dillapiol should reflect the importance of lipophilicity in the activity of dillapiol and its derivatives. The preparation of **48** involved alkylating the phenol **26** with octyl bromide in a basic medium. The reaction proceeded in moderate yield (60%) and afforded the desired product as a yellow oil following purification of the product by flash chromatography. Analysis of **48** by ^{1}H NMR revealed a triplet at 0.87 ppm followed by a series of multiplets ranging from 1.24 ppm to 1.75 ppm arising from the resonances of the six central methylene groups. The ^{13}C spectrum contains 19 signals including the required 7 methylene resonances between 22.6 and 72.6 ppm.

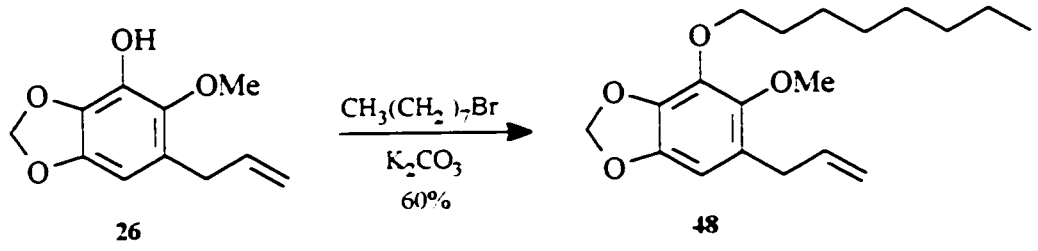

26 **48**

Scheme 2.12 - Synthesis of Dillapiol Derivative **48**

The final set of derivatives was obtained directly from dillapiol by modification of its allylic side chain. We anticipated that reaction of dillapiol with nBuLi would yield preferentially the allylic carbanion rather than an aryl anion. Typically, an OCH_3 group (an OR group in general) activates lateral metallation more strongly than ortho-metallation. In the event, reaction of dillapiol with nBuLi in THF at -78°C followed by the addition of benzophenone afforded the γ-addition product **49** in 42% yield; no evidence of the

α-condensation product **50** was observed. The preference for γ-addition of ketones and aldehydes to what appears to be the more stable resonance structure of an allylic carbanion is the usual result.

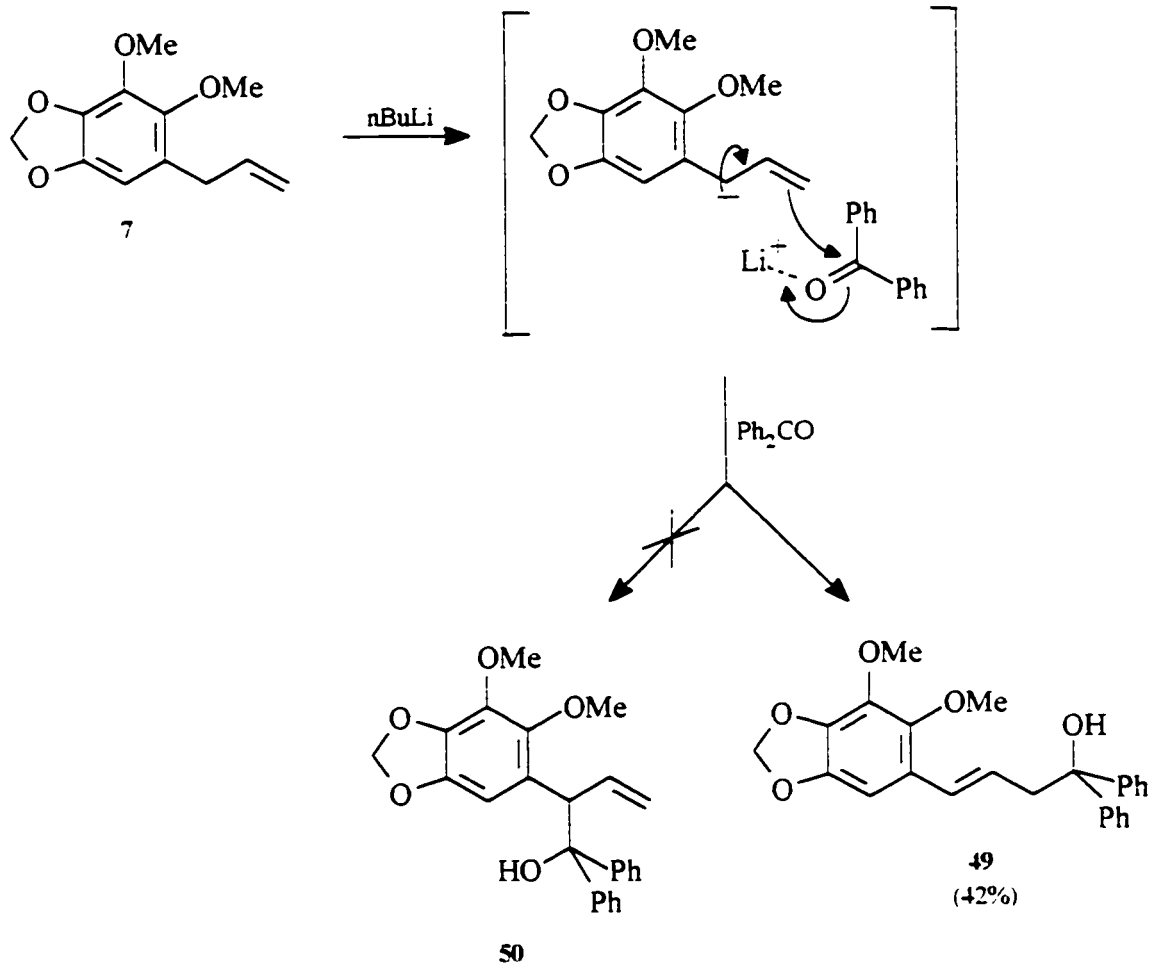

Scheme 2.13 - Synthesis of Dillapiol Derivative **49**

Assignment of the trans configuration to the double bond was based on the large coupling constant (J = 16.0 Hz) of the vinylic hydrogens. The remaining peaks in the ^{1}H spectrum are as expected, including a broad OH peak at 2.57 ppm (Figure 2.17). The ^{13}C

spectrum, Figure 2.18, contains 17 signals including a methylene signal at 46.2 ppm, two methoxy resonances at 60.0 ppm and 61.5 ppm and 6 methine resonances. It is somewhat surprising that **49** does not easily eliminate water to give a conjugated diene. Dehydration only seems to occur at high temperature as indicated by the M^{+}-H_2O peak in the EI-MS.

We had anticipated that the allylic carbanion would serve as a valuable intermediate to many other compounds via reaction with readily available electrophiles.

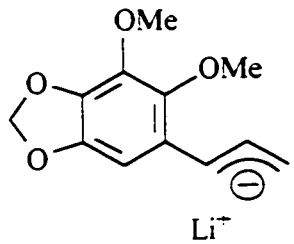

51

In initial studies of the reaction of **51** with such electrophiles as alkyl halides, trimethylsilanes, aldehydes, and esters, mixtures of compounds were obtained. Several attempts at separating these mixtures or developing reaction conditions which might favor one product were not successful and this direction was abandoned.

The presence of a double bond in the side chain of dillapiol and the numerous reactions available to it could potentially lead to a variety of compounds. One reaction, oxymercuration-demercuration, is highly regioselective and has been shown to react with aqueous solutions of mercuric acetate to afford alcohols in high (>90%) yield (Scheme 2.14). The reaction can also be carried out in other nucleophilic solvents such as alcohols

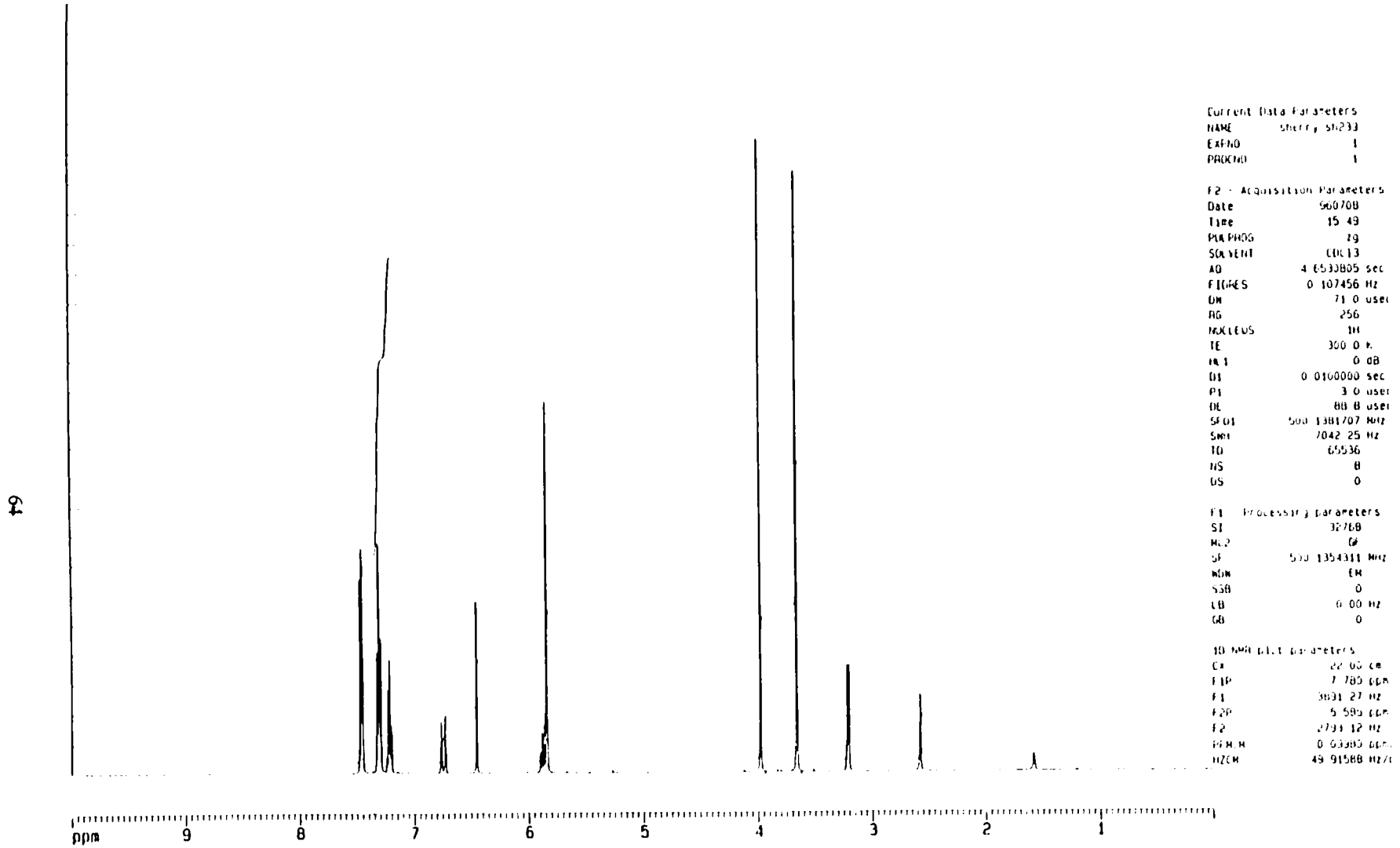

Figure 2.17 500 MHz ^{1}H-NMR Spectrum of Alcohol **49** in $CDCl_3$

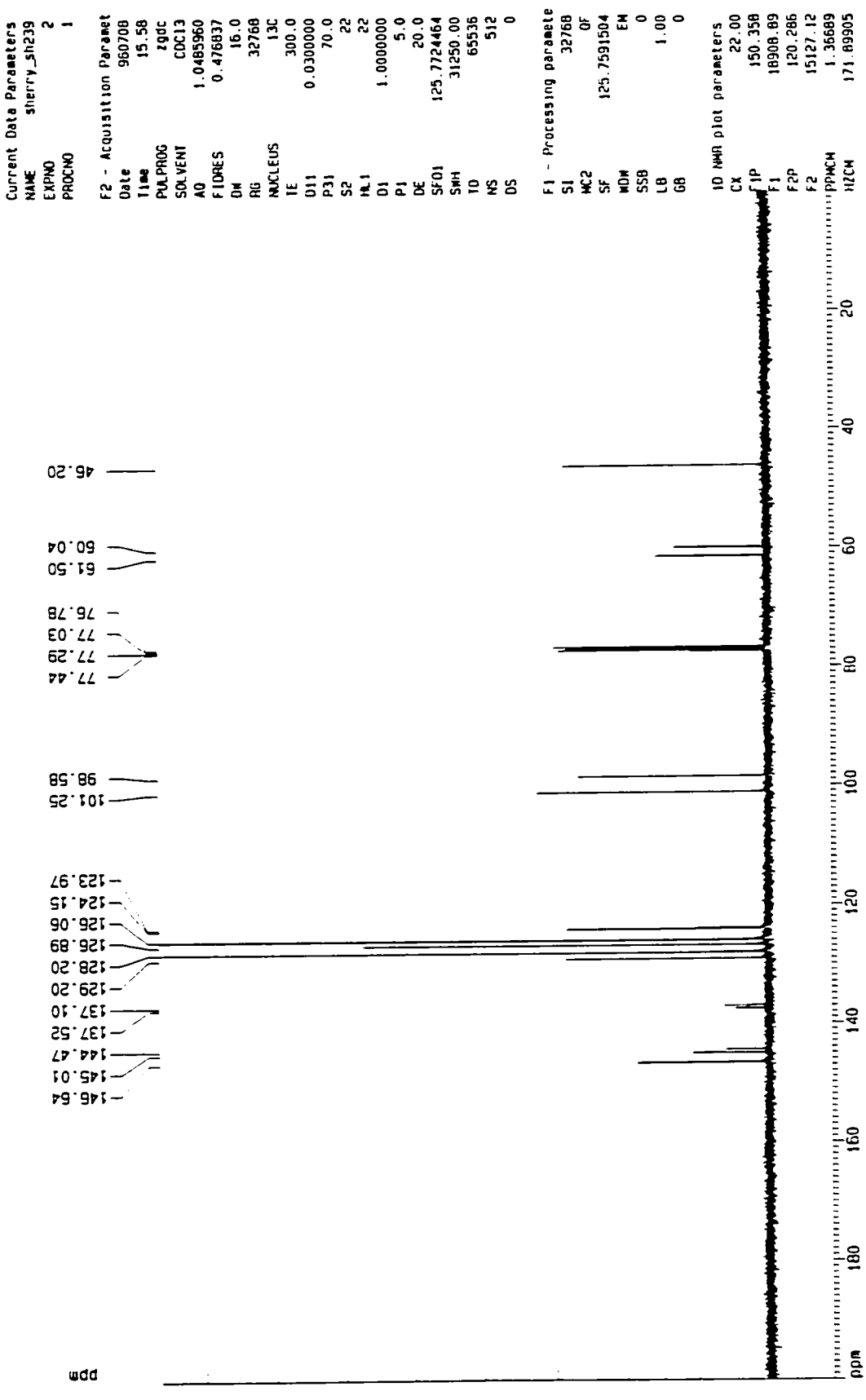

Figure 2.18 125 MHz ^{13}C-NMR Spectrum of Alcohol **49** in $CDCl_3$

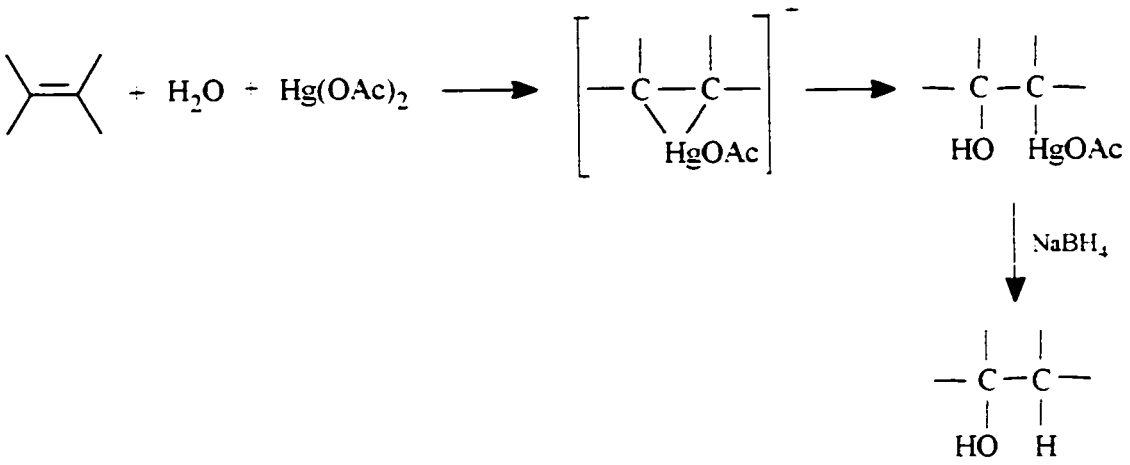

Scheme 2.14 The oxymercuration-demercuration reaction

to give a variety of ethers. In the synthesis of ether **52**, this nucleophilic solvent was 1-propanol. Treatment of a solution of dillapiol 7 with 1.2 eq. of mercuric acetate in 1-propanol followed by reduction of the organomercurial compound with $NaBH_4$ afforded 17% of ether **52** as a yellow liquid. ^1H NMR resonances include a high field methyl triplet and doublet at 0.86 ppm and 1.09 ppm, two doublet of doublets at 2.51 ppm and 2.81 ppm arising from the resonances of the benzylic hydrogens, and multiplets at 1.50-1.58 ppm, 3.31-3.34 ppm (1H), 3.39-3.42 ppm (1H), and 3.53-3.54 ppm (1H) (Figure 2.19). The ^{13}C spectrum, Figure 2.20, shows a methine carbon at 76.0 ppm which confirms the regiochemistry shown in **52**.

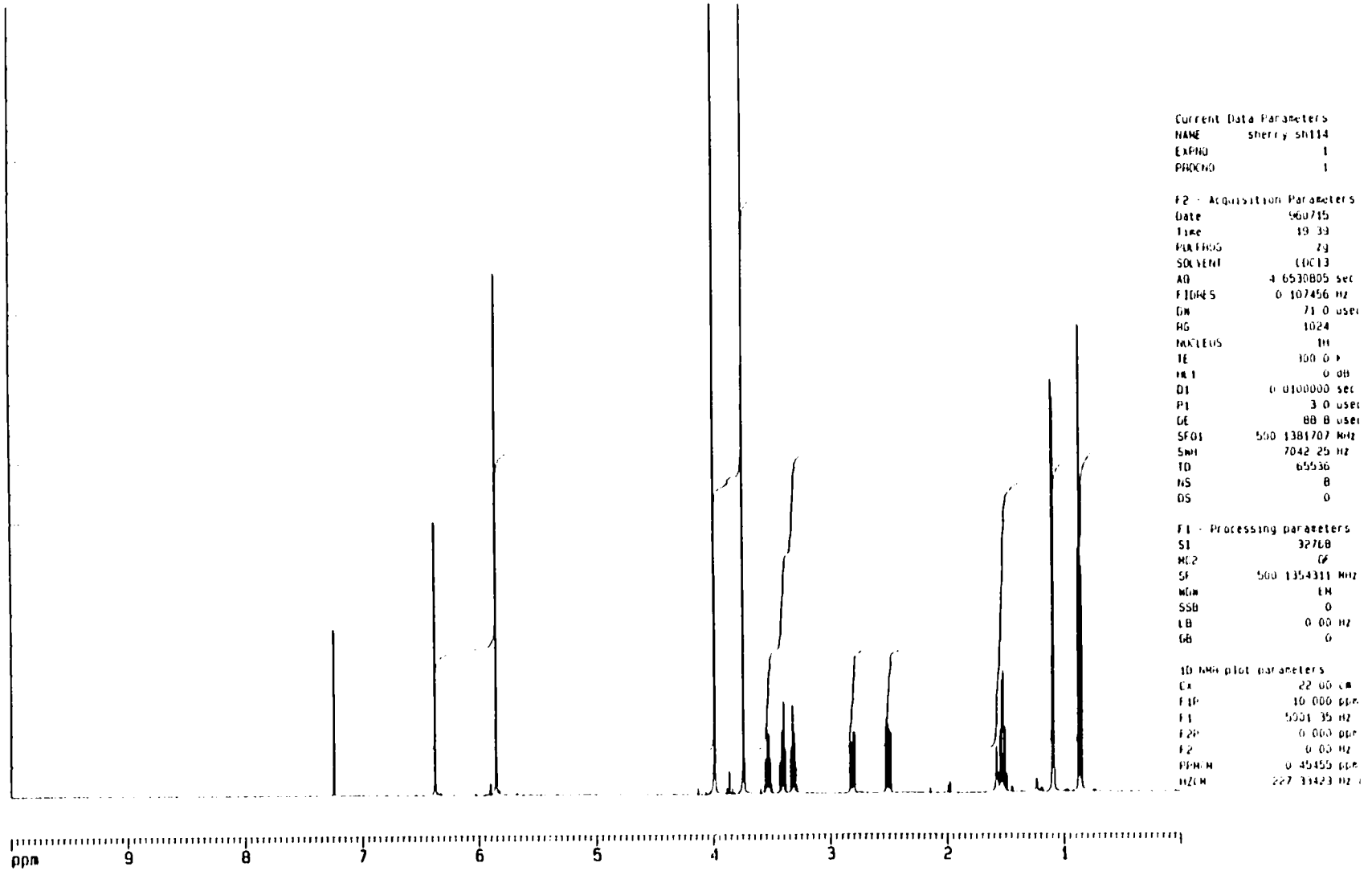

Figure 2.19 500 MHz ^{1}H-NMR Spectrum of Polyether **52** in $CDCl_3$

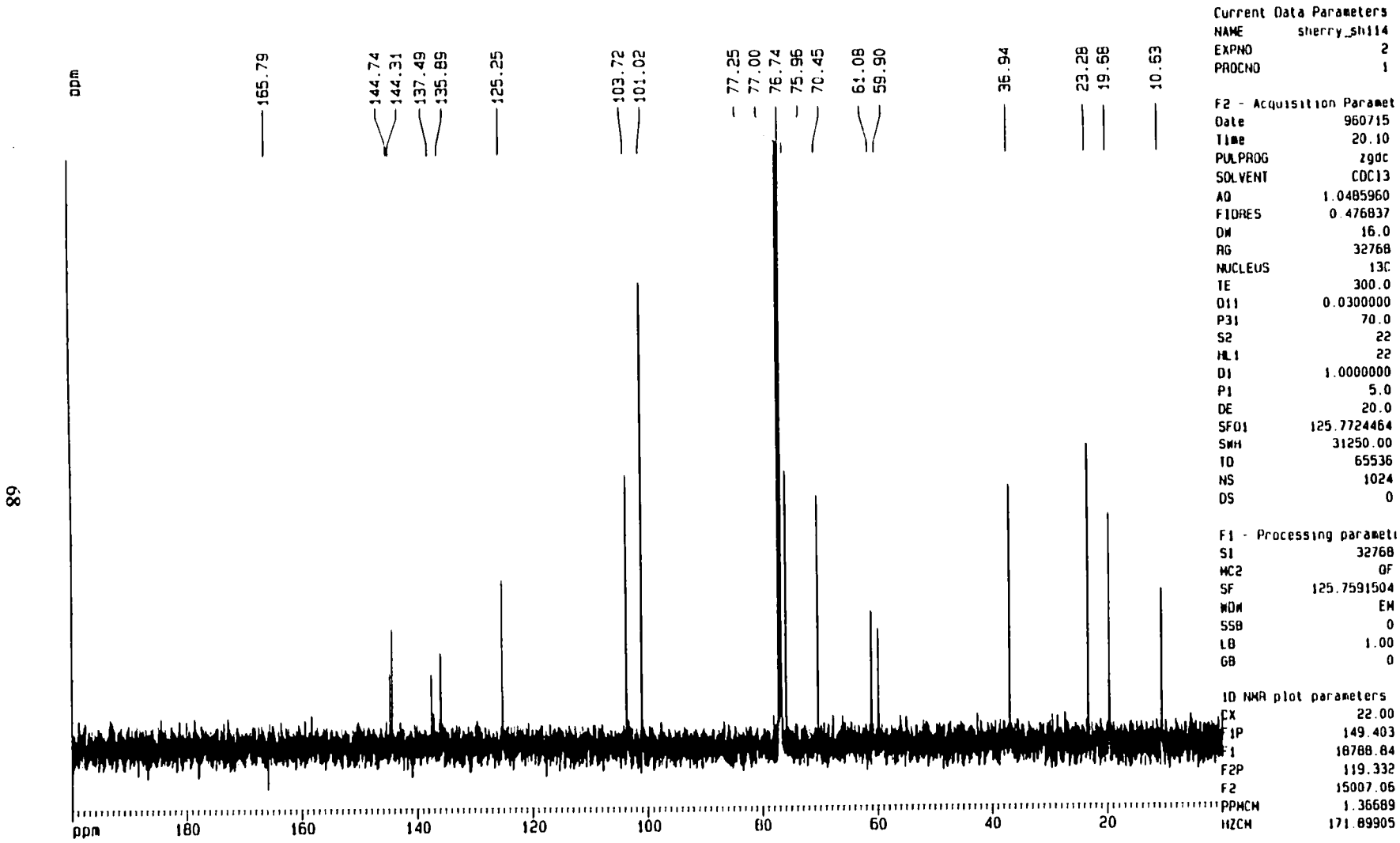

Figure 2.20 125 MHz ^{13}C-NMR Spectrum of Polyether **52** in $CDCl_3$

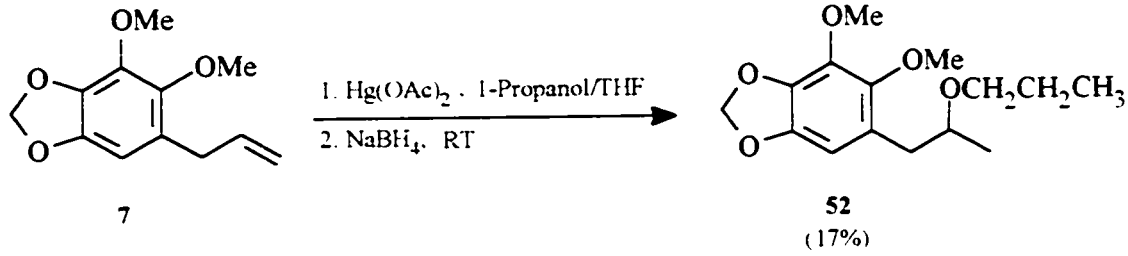

7

52
(17%)

Scheme 2.15 - Synthesis of Dillapiol Derivative **52**

As anticipated, treatment of dillapiol with borane methyl sulfide followed by hydrogen peroxide resulted in the preferential formation of alcohol **53** (26% yield). Only a trace (2%) of the secondary alcohol was detected by ^{1}H NMR. Formation of the primary alcohol was indicated in the ^{1}H NMR spectrum by a multiplet at 1.67-1.73 ppm for the central methylene hydrogens, two methylene triplets at 2.54 and 3.50 ppm and a broad singlet at 2.74 ppm arising from the resonance of the hydroxyl hydrogen (Figure 2.21). The methylene signals at 25.7, 33.5 and 61.4 ppm in the ^{13}C spectrum also confirm the transformation (Figure 2.22).

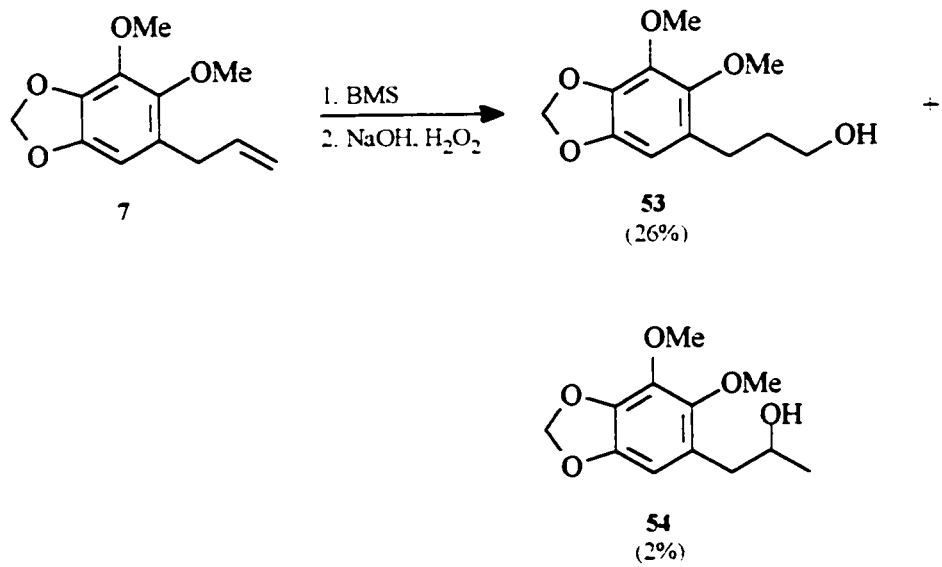

7

53
(26%)

54
(2%)

Scheme 2.16 - Synthesis of Dillapiol Derivatives **53** and **54**

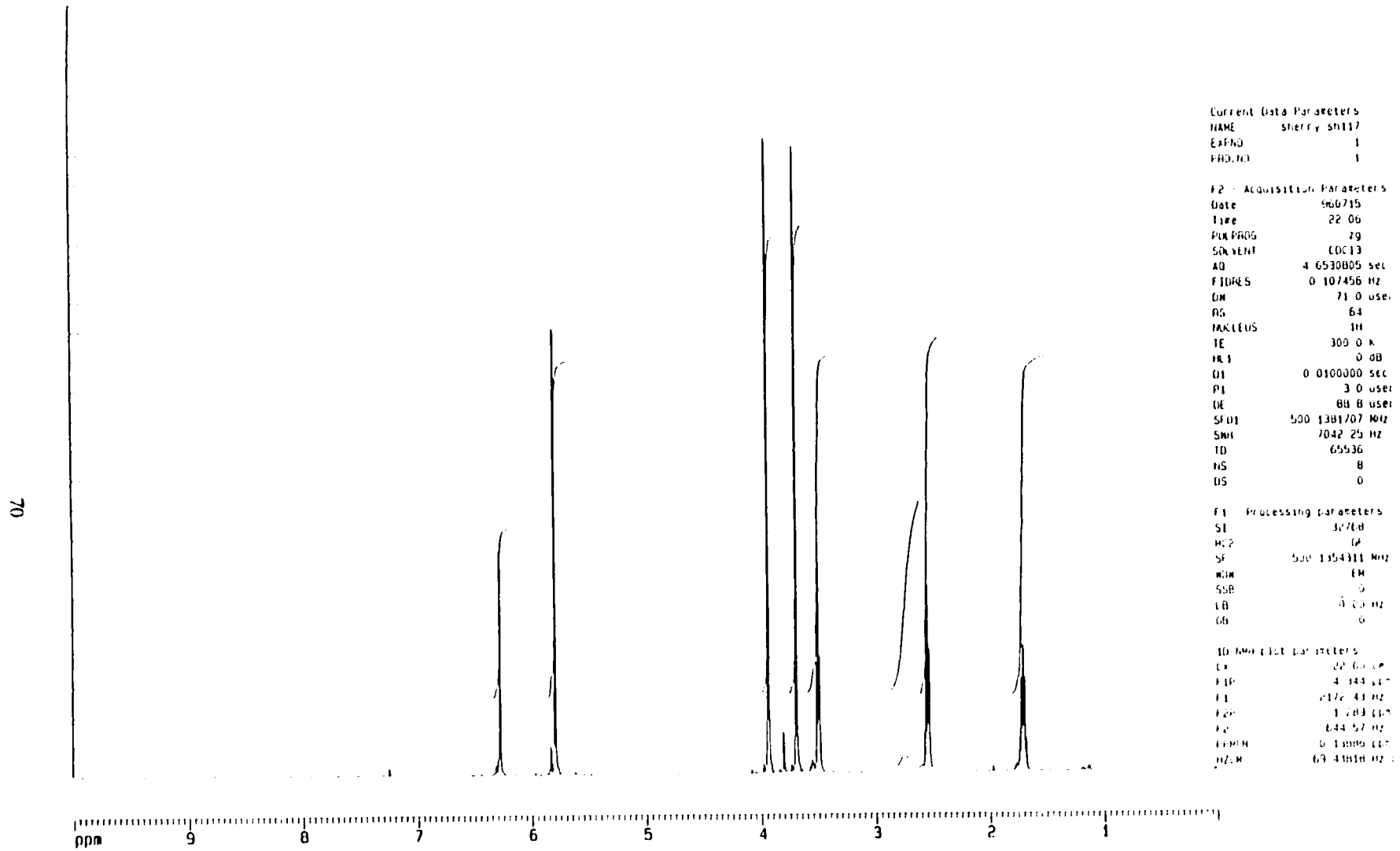

Figure 2.21 500 MHz ^{1}H-NMR Spectrum of Alcohol **53** in $CDCl_3$

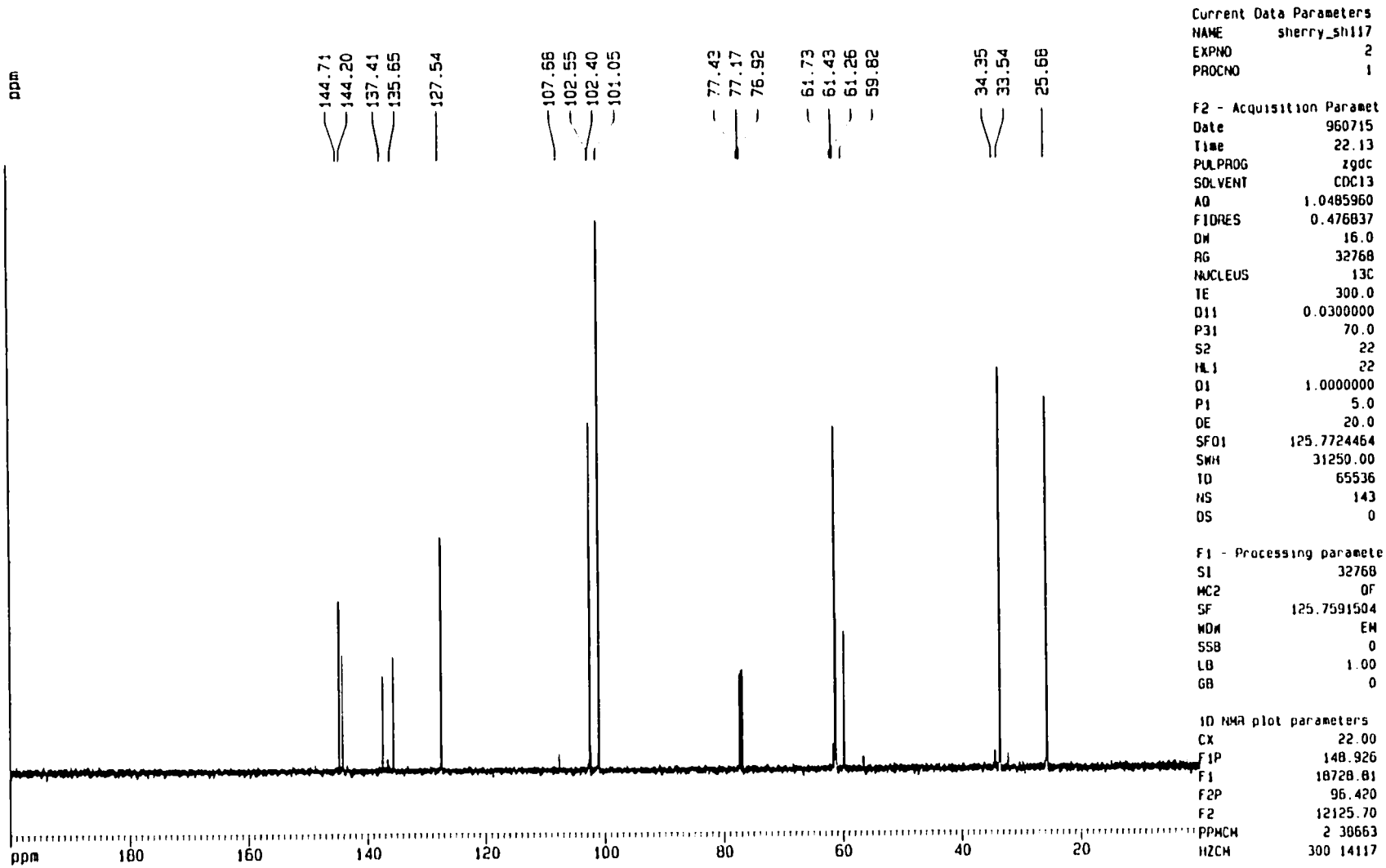

Figure 2.22 125 MHz ^{13}C-NMR Spectrum of Alcohol **53** in $CDCl_3$

^{1}H resonances of alcohol **54** include a doublet at 1.19 ppm (3H), an OH doublet at 2.13 ppm, a pair of doublet of doublets at 2.61 ppm and 2.68 ppm, and a multiplet at 3.95-3.99 ppm due to the CH group (Figure 2.23). Corresponding carbon resonances can be found at 23.1 ppm, 40.0 ppm and 68.6 ppm (Figure 2.24).

Dillapiol also served as the precursor for the furan derivative **55**. The reaction consisted of Markovnikov addition of H^- to the double bond of dillapiol followed by nucleophilic attack of the methoxy oxygen onto the carbocation. After refluxing a mixture of dillapiol, NaI and TsOH for 72 h in CH_2Cl_2, and purifying the product by flash chromatography, ether **55** was obtained in 30% yield as a colorless oil. The ^{1}H NMR spectrum of **55** showed a 3H doublet at 1.44 ppm, a multiplet at 4.88–4.92 ppm for the methine proton and a pair of doublet of doublet of doublets at 2.71 ppm and 3.17 ppm arising from the coupling of the methylene hydrogens with each other and the methine proton. The appearance of 11 signals in the ^{13}C spectrum and the peak at a mass of 208 in the EI-MS were in agreement with the structural assignment.

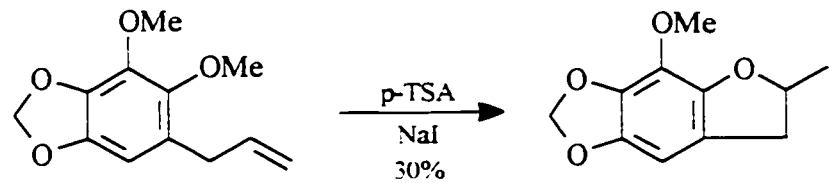

7 55

Scheme 2.17 - Synthesis of Dillapiol Derivative **55**

The final derivative, ester **56**, was easily synthesized from alcohol **53** in 64% yield by acylation with benzoyl chloride in the presence of pyridine. The ^{1}H and ^{13}C NMR

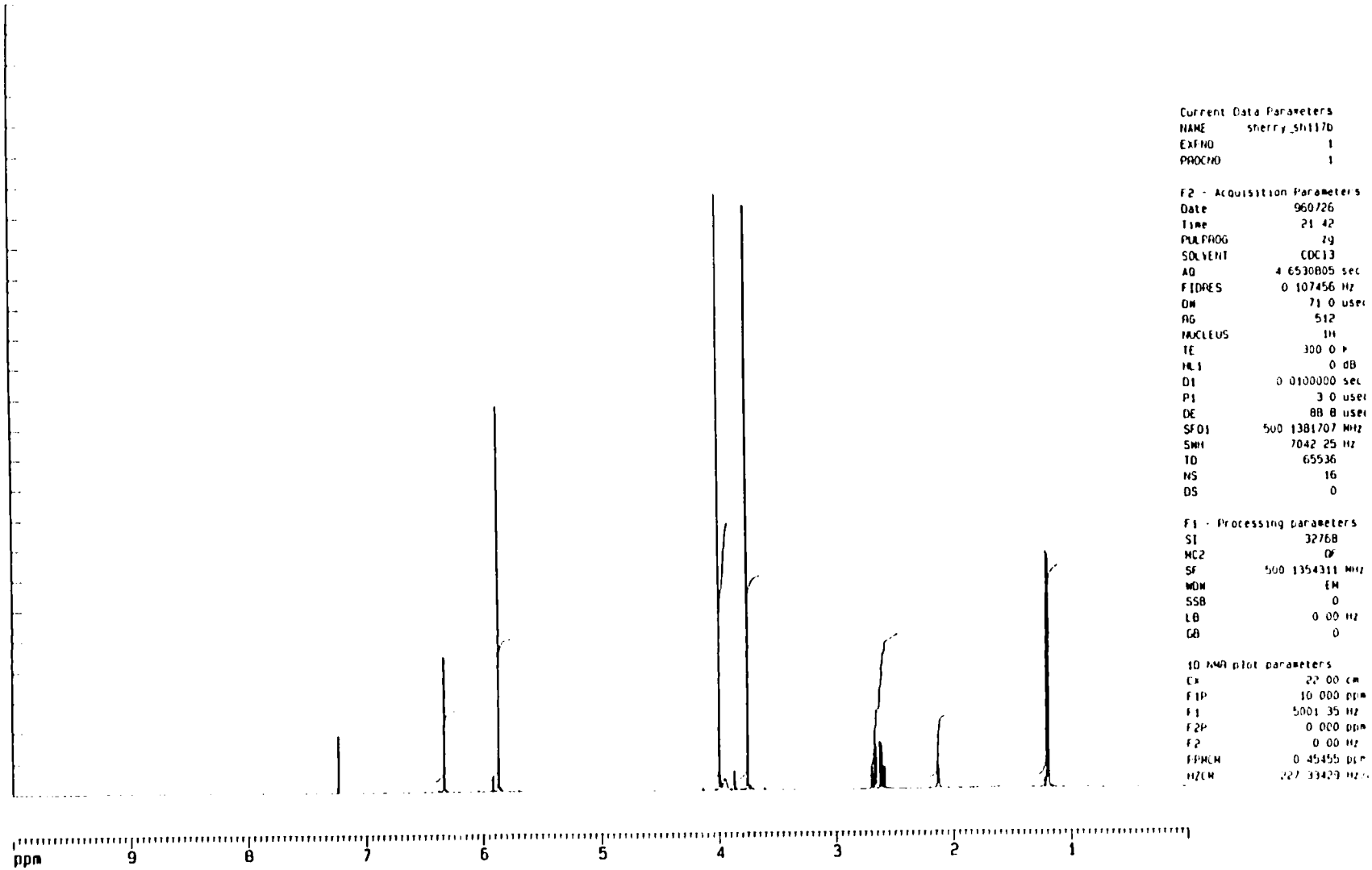

Figure 2.23 500 MHz ^{1}H-NMR Spectrum of Alcohol **54** in $CDCl_3$

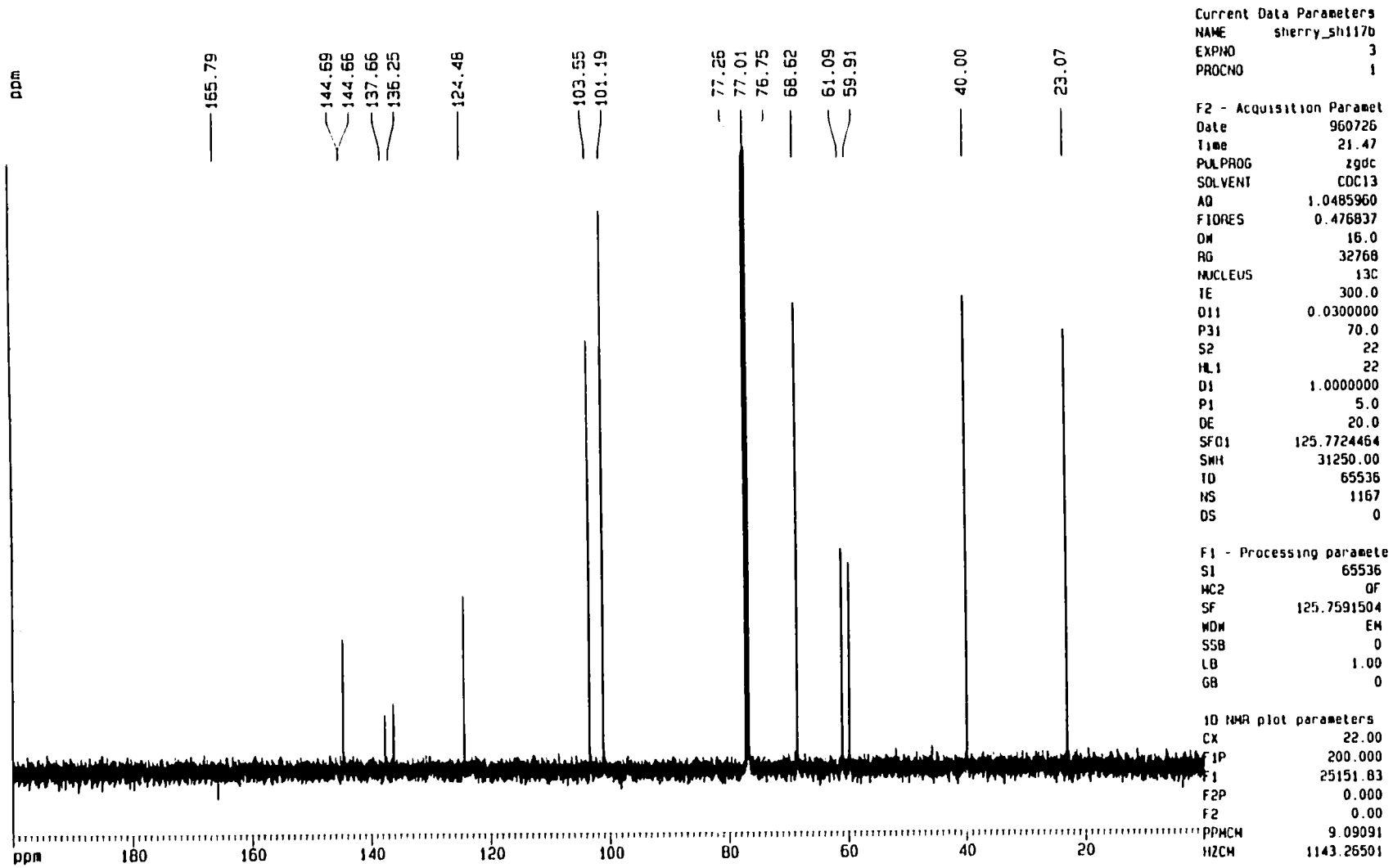

Figure 2.24 125 MHz ^{13}C-NMR Spectrum of Alcohol **54** in $CDCl_3$

spectra closely resemble those of alcohol **53**. ^{1}H signals include the three multiplets at 7.40-7.43 ppm, 7.51-7.54 ppm, and 8.01-8.02 ppm arising from the resonance of the aromatic hydrogens. The 17 signals in the ^{13}C spectrum, including the carbonyl signal at 166.6 ppm, and the carbonyl stretching vibration at 1715 cm^{-1} in the infrared spectrum were expected.

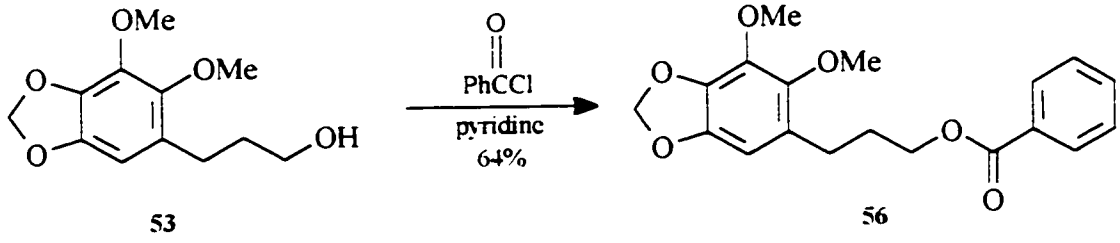

53 **56**

Scheme 2.18 - Synthesis of Dillapiol Derivative **56**

CHAPTER 3

EFFECT OF DILLAPIOL AND ITS DERIVATIVES ON MULTIDRUG RESISTANCE PHENOTYPES[1]

3.1 Introduction

Multi-resistance to insecticides most probably arises from a combination of defense mechanisms. One of them is the biotransformation of these often lipophilic compounds, by PSMOs, to excretable metabolites. The other mechanism of defense which may be involved in the development of multi-resistance by insects is the extrusion of insecticides out of cells by a P-glycoprotein-like pump. Such a pump has been identified in the blood-brain barrier of the tobacco hornworm as well as in the epithelial wall of its Malpighian tubules[36]. The activity of this pump, along with that of such detoxification enzymes as PSMOs, have been attributed to the development of resistance by this insect to nicotine.

The idea that multi-resistance in insects could be due in part to a P-glycoprotein-like pump stemmed from numerous studies of multi-resistance in mammals. Multi-resistance, the cause of failed chemotherapy, has been associated with the overexpression of a highly conserved multidrug resistance gene family which codes for a transmembrane protein, called P-glycoprotein. As mentioned in Chapter 1, this transmembrane protein appears to pump out a range of different drugs from within cells thus maintaining the exposure and binding of the drugs to their intracellular target at a non-toxic level. Several

1. Dillapiol and some of the analogs described in the previous chapter were assayed for MDR activity by Dr Claude Bernard. This discussion of her experimental results is included in order to give a more complete picture of the potential importance of these compounds.

compounds exist which inhibit the extrusion of drugs by this pump but the major and potentially dangerous side effects which accompany their reversal of multidrug resistance limit their clinically achievable concentrations. Consequently, new, better, and less toxic chemosensitizers need to be developed.

Dr Bernard investigated the activity of dillapiol and several of its derivatives on multidrug resistance phenotypes in a cultured cell model which includes hamster cell lines selected for multidrug resistance (B30) as well as murine cells transfected with the MDR1 gene that confers the human P-glycoprotein phenotype (G185)[62].

3.2 Resistance Levels

In a preliminary investigation of the toxicity of dillapiol to resistant and drug-sensitive cell lines, dillapiol was found to have a surprising and potentially significant effect. In contrast to other lignans, dillapiol as well as piperonyl butoxide were more toxic to the P-glycoprotein-rich multidrug-resistant cells than to their parental cells with normal P-glycoprotein levels, a phenomenon known as collateral sensitivity. Specifically, multidrug-resistant B30 cells were killed with doses of dillapiol and piperonyl butoxide of 0.5 ng/mL while the parental AUXB1 cells were killed with the much higher doses of >500 ng/mL and 50 ng/mL, respectively. The degree of collateral sensitivity was much less pronounced with the murine fibroblast multidrug-resistant G185 cells. While a dose of only 5 ng/mL was required to toxify the resistant G185 cells, the parental NIH cells were killed by 50 ng/mL of piperonyl butoxide. Collateral sensitivity of G185 cells to dillapiol could not be demonstrated because of the limited solubility of the compound in

the culture media. However, Bernard showed that G185 and NIH cells are killed by >500 ng/mL of dillapiol.

Collateral sensitivity of multidrug-resistant cells, a multidrug resistance phenotype leading to hypersensitivity to drugs, has been reported with various detergents and detergent-like compounds[63]. The phenomenon, however, is poorly understood. It has been suggested that changes in membrane permeability and composition accompanying the multidrug resistance phenotype may be a mechanism for collateral sensitivity. Ultrastructural changes in the membrane layer of multidrug-resistant cells and modifications of its physical properties have also been described by Arsenault and coworkers[64], and by Kessel[65].

Since the effect of dillapiol could prove to be of significance in the management of resistant tumor cells and potentially resistant insect pests, further attention was given to the mechanism of action of dillapiol on these cells.

3.3 Uptake of ^{3}H-vinblastine in Resistant and Sensitive Cell Lines

The major role of P-glycoprotein in the resistance of B30 cells (the Chinese hamster ovarian multidrug-resistant cell line) was demonstrated by Bernard by the ability of verapamil to inhibit P-glycoprotein activity and to restore the level of vinblastine accumulated by B30 cells to that of the drug-sensitive AUXB1 cells (Figure 3.1). This established the validity of the system and served as a positive control run in each experiment.

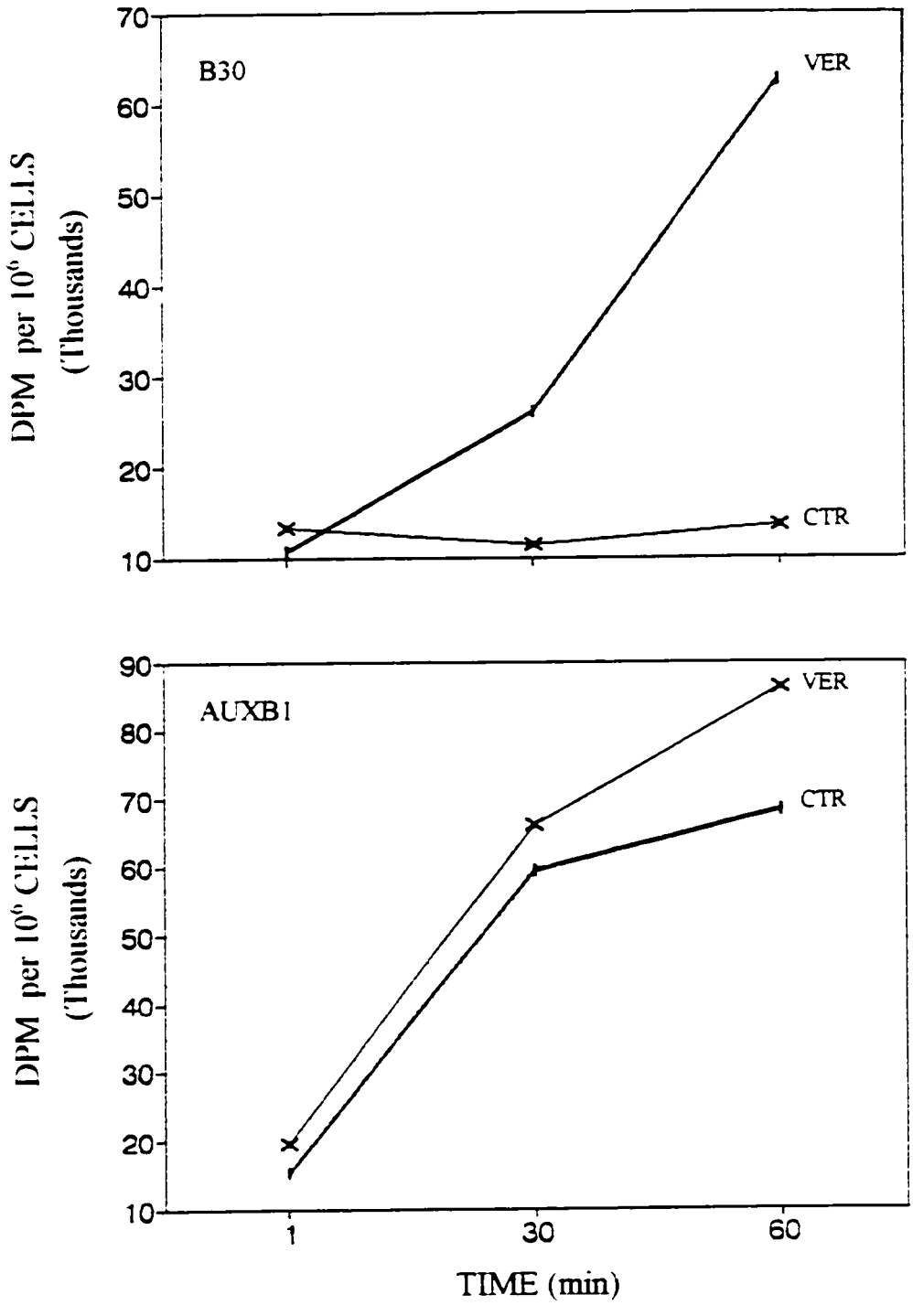

Figure 3.1: Differential Uptake of ^{3}H-vinblastine by B30 and AUXB1 Cells with the Known Inhibitor of the P-glycoprotein Pump, Verapamil (VER)

When tested at various concentrations, dillapiol was found to have a major effect on the net accumulation of ^{3}H-vinblastine in the multidrug-resistant hamster cells (B30) but only a limited effect on the sensitive AUXB1 cells (Figure 3.2). As the figure illustrates, the lower doses (9 nM and 18 nM) of dillapiol had a very minimal effect on the net uptake of parental AUXB1 cells but they increased ^{3}H-vinblastine uptake ten times in the resistant cells. This selective modulating effect of dillapiol on ^{3}H-vinblastine uptake is more rapid and obtained with much lower concentrations than with verapamil. After 15 min, the net accumulation of vinblastine in dillapiol-treated resistant cells is three times that of verapamil-treated cells.

None of the doses of dillapiol in the vinblastine uptake assays were toxic to AUXB1 cells. This is true until 500 ng/mL. On the other hand, B30 cells are killed with a much lower dose of dillapiol (0.5 ng/mL). Therefore dillapiol could be administered at a dose that is non toxic to normal cells yet is sufficient to reverse multidrug resistance. The other consequence of this selective toxicity is that the anticancer drug could be administered at a dose which does not produce unacceptable side effects.

At high doses of dillapiol (135 nM, data not shown), the retention of ^{3}H-vinblastine in the multidrug-resistant B30 cell pellet decreased after 30 min. According to Bernard, this seems to indicate an efflux of labeled material, possibly by cell lysis. This concentration of dillapiol was extremely toxic to B30 cells.

As mentioned earlier, collateral sensitivity of multidrug-resistant G185 cells to dillapiol could not be shown because of the limited solubility of dillapiol in the culture media. However, the increase of ^{3}H-vinblastine uptake in G185 cells with dillapiol

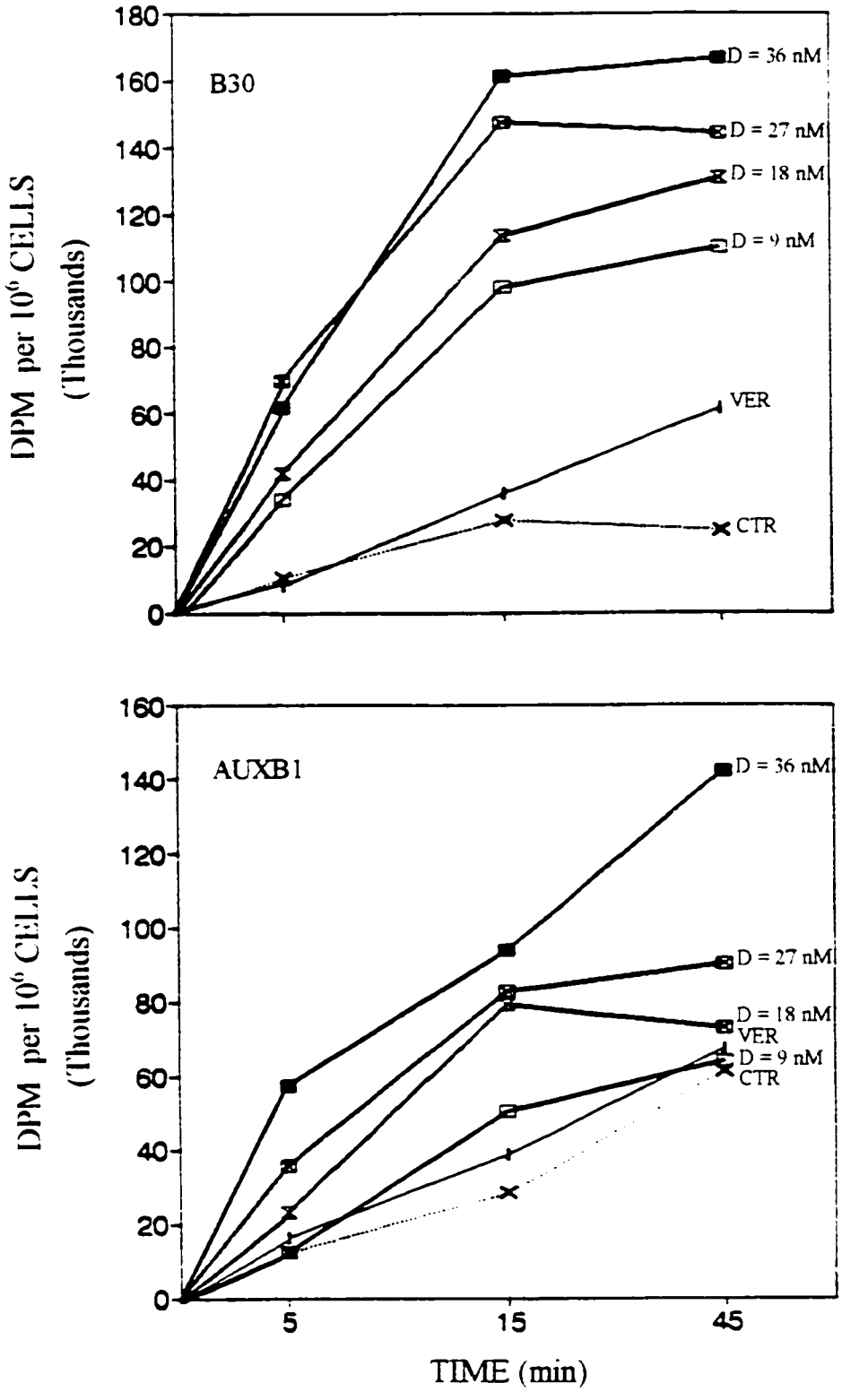

Figure 3.2: Differential Uptake of ^{3}H-vinblastine by B30 and AUXB1 Cells with 160 μM of Verapamil (VER) and Various Concentrations of Dillapiol (D)

effect on vinblastine uptake in multidrug-resistant G185 cells (six-fold increase). A similar response was observed with piperonyl butoxide and five of the synthetic derivatives of dillapiol (**52-56**).

Among the derivatives tested for vinblastine uptake (**52-56**), **53**, **54**, and **56** displayed the highest degree of collateral sensitivity (Figure 3.3). Derivative **54** was the most active of the three and is also the most polar. Ester **56** is the least polar and displayed the lowest activity. Although for these compounds polarity parallels activity, this is not true for dillapiol which is even less polar than derivative **56** yet is considerably more active. Obviously, polarity alone can not explain the superior modulating effect of dillapiol. A study of ^{3}H-vinblastine uptake with a larger library of dillapiol derivatives should help shed some light on the structural elements needed for increased collateral sensitivity.

Dillapiol and piperonyl butoxide are known inhibitors of PSMOs. Although an elevation of the level or activity of the PSMOs possibly limiting the metabolism of vinblastine can not be ruled out in drug-selected multidrug-resistant B30 cells, the G185 cells transfected with the multidrug resistance phenotype should not be expected to experience altered levels of the intracellular enzymes. This leaves the possibility that dillapiol and its derivatives act on the cell membrane.

The fact that dillapiol is an inhibitor of PSMOs and acts preferentially on multiresistant cells with a high expression of P-glycoprotein, both point at a possible role of dillapiol as antagonist of resistance mechanisms. The co-evolution of insects and plants may have favored the selection of lignans in plants to act on particular mechanisms related to resistance in insects. Future research may reveal the potential of such compounds in the major area of management of insect pests.

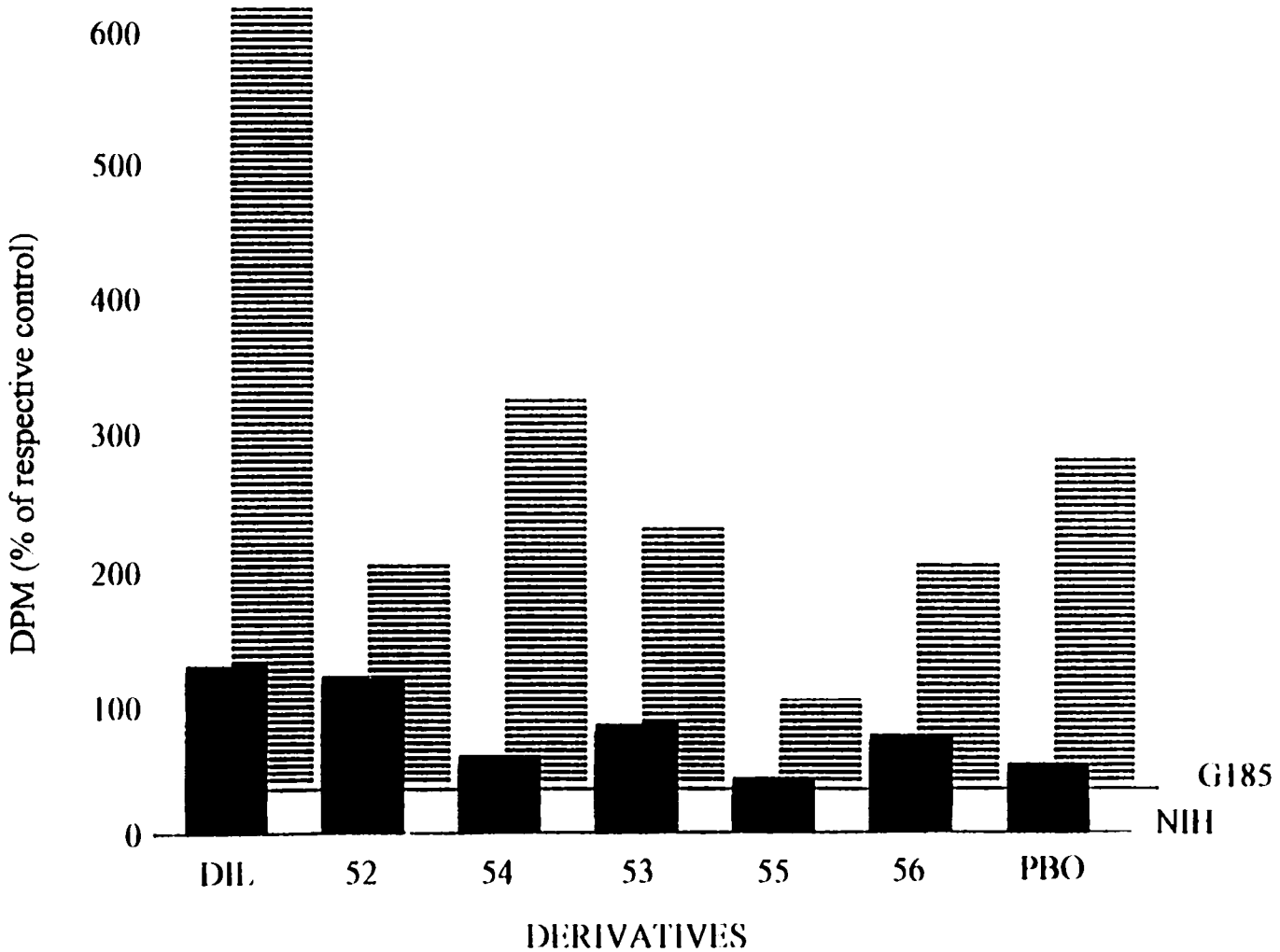

Figure 3.3: Differential Uptake of ^{3}H-vinblastine by NIH and G185 Cells after 60 Minutes of Incubation with 65 nM of Piperonyl Butoxide (PBO), 65 nM of Dillapiol (DIL) and 150 nM of Dillapiol Derivatives **52** to **56**

3.4 Toxicity and Drug-Fate Studies of Dillapiol

The presence of dillapiol in several widely consumed food substances (dill, celery seeds) seems to indicate a low dietary toxicity. Although this constitutes a promising starting point for its development as a safe chemosensitizer, its toxicity to mammals must be determined with certainty before it can be considered for the treatment of cancer. The results of a preliminary study done by Dr Claude Bernard[96] on the toxicity and fate of dillapiol in the Sprague-Dawley rat are presented and discussed briefly in the following paragraphs.

The toxicity results were quite positive. All rats survived after being administered a dose of dillapiol that is considered to be 10x the proposed therapeutic dose. The rats also displayed no negative effects with respect to weight changes or behavior. Finally, histological examination of the brain, liver, heart, kidney and lungs revealed no abnormalities.

In addition to its toxicity, it was important to determine the distribution of dillapiol among the various organs of the Sprague-Dawley rat. This required the preparation of ^{14}C-dillapiol. The synthesis involved adding 1 eq. of a mixture of $^{14}CH_3I$ and unlabeled CH_3I to a solution of phenol **26** in acetone at RT for 2 d. A single dose I.V. of 0.5 mg/kg of labeled material resulted in the distributions shown in Figure 3.4. As the chart indicates, the radiolabeled material is concentrated mainly in the liver, kidney and gut. Very little, if any, enters the brain. The detection of a large amount of radioactivity in the kidney indicated that the majority of dillapiol would be excreted in the urine. This was the

desired result. Confirmation was obtained after daily analysis of the urine and feces. After 3 d, essentially all of the labeled material had been excreted via the urine (Figure 3.5); only a trace of dillapiol was detected in the feces.

Analysis of the excreted material by TLC revealed several spots, none of which corresponded to dillapiol. The R_f of the spots indicated that dillapiol had been metabolized to more polar compounds before being excreted. None of these compounds have yet been identified.

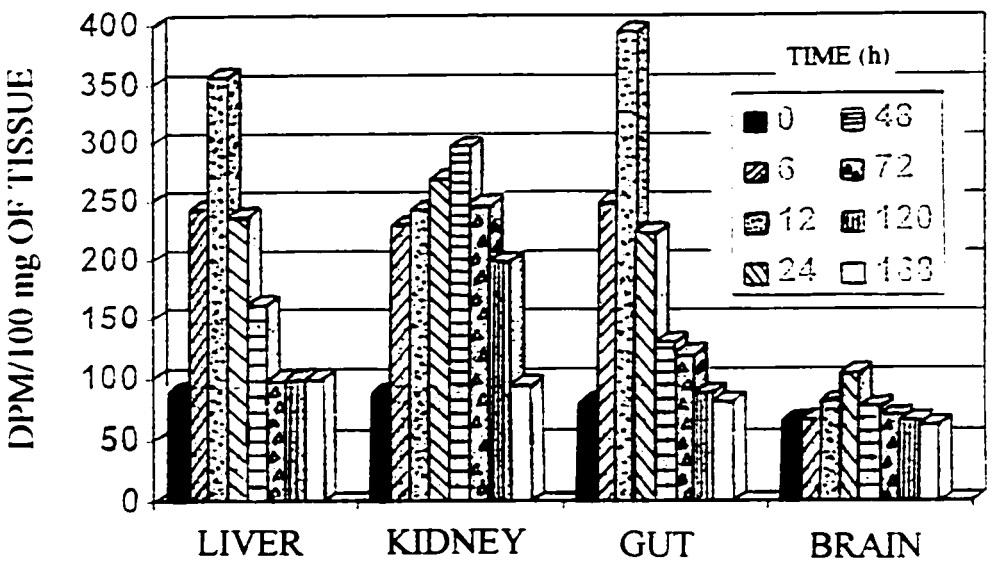

Figure 3.4: Distribution of ^{14}C-Dillapiol in the Sprague-Dawley Rat

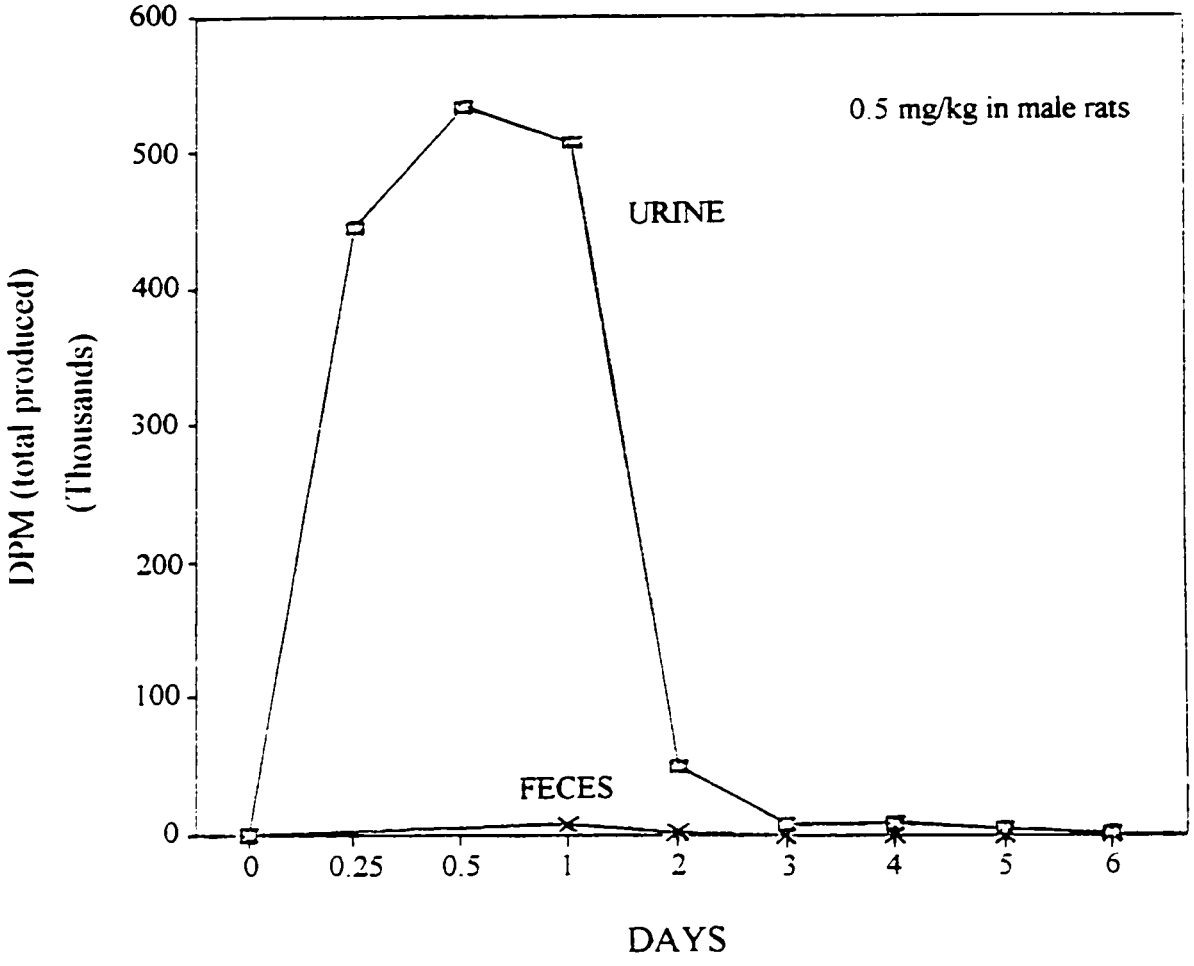

Figure 3.5: Elimination of ^{14}C-Dillapiol in the Feces and Urine

CHAPTER 4

INVESTIGATION OF THE SYNERGISTIC ACTIVITY OF DILLAPIOL AND ITS DERIVATIVES ON *Aedes atropalpus* Coq. LARVAE

4.1 Introduction

Among the various insecticides that are used for controlling insect populations, thiophenes have revealed themselves to be very potent against mosquito larvae[67]. When light activated, these compounds, in particular α-terthienyl (α-T, **57**), produce singlet oxygen which causes the peroxidation of phospholipids and the oxidation of enzymes and other proteins[68]. As with any insecticide, these compounds face the risk of becoming inefficient due to the development of multi-resistance by insects. As discussed in Chapter 1, one strategy for reversing multi-resistance is to inhibit the enzymes (PSMOs) responsible for transforming the toxic lipophilic compounds into excretable hydrophilic substances. This strategy has been successful for many commercial insecticides including pyrethrins, carbamates and organophosphates for which dillapiol served as the inhibitor[8,9].

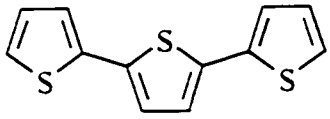

57

As a result of the success that has been achieved with dillapiol in reversing multi-resistance in insects, an investigation of its activity towards α-T was undertaken. Several of its derivatives were also tested in the hopes of enhancing its effectiveness.

4.2 Synergistic Insecticidal Effect of Dillapiol and its Derivatives on α-T

The toxicity tests, presented briefly below, represent the work done by two students at the University of Ottawa. Investigation of the synergistic effect of dillapiol, along with derivatives **36**, **49** and **52-55** was carried out by undergraduate student Catherine Podeszfinski[69]. Derivatives **37**, **40**, **41**, **43**, **44** and **48** were tested at a later date by MSc student Anne-Sophie Belzile using the same protocol[2].

When administered at a concentration of 800 ppb, neither dillapiol nor its derivatives were toxic to the mosquito larvae. However, when combined with α-T, LC_{50}s between 41 and 65 ppb were observed (Table 4.1). Dillapiol, **48** and **36** were the most efficient in increasing the toxicity of α-T with synergism factors of 1.9, 1.8 and 1.7, respectively. With the exception of derivatives **53** and **54**, all other derivatives displayed moderate synergistic activity. Alcohols **53** and **54** did not have any effect on α-T toxicity as indicated by their synergism factors.

In general, the alcohols were poorer synergists of α-T than the ethers. Although this suggests that molecules of lower polarity are less effective, dillapiol, which is less polar than derivative **48**, had a higher synergism factor. Since these two compounds only differ in the size of the alkyl chain attached to the oxygen at C-3, it may be possible that the bulk of the substituent plays a role in determining the synergistic ability of a compound. A quantitative structure-activity relationship (QSAR) study was carried out in order to gain further insight on the link between structure and α-T toxicity.

---

2. As with Chapter 3, these results are included in order to give a more complete picture of the potential importance of dillapiol and its analogs.

Table 4.1: Lethal Concentrations of α-T on Mosquito Larvae and the Synergism Factors for Dillapiol and its Derivatives

Compound	LC_{50} (ng/g)	Synergism factor
α-T + Dillapiol	41	1.9
α-T + **36**	45	1.7
α-T + **37**	61	1.3
α-T + **40**	60	1.3
α-T + **41**	49	1.6
α-T + **43**	65	1.2
α-T + **44**	64	1.2
α-T + **48**	44	1.8
α-T + **49**	63	1.2
α-T + **52**	53	1.5
α-T + **53**	86	0.9
α-T + **54**	85	0.9
α-T + **55**	50	1.6
α-T	78	----

4.3 Quantitative Structure-Activity Relationships of Dillapiol Derivatives

Due to time constraints and the availability of derivatives, only dillapiol and **36**, **49** and **52-55** were used in this QSAR study. The results presented below can be found in the 1996 undergraduate thesis of Catherine Podeszfinski[69], University of Ottawa.

4.3.1 Partition coefficients

Prior to calculating octanol/water partition coefficients (P) for dillapiol and its derivatives, four standards with known partition coefficients were eluted through a reverse-phase HPLC column from which their capacity factors (K') were determined (Table 4.2). Subsequent regression analysis of the plot of the logarithm of the partition coefficient versus the logarithm of the capacity factor for these four standards (Figure 4.1) afforded the equation

$$\log P = 2.327(\log K') + 2.689 \quad (r^2 = 0.958) \qquad (1)$$

This relationship between lipophilicity and the capacity factor was then used to determine octanol/water partition coefficients for dillapiol and its derivatives (Table 4.2)

Table 4.2: Capacity Factors and Octanol/Water Partition Coefficients of Four Standards, Dillapiol and its Derivatives

Compound	Log of the capacity factor (logK')	Log of the octanol/water partition coefficient (logP)
Metalaxyl	-0.186	1.270
Monuron	-0.207	1.950
Diuron	0.046	2.890
p,p'-DDT	1.367	5.940
Dillapiol	0.341	3.498
36	0.280	3.352
49	0.569	4.037
52	0.418	3.679
53	-0.408	1.722
54	-0.383	1.781
55	0.013	2.720

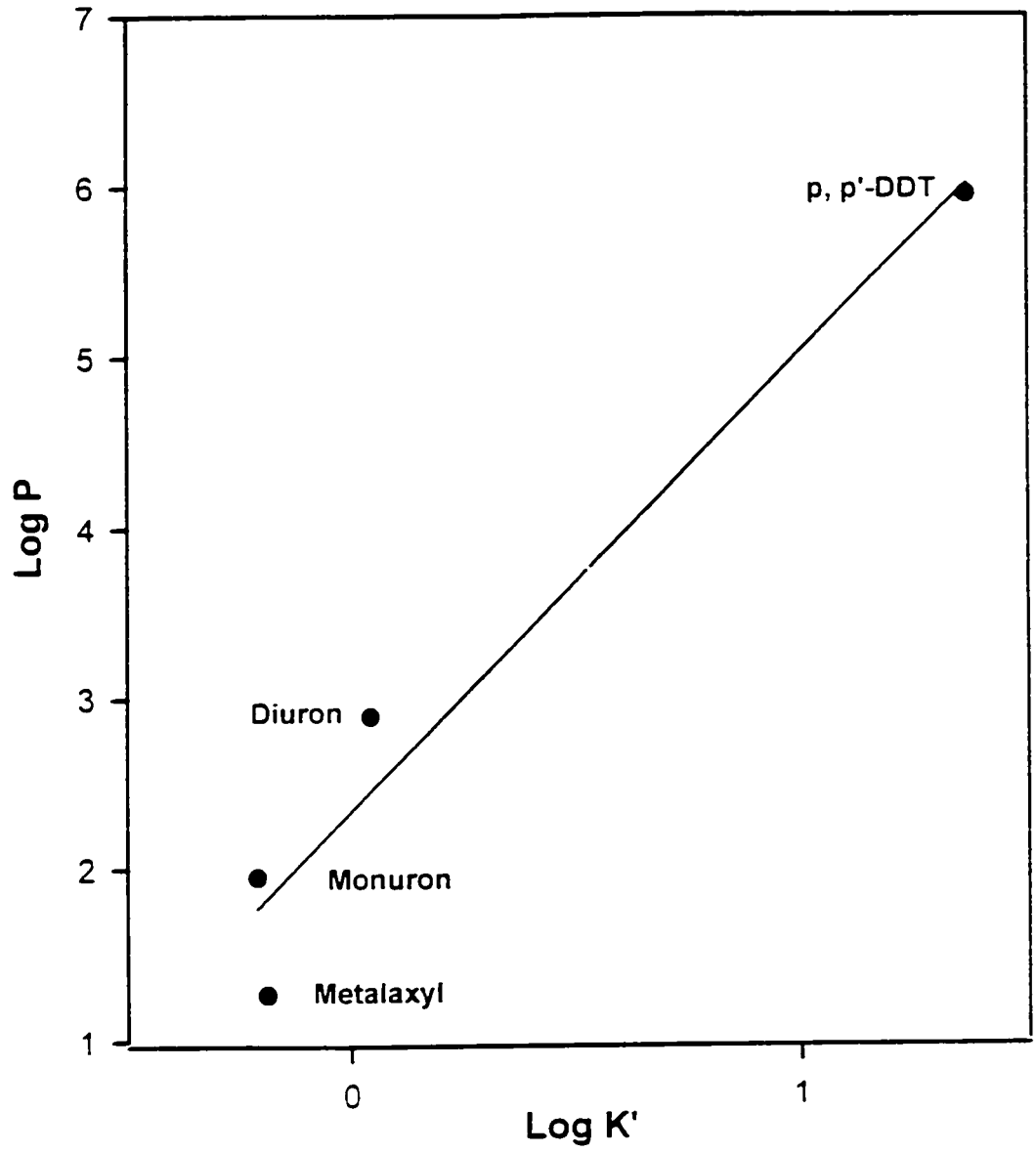

Figure 4.1: Relationship between the Octanol/Water Partition Coefficient and Capacity Factor of Four Standards

4.3.2 Relationship between α-T toxicity and the partition coefficient of dillapiol and its derivatives

Previous work done by Marles and coworkers[70] showed that the lipophilicity of α-T derivatives correlated with their phototoxic properties. The different combinations of α-T and dillapiol derivatives showed the same kind of response (Figure 4.2). A plot of the

logarithm of $1/LC_{50}$ versus the logarithm of the octanol/water partition coefficients showed that a parabolic relationship exists between α-T toxicity and the lipophilicity of the various derivatives (Figure 4.2, equation 2).

$$\log (1/LC_{50}) = - 0.198 (\log P)^2 + 1.194 \log P - 3.411 \qquad (r^2 = 0.945) \qquad (2)$$

This parabolic relationship indicates that the toxicity of α-T will continue to increase up to a maximum octanol/water partition coefficient. Any deviation from this optimal value

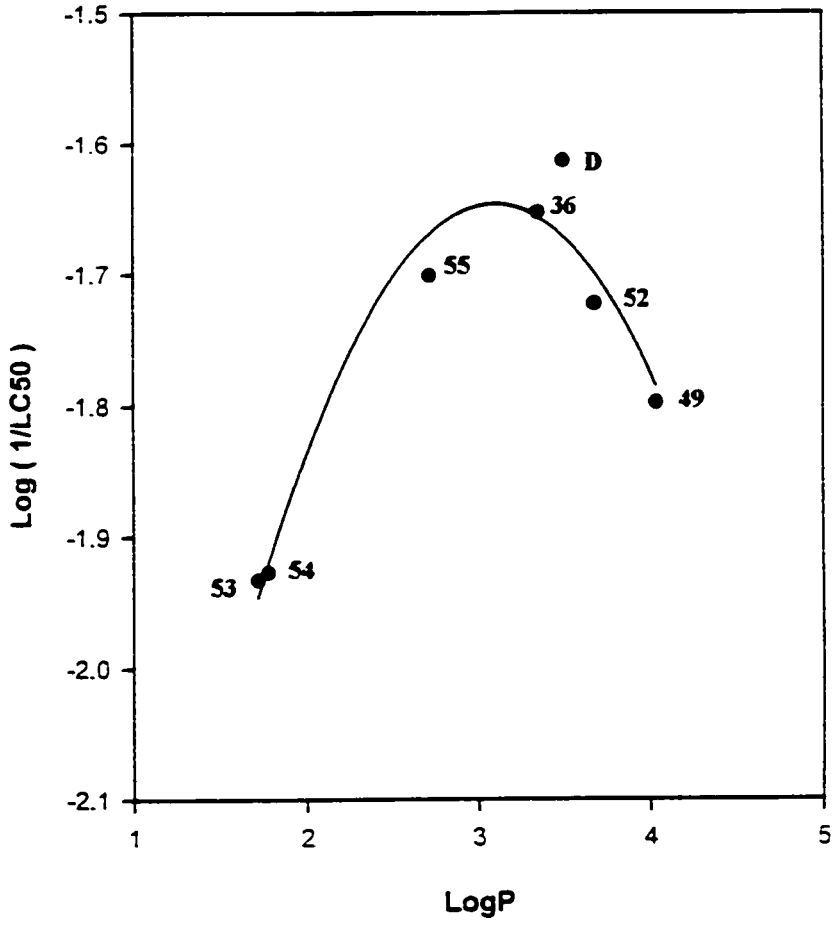

Figure 4.2: Relationship between α-T Toxicity and the Partition Coefficient of Dillapiol and its Derivatives

will ultimately lead to lower synergism factors and possibly even to an activity below that of α-T alone as in the case of **53** and **54**. Similar results were reported by Tomar and coworkers in a study of the synergistic activity of dillapiol and other lignans on carbaryl[25]. This study did not, however, involve the modern bilinear model as does the present study. The bilinear relationship between toxicity and lipophilicity can become an important tool to predict the synergistic effect of a compound.

4.3.3 Relationship between the retention of α-T in insects and its toxicity

As with any insecticide, a higher retention of α-T in the larval tissues should translate into greater toxicity. It is not surprising then, that a significant linear regression (r^2 = 0.808) was found between the toxicity of this insecticide and its retention in the larvae (Figure 4.3).

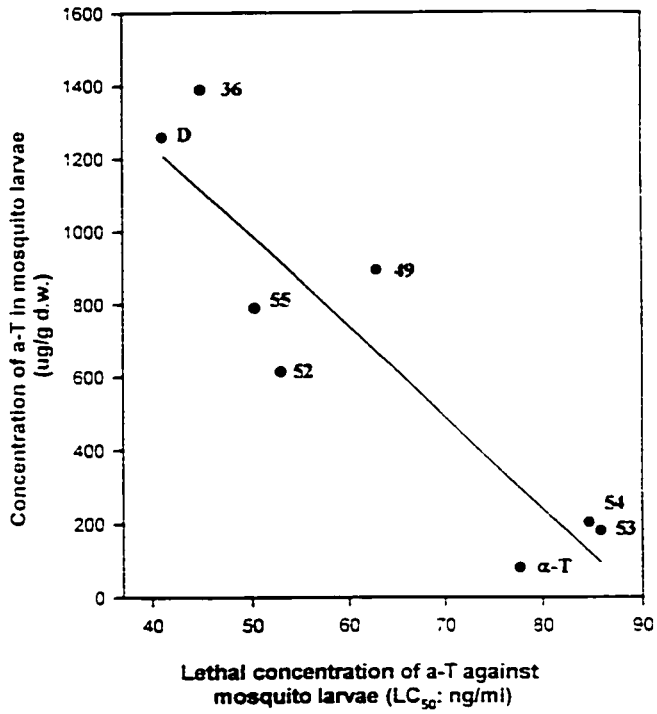

Figure 4.3: Relationship between the Retention of α-T in Mosquito Larvae and its Toxicity

4.3.4 Relationship between the retention of α-T in mosquito larvae and the partition coefficient of dillapiol and its derivatives

Since a relationship exists between the retention of α-T in the larvae and its toxicity, and between lipophilicity and α-T toxicity, , it seemed logical to assume that a significant relationship would also be found between the retention of α-T in the larvae and the octanol/water partition coefficient of dillapiol and its derivatives. Not surprisingly, this proved to be the case. A high correlation was found between these two variables.

$$\log [\alpha\text{-T}] = - 0.395 \log P^2 + 2.509 \log P - 0.865 \quad (r^2 = 0.891) \qquad (3)$$

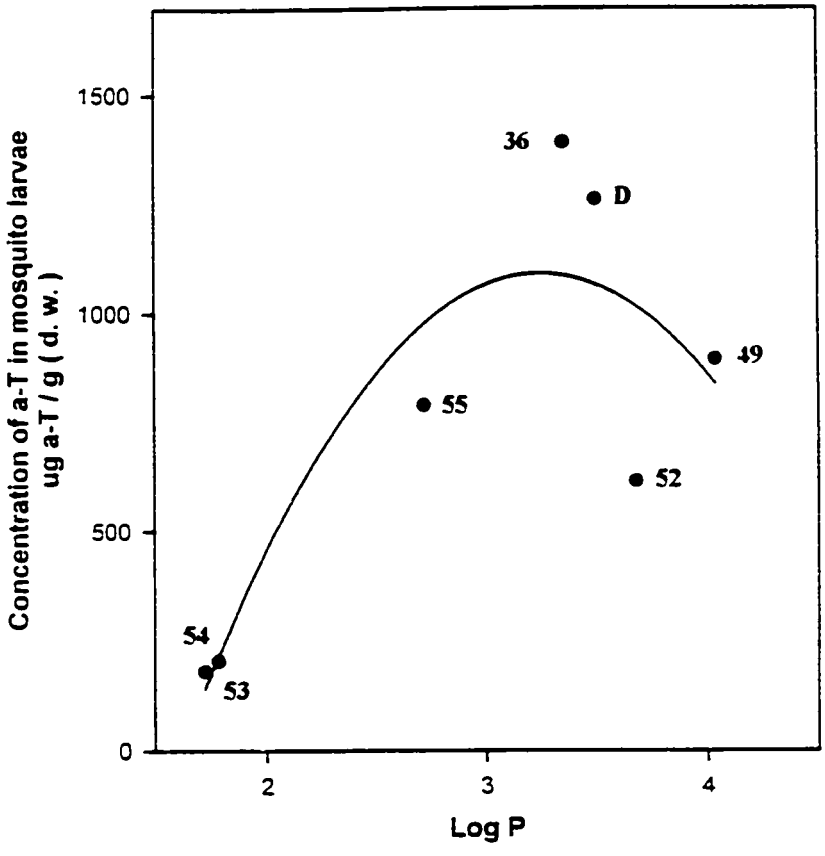

Figure 4.4: Relationship between the Retention of α-T in Mosquito Larvae and the Partition Coefficient of Dillapiol and its Derivatives

CHAPTER 5

EXPERIMENTAL

5.1 Synthesis of Dillapiol and its Derivatives

General

All reactions were carried out in flame-dried glassware that had been cooled under a stream of nitrogen. Melting points were determined with a Fisher-Johns Unimelt melting point apparatus and are uncorrected. Infrared spectra were recorded with a Bomem MB 101 FT-IR spectrometer with solution cells using reagent grade methylene chloride as solvent. Proton and carbon nuclear magnetic resonance spectra were recorded in deuterated chloroform on a Bruker AMX 500 operating at a frequency of 500 MHz for proton and 125 MHz for carbon. Chemical shifts are in parts per million relative to tetramethylsilane. Multiplets are reported as s, singlet; d, doublet; dd, doublet of doublets; ddd, doublet of doublet of doublets; dt, doublet of triplets; t, triplet; q, quartet; and m, multiplet. Low and high resolution mass spectra were recorded on a VG 7070 Mass Spectrometer. MS peak intensities are reported as a percent of the base peak.

Flash column chromatography was performed using 230–400 mesh silica gel supplied by Terochem Laboratories in the solvent system specified. All solvents were routinely dried and distilled prior to use. All starting materials were used as received from Aldrich Chemical Co..

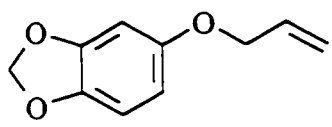

21

To a solution of sesamol (15 g, 0.109 mol) and freshly distilled allyl bromide (12.0 mL, 0.139 mol) in acetone (110 mL) was added anhydrous K_2CO_3 (20 g, 0.145 mol). The resulting mixture was stirred at reflux for 23 h. After cooling the mixture to RT, the solvent was concentrated in vacuo. The remaining K_2CO_3 was dissolved in water and the aqueous phase extracted with Et_2O (3 x 40 mL). The combined organic extracts were dried over Na_2SO_4, filtered and concentrated to provide **21** as an orange liquid (19.48 g, >99%). The spectral data for this compound matched those given in the literature[46].

^{1}H NMR: δ 4.44 (dt, 2H, J = 5.3, 1.5 Hz), 5.25 (dd, 1H, J = 10.5, 1.4 Hz), 5.37 (ddt, 1H, J = 17.3, 1.6, 1.5 Hz), 5.89 (s, 2H), 5.98-6.04 (m, 1H), 6.32 (dd, 1H, J = 8.5, 2.5 Hz), 6.50 (d, 1H, J = 2.5 Hz), 6.68 (d, 1H, J = 8.5 Hz)

^{13}C NMR: δ 69.8, 98.3, 101.1, 106.1, 107.9, 117.6, 133.4, 141.7, 148.2, 154.1

EI-MS (m/z, %): 178(M^+, 40), 137(100), 107(40)

HRMS: Calc. for $C_{10}H_{10}O_3$: 178.0630; Found: 178.0632

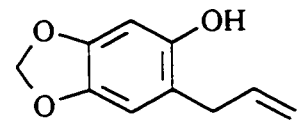

22

A solution of allyl ether **21** (12.77 g, 0.072 mol) in N,N-dimethylaniline (19 mL) was heated at 190 °C for 2.5 h by means of an oil bath and then cooled to RT. The solution was diluted with Et_2O (15 mL) and washed several times with 1N NaOH. The alkaline extract was acidified with concentrated HCl and the aqueous phase extracted with Et_2O (3 x 40 mL). The combined organic extracts were dried over $MgSO_4$, dried, filtered, and concentrated in vacuo. The crude residue was purified by flash chromatography (5:1 Hex:EtOAc) to provide the product **22** as colorless needles (10.29 g, 81%). The physical and spectral data matched those cited in the literature[46].

^{1}H NMR: δ 3.29 dt, 2H, J = 6.3, 1.5 Hz), 4.64 (s, 1H), 5.11-5.15 (m, 2H), 5.86 (s, 2H), 5.92-5.97 (m, 1H), 6.41 (s, 1H), 6.56 (s, 1H)

^{13}C NMR: δ 35.0, 98.7, 101.0, 109.5, 116.4, 116.9, 136.4, 141.5, 146.7, 148.6

IR: 3563 cm^{-1}

EI-MS(m/z, %): 178 (M^+, 100), 151 (30)

HRMS: Calc. for $C_{10}H_{10}O_3$: 178.0630; Found: 178.0625

mp: 74-76°C

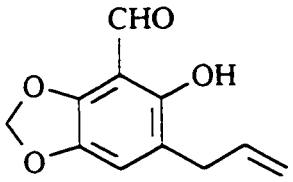

23

To a three-neck flask equipped with a reflux condenser, thermometer, and a nitrogen source was added anhydrous toluene (5.6 mL), **22** (1.5 g, 8.42 mmol), tin tetrachloride (0.1 mL, 0.84 mmol), and tri-n-butylamine (0.8 mL, 3.37 mmol). The reaction mixture was stirred at RT for 20 min and then paraformaldehyde (0.56 g, 18.52 mmol) was added. The resulting yellowish solution was heated for 8 h at 100 °C. After cooling to RT, the reaction mixture was poured into water (25 mL), acidified to pH 2 with 2N HCl and extracted with ether. The ether extracts were dried over $MgSO_4$, filtered and concentrated. The crude residue was purified by flash chromatography (1:1 Hex:CH_2Cl_2) and the product was obtained as a bright yellow solid (1.05 g, 60%).

^{1}H NMR: δ 3.27-3.29 (m, 2H), 5.03-5.07 (m, 2H), 5.86-5.94 (m, 1H), 6.00 (s, 2H), 6.87 (s, 1H), 10.09 (s, 1H), 10.65 (s, 1H)

^{13}C NMR: δ 32.8, 102.5, 106.7, 116.0, 117.6, 119.0, 136.1, 140.1, 148.5, 152.3, 191.3

IR: 1658, 3215 cm^{-1}

EI-MS (m/z, %): 206 (M^+, 100)

HRMS: Calc. for $C_{11}H_{10}O_4$: 206.0579; Found: 206.0568

mp: 68-70 °C

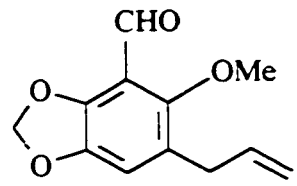

24

Potassium carbonate (1.31 g, 9.45 mmol) and methyl iodide (3.92 mL, 63.0 mmol) were added sequentially to a solution of aldehyde **23** (1.30 g, 6.30 mmol) in acetone (10 mL). The resulting solution was allowed to stir at RT for 48 h, after which time the solvent was evaporated in vacuo. The remaining K_2CO_3 was dissolved in water and the aqueous phase extracted with Et_2O (3 x 15 mL). The combined organic extracts were dried over Na_2SO_4, filtered and concentrated affording, after flash chromatography (5:1 Hex:EtOAc), the desired product as a pale yellow solid (1.35 g, 97%).

^{1}H NMR: δ 3.32 (dt, 2H, J = 6.4, 1.5 Hz), 3.77 (s, 3H), 5.03-5.08 (m, 2H), 5.86-5.91 (m, 1H), 6.05 (s, 2H), 6.83 (s, 1H), 10.23 (s, 1H)

^{13}C NMR: δ 33.0, 64.1, 102.9, 114.2, 114.7, 116.4, 125.7, 136.5, 144.9, 146.9, 153.6, 188.1

IR: 1689 cm^{-1}

EI-MS (m/z, %): 220 (M^+, 100)

HRMS: Calc. for $C_{12}H_{12}O_4$: 220.0736; Found: 220.0754

mp: 101-102 °C

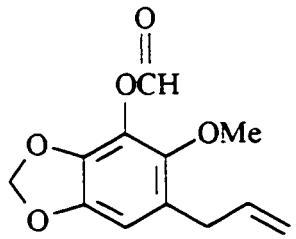

25

To a cooled (0 °C) solution of aldehyde **24** (210 mg, 0.95 mmol) in dry $CHCl_3$ (6 mL) was added in one portion mCPBA (0.30 g, 0.95 mmol, 55%). After 18 h, the reaction mixture was allowed to reach RT and washed with sodium sulfite (sat., 2 x 10 mL), sodium bicarbonate (sat., 1 x 10 mL) and water (1 x 10 mL). The extract was dried over Na_2SO_4, filtered and evaporated to dryness. The resulting oily residue was purified by flash chromatography (3:1 Hex/EtOAc) affording **25** as a colorless oil (160 mg, 71%).

^{1}H NMR: δ 3.32 (d, 2H, J = 6.5 Hz), 3.69 (s, 3H), 5.03-5.06 (m, 2H), 5.86-5.93 (m, 1H), 5.94 (s, 2H), 6.56 (s, 1H), 8.26 (s, 1H)

^{13}C NMR: δ 33.6, 61.8, 102.3, 107.0, 116.1, 126.3, 126.8, 136.8, 138.0, 144.6, 144.8, 157.9

IR: 1759 cm^{-1}

EI-MS (m/z, %): 236 (M^+, 100), 208 (73), 163 (79)

HRMS: Calc. for $C_{12}H_{12}O_5$: 236.0685; Found: 236.0690

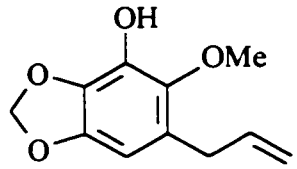

26

To a solution of **25** (250 mg, 1.06 mmol) in THF (9 mL) was added 1 mL of a 3N NaOH solution. The resulting homogeneous solution was stirred at RT for 1 h and diluted with brine. After separating the organic layer, the aqueous layer was acidified with 2N HCl and extracted with CH_2Cl_2 (3 x 10 mL). The combined organic extracts were dried over $MgSO_4$, filtered, and evaporated to dryness affording phenol **26** as a pale yellow solid (180 mg, 82%).

^{1}H NMR: δ 3.31 (dt, 2H, J = 6.5, 1.4 Hz), 3.73 (s, 3H), 5.03-5.07 (m, 2H), 5.50 (s, 1H), 5.87-5.93 (m, 1H), 5.90 (s, 2H), 6.25 (s, 1H)

^{13}C NMR: δ 33.6, 61.8, 101.0, 101.7, 115.9, 125.2, 132.7, 133.5, 137.0, 141.1, 144.9

IR: 3523 cm^{-1}

EI-MS (m/z, %): 208 (M^+, 98), 163 (40), 84 (63), 49 (100)

HRMS: Calc. for $C_{11}H_{12}O_4$: 208.0736; Found: 208.0740

mp: 61-63 °C

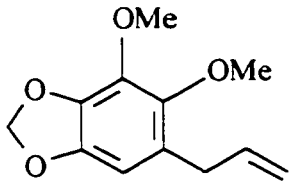

7

To a stirred solution of phenol **26** (100 mg, 0.48 mmol) in acetone (5 mL) was added an equimolar amount of MeI (28.6 μL) and K_2CO_3 (0.1 g, 0.72 mmol). The resulting mixture was vigorously stirred at RT for 72 h, after which time the solvent was concentrated. Water (5 mL) was added to the crude residue and the aqueous phase was extracted with Et_2O (3 x 5 mL). The combined organic extracts were dried over Na_2SO_4, filtered and concentrated. Flash chromatography (5:1 Hex:EtOAc) provided the desired product 7 as a colorless oil (80 mg, 78%). The physical and spectral data for this compound matched those given in the literature[44].

^{1}H NMR: δ 3.29 (dt, 2H, J = 6.5, 1.4 Hz), 3.74 (s, 3H), 3.99 (s, 3H), 5.00-5.05 (m, 2H), 5.86 (s, 2H), 5.85-5.93 (m, 1H), 6.33 (s, 1H)

^{13}C NMR: δ 33.9, 60.0, 61.3, 101.1, 102.8, 115.5, 126.1, 136.0, 137.4, 137.7, 144.4, 144.6

EI-MS (m/z, %): 222 (M^+, 100), 177 (39)

HRMS: Calc. for $C_{12}H_{14}O_4$: 222.0892; Found: 222.0874

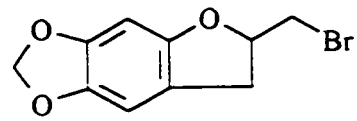

36

Bromine (0.21 mL, 4.1 mmol) was added over 5 min to a cooled (-20 to -30 °C) mixture of t-butylamine (0.50 mL, 4.8 mmol) and dry toluene (15 mL). The solution was then cooled to -78 °C at which time 0.36 g (2.0 mmol) of phenol **22** dissolved in toluene (5 mL) was added. The resulting solution was allowed to warm to RT over 6 h, then diluted with hexane (50 mL) and washed with water (4 x 50 mL). The organic phase was dried over $MgSO_4$, filtered, and evaporated to dryness. Purification of the crude residue by flash chromatography (5:1 Hex:EtOAc) provided **36** as a yellow oil (0.49 g, 95%).

^{1}H NMR: δ 3.00 (dd, 1H, J = 15.6, 6.5 Hz), 3.27 (dd, 1H, J = 15.5, 9.2 Hz), 3.47 (dd, 1H, J = 10.4, 6.8 Hz), 3.56 (dd, 1H, J = 10.4, 5.2 Hz), 4.94–4.99 (m, 1H), 5.86 (s, 2H), 6.36 (s, 1H), 6.61 (s, 1H)

^{13}C NMR: δ 34.5, 34.6, 82.0, 93.1, 101.2, 105.0, 116.3, 141.8, 147.4, 153.6

EI-MS (m/z, %): 258 (M^++2, 71), 256 (M^+, 72), 147 (100), 119 (60)

HRMS: Calc. for $C_{10}H_9O_3Br$: 255.9735; Found: 255.9729

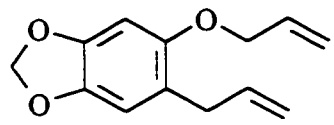

37

To a solution of phenol **22** (300 mg, 1.68 mmol) in acetone (2 mL) were added K_2CO_3 (0.35 g, 2.52 mmol) and allyl bromide (0.19 mL, 2.14 mmol). The resulting mixture was vigorously stirred at reflux for 21.5 h. After this time, the mixture was cooled to RT and the solvent was evaporated in vacuo. Water (5 mL) was added and the aqueous phase extracted with Et_2O (3 x 5 mL). The combined organic extracts were washed with 1N NaOH, dried over Na_2SO_4, filtered, and evaporated to dryness. Purification by flash chromatography (5:1 Hex:EtOAc) provided **37** as a yellow liquid (329 mg, 90%).

^{1}H NMR: δ 3.31 (dt, 2H, J = 6.6, 1.2 Hz), 4.44 (dt, 2H, J = 5.1, 1.6 Hz), 5.00-5.05 (m, 2H), 5.24 (dd, 1H, J = 10.6, 1.5 Hz), 5.39 (dd, 1H, J = 17.3, 1.6 Hz), 5.87 (s, 2H), 5.90-6.04 (m, 2H), 6.49 (s, 1H), 6.64 (s, 1H)

^{13}C NMR: δ 34.1, 70.3, 96.5, 101.0, 109.6, 115.3, 117.1, 121.5, 133.6, 137.2, 141.3, 146.2, 151.0

EI-MS (m/z, %): 218 (M^+, 50), 177 (42), 147 (100), 119 (50)

HRMS: Calc. for $C_{13}H_{14}O_3$: 218.0943; Found: 218.0930

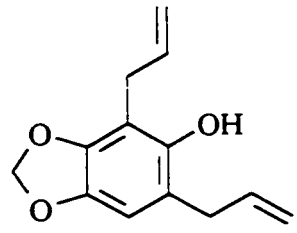

38

A solution of allyl ether **37** (4.51 g, 20.7 mmol) in N,N-dimethylaniline (10 mL) was heated at 190 °C for 2.5 h. After this time, the solution was cooled to RT, diluted with Et_2O (10 mL) and shaken several times with 1N NaOH. The alkaline extract was acidified with concentrated HCl and the aqueous phase extracted with Et_2O (3 x 20 mL). The combined organic extracts were dried over $MgSO_4$, filtered, and concentrated. The crude residue was purified by flash chromatography (5:1 Hex: EtOAc) to give the desired product **38** as a yellow liquid (1.8 g, 40%).

^{1}H NMR: δ 3.29 (dtd, 2H, J = 6.4, 1.6, 0.3 Hz), 3.38 (dt, 2H, J = 6.1, 1.6 Hz), 4.82 (s, 1H), 5.09-5.15 (m, 4H), 5.86 (s, 2H),5.91-6.02 (m, 2H), 6.49 (s, 1H)

^{13}C NMR: δ 28.5, 35.2, 100.8, 107.5, 109.4, 116.1, 116.1, 117.4, 135.4, 136.7, 140.8, 144.9, 147.3

IR: 3539 cm^{-1}

EI-MS (m/z, %): 218 (M^+, 100)

HRMS: Calc. for $C_{13}H_{14}O_3$: 218.0943; Found: 218.0955

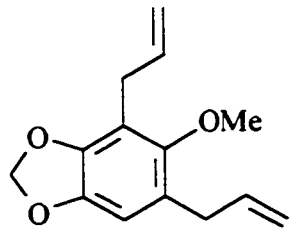

39

Potassium carbonate (3.17 g, 22.9 mmol) and MeI (2.85 mL, 45.8 mmol) were added sequentially to a solution of phenol **38** (1.00 g, 4.58 mmol) in acetone (15 mL). The resulting mixture was stirred vigorously at reflux for 60 h. After cooling the mixture to RT, the solvent was concentrated in vacuo. Water (15 mL) was added and the aqueous phase was extracted with CH_2Cl_2 (3 x 20 mL). The combined organic extracts were dried over Na_2SO_4, filtered, and concentrated. Purification of the crude residue by flash chromatography (5:1 Hex:EtOAc) afforded the desired product **39** as a yellow liquid (0.822 g, 77%).

^{1}H NMR: δ 3.33 (dt, 2H, J = 6.5, 1.5 Hz), 3.37 (dt, 2H, J = 6.1, 1.6 Hz), 3.66 (s, 3H), 5.02-5.07 (m, 4H), 5.88-6.03 (m, 2H), 5.89 (s, 2H), 6.54 (s, 1H)

^{13}C NMR: δ 28.8, 33.9, 62.0, 101.1, 107.4, 115.3, 115.5, 115.7, 125.3, 135.7, 137.5, 143.3, 144.9, 150.8

EI-MS (m/z, %): 232 (M^+, 100), 176 (50)

HRMS: Calc. for $C_{14}H_{16}O_3$: 232.1100; Found: 232.1083

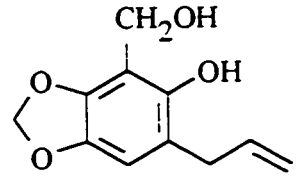

40

To a solution of aldehyde **23** (237.5 mg, 1.15 mmol) in EtOH (2.5 mL) was added $NaBH_4$ (44 mg, 1.16 mmol) at RT. The resulting colorless solution was stirred at this temperature for 40 min and then water (2 mL) was added. The aqueous phase was acidified with 2N HCl and extracted with EtOAc (3 x 10 mL). The combined organic extracts were dried over $MgSO_4$, filtered and concentrated to afford 255.7 mg of crude material. Purification by flash chromatography (1:1 Hex:EtOAc) provided the desired compound as a white crystalline solid (198 mg, 83%).

^{1}H NMR: δ 2.55 (s, 1H), 3.28 (dt, 2H, J = 6.5, 1.4 Hz), 4.81 (s, 2H), 5.05-5.10 (m, 2H), 5.83 (s, 2H), 5.91-5.96 (m, 1H), 6.53 (s, 1H), 6.85 (s, 1H)

^{13}C NMR: δ 34.2, 57.8, 101.0, 108.6, 108.9, 115.7, 118.3, 136.9, 140.4, 143.3, 148.4

IR: 3404, 3587 cm^{-1}

EI-MS (m/z, %): 208 (M^+, 26), 190 (100), 189 (50)

HRMS: Calc. for $C_{11}H_{12}O_4$: 208.0736; Found: 208.0736

mp: 82-84 °C

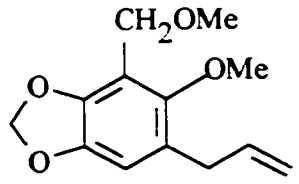

41

To a solution of **40** (296 mg, 1.33 mmol) in dry THF (5 mL) were added NaH (64 mg, 2.66 mmol) and MeI (0.41 mL, 6.65 mmol). After 22 h at reflux, the reaction mixture was cooled to RT, and the solvent was concentrated. Water (5 mL) was added and the organic phase extracted with CH_2Cl_2 (3 x 10 mL). The combined organic extracts were dried over Na_2SO_4, filtered, and evaporated to dryness affording, after flash chromatography (5:1 Hex:EtOAc), **41** as a yellow oil (230 mg, 73%).

^{1}H NMR: δ 3.31 (dt, 2H, J = 6.5, 1.5 Hz), 3.40 (s, 3H), 3.72 (s, 3H), 4.45 (s, 2H), 5.02-5.06 (m, 2H), 5.87-5.93 (m, 1H), 5.92 (s, 2H), 6.61 (s, 1H)

^{13}C NMR: δ 33.7, 58.3, 62.8, 64.3, 101.4, 109.3, 113.7, 115.7, 125.3, 137.3, 143.5, 145.8, 151.4

EI-MS (m/z, %): 236 (M^+, 93), 45 (100)

HRMS: Calc. for $C_{13}H_{16}O_4$: 236.1049; Found: 236.1038

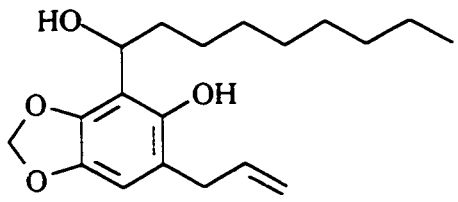

42

To a 2-neck flask fitted with a condenser and a nitrogen source were added magnesium turnings (0.07 g, 3.05 mmol). After flame-drying the apparatus, dry Et_2O (1 mL) and a crystal of iodine were added. A solution of 1-bromooctane (0.53 mL, 3.05 mmol) in the same solvent (1.5 mL) was then syringed dropwise into the flask. Since spontaneous reflux was not observed, the reaction mixture was slightly heated after 0.8 mL of the 1-bromooctane solution had been added. After all of the solution had been delivered, the mixture was further refluxed for 45 min, after which time a solution of aldehyde **23** (300 mg, 1.45 mmol) in dry Et_2O (2 mL) was added. After 1 h at reflux, the mixture was quenched with saturated NH_4Cl (5 mL), the organic phase was separated and the aqueous phase extracted with Et_2O (2 x 10 mL). The combined organic extracts were dried over $MgSO_4$, filtered and evaporated to dryness. Purification by flash chromatography (3:1 Hex:EtOAc) afforded **42** as a white solid (108 mg, 23%)

^{1}H NMR: δ 0.86 (t, 3H, J = 6.7 Hz), 1.24-1.33 (m, 11H), 1.41-1.46 (m, 1H), 1.75-1.81 (m, 1H), 1.85-1.91 (m, 1H), 2.54 (s, 1H), 3.23-3.33 (m, 2H), 5.02-5.07 (m, 3H), 5.79 (d, 1H, J = 1.3 Hz), 5.83 (d, 1H, J = 1.4 Hz), 5.91-5.99 (m, 1H), 6.52 (s, 1H), 7.65 (d, 1H, J = 4.5 Hz)

^{13}C NMR: δ 14.1, 22.6, 25.5, 29.2, 29.3, 29.5, 31.8, 33.9, 36.6, 70.4, 100.8, 108.4, 111.4, 115.4, 119.0, 137.1, 139.8, 142.6, 147.8

IR: 3372, 3586 cm^{-1}

EI-MS (m/z, %): 320 (M^{+}-H_2O, 100), 191 (53)

HRMS: Calc. for $C_{19}H_{28}O_4$: 320.1988; Found 320.1998

mp: 91-93 °C

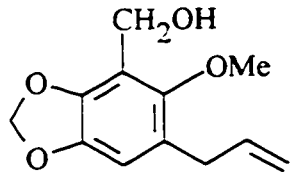

43

To a stirred solution of aldehyde **24** (350 mg, 1.59 mmol) in EtOH (3 mL) was added $NaBH_4$ (60.1 mg, 1.59 mmol) at RT. The resulting solution was stirred for 10 min. After diluting the reaction mixture with water, the aqueous phase was acidified with 2N HCl and extracted with EtOAc (3 x 10 mL). The combined organic phases were dried over $MgSO_4$, filtered, and evaporated to dryness. Purification of the crude material by flash chromatography (3:1 Hex:EtOAc) afforded the product as a yellow oil (264.5 mg, 75%).

^{1}H NMR: δ 2.45 (s, 1H), 3.30 (dt, 2H, J = 6.5, 1.4 Hz), 3.72 (s, 3H), 4.68 (s, 2H), 5.01-5.05 (m, 2H), 5.85-5.93 (m, 1H), 5.90 (s, 2H), 6.58 (s, 1H)

^{13}C NMR: δ 33.6, 55.7, 62.5, 101.4, 108.9, 115.9, 116.4, 125.4, 137.2, 143.7, 144.7, 150.8

IR: 3598 cm^{-1}

EI-MS (m/z, %): 222 (M^+, 100)

HRMS: Calc. for $C_{12}H_{14}O_4$: 222.0892; Found: 222.0906

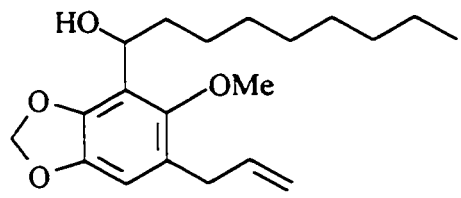

44

Alcohol **44** was prepared in a manner identical to that described for the preparation of **42**. The synthesis started with aldehyde **24** (308 mg, 1.40 mmol) which was converted into the desired product **44**, obtained as a yellow oil (304 mg, 65%) after purification by flash chromatography (3:1 Hex:EtOAc).

^{1}H NMR: δ 0.84-0.87 (m, 3H), 1.24-1.30 (m, 11H), 1.45-1.50 (m, 1H), 1.76-1.78 (m, 1H), 1.90-1.91 (m, 1H), 3.31 (dd, 2H, J = 6.4, 1.0 Hz), 3.70 (s, 3H), 4.88 (s, 1H), 5.02-5.06 (m, 2H), 5.87-5.93 (m, 1H), 5.91 (s, 2H), 6.56 (s, 1H)

^{13}C NMR: δ 14.1, 22.6, 26.1, 29.2, 29.5, 29.7, 31.9, 33.7, 37.6, 62.5, 68.3, 101.3, 108.4, 115.9, 120.8, 125.5, 137.2, 143.6, 143.9, 149.7

IR: 3588 cm^{-1}

EI-MS (m/z, %): 334 (M^+, 5), 316 (100), 190 (42), 43 (75)

HRMS: Calc. for $C_{20}H_{30}O_4$: 334.2145; Found: 334.2157

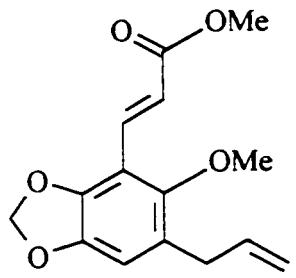

45

Methyl(triphenylphosphoranylidene)acetate (0.16 g 0.47 mmol) was added to a solution of aldehyde **24** (85.5 mg, 0.39 mmol) in toluene (2 mL) and the mixture was refluxed for 22 h. After this time, the mixture was cooled to RT and the solvent was removed under vacuum. Purification by flash chromatography (5:1 Hex:EtOAc) afforded the desired product **45** as a pale yellow solid (98.4 mg, 91%).

^{1}H NMR: δ 3.32 (dt, 2H, J = 6.5, 1.4 Hz), 3.69 (s, 3H), 3.79 (s, 3H), 5.03-5.07 (m, 2H), 5.87-5.93 (m, 1H), 6.00 (s, 2H), 6.66 (s, 1H), 6.78 (d, 1H, J = 16.3 Hz), 7.81 (d, 1H, J = 16.3 Hz)

^{13}C NMR: δ 33.6, 51.6, 62.7, 101.8, 110.7, 112.3, 116.0, 121.8, 125.5, 135.0, 137.0, 143.9, 145.6, 151.2, 167.9

IR: 1713 cm^{-1}

EI-MS (m/z, %): 276 (M^+, 100), 245 (41)

HRMS: Calc. for $C_{15}H_{16}O_5$: 276.0998; Found: 276.0999

mp: 76-78 °C

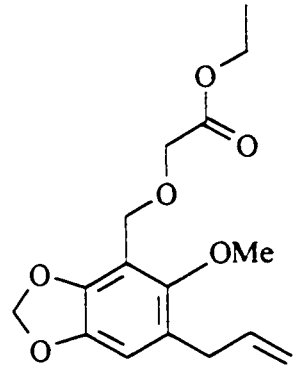

46

Alcohol **43** (200 mg, 0.90 mmol) was dissolved in dry THF (3 mL) and to this was added an equimolar amount of NaH (22 mg). The resulting solution was stirred at RT for 5 min after which time ethyl bromoacetate (0.1 mL, 0.90 mmol) was added dropwise. After 22 h at reflux, the solution was cooled to RT, and the solvent was concentrated. Water (5 mL) was added and the organic phase extracted with CH_2Cl_2 (3 x 10 mL). The combined organic extracts were dried over Na_2SO_4, filtered, and evaporated to dryness. Purification of the crude residue by flash chromatography (5:1 Hex:EtOAc) provided **46** as a colorless oil (58 mg, 19%).

^{1}H NMR: δ 1.25 (t, 3H, J = 7.1 Hz), 3.30 (dt, 2H, J = 6.5, 1.3 Hz), 3.74 (s, 3H), 4.11 (s, 2H), 4.19 (q, 2H, J = 7.1 Hz), 4.63 (s, 2H), 5.01-5.05 (m, 2H), 5.85-5.93 (m, 1H), 5.91 (s, 2H), 6.61 (s, 1H)

^{13}C NMR: δ 14.2, 33.7, 60.8, 62.9, 63.0, 67.5, 101.5, 109.6, 112.7, 115.8, 125.4, 137.2, 143.5, 146.0, 141.6, 170.4

IR: 1746 cm^{-1}

EI-MS (m/z, %): 308 (M^+, 100)

HRMS: Calc. for $C_{16}H_{20}O_6$: 308.1260; Found: 308.1255

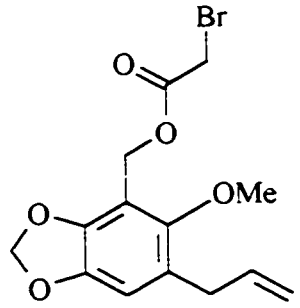

47

Ester **47** was obtained as a second product from the reaction described for **46**. Purification by flash chromatography (5:1 Hex:EtOAc) afforded the desired product **47** as a colorless oil (67 mg, 22%).

^{1}H NMR: δ 3.32 (dt, 2H, J = 6.5, 1.4 Hz), 3.71 (s, 3H), 3.84 (s, 2H), 5.03-5.07 (m, 2H), 5.23 (s, 2H), 5.86-5.92 (m, 1H), 5.93 (s, 2H), 6.65 (s, 1H)

^{13}C NMR: δ 25.8, 33.6, 58.4, 62.9, 101.7, 110.2, 110.6, 116.1, 125.4, 137.0, 143.8, 146.0, 151.4, 167.0

IR: 1742 cm^{-1}

EI-MS (m/z, %): 344 (M^++2, 97), 342 (M^+, 100), 189 (68)

HRMS: Calc. for $C_{14}H_{15}O_5Br$: 342.0103; Found: 342.0093

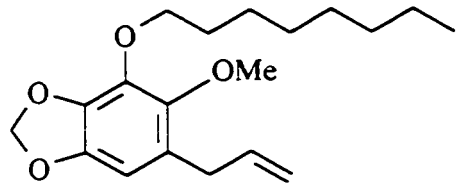

48

To a solution of phenol **26** (88.3 mg, 0.42 mmol) in acetone (6 mL) were added K_2CO_3 (0.09 g, 0.63 mmol), octyl bromide (0.09 mL, 0.51 mmol), and a few crystals of iodine. The resulting mixture was refluxed for 64 h and then cooled to RT. After concentrating the acetone, water was added to dissolve the remaining K_2CO_3 and the aqueous phase was extracted with Et_2O (3 x 5 mL). The combined organic extracts were dried over Na_2SO_4, filtered and concentrated. The crude residue was purified by flash chromatography (20:1 Hex:EtOAc) affording **48** as a yellow oil (80.4 mg, 60%).

^{1}H NMR: δ 0.87 (t, 3H, J = 6.8 Hz), 1.24-1.32 (m, 8H), 1.42-1.45 (m, 2H), 1.72-1.75 (m, 2H), 3.29 (dt, 2H), J = 6.6, 1.1 Hz), 3.75 (s, 3H), 4.16 (t, 2H, J = 6.7 Hz), 5.00-5.04 (m, 2H), 5.85 (s, 2H), 5.87-5.93 (m, 1H), 6.33 (s, 1H)

^{13}C NMR: δ 14.1, 22.6, 25.8, 29.2, 29.3, 30.1, 31.8, 34.0, 61.2, 72.6, 101.0, 102.7, 115.4, 126.0, 136.3, 136.9, 137.5, 144.4, 144.7

EI-MS (m/z, %): 320 (M^+, 64), 208 (74), 84 (62), 49 (100)

HRMS: Calc. for $C_{19}H_{28}O_4$: 320.1988; Found: 320.1984

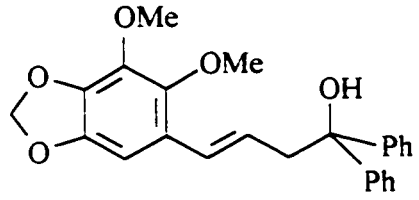

49

A solution of nBuLi (0.60 mL, 1.49 mmol, 2.5 M in Hexanes) was added dropwise to a cooled (-78 °C) solution of dillapiol **7** (276 mg, 1.24 mmol) in THF (4 mL). Stirring was continued for 30 min, after which time benzophenone was added in one portion. The reaction mixture was slowly allowed to warm to RT, quenched with saturated ammonium chloride (15 mL) and extracted with Et_2O (3 x 10 mL). The etheral extracts were combined, dried over $MgSO_4$, filtered, and concentrated. Recrystallization of the greyish solid from CH_2Cl_2/hexanes provided compound **49** as a white solid (200 mg, 42%).

^{1}H NMR: δ 2.57 (s, 1H), 3.21 (dd, 2H, J = 7.3, 1.1 Hz), 3.66 (s, 3H), 3.98 (s, 3H), 5.84 (s, 2H), 5.85-5.90 (m, 1H), 6.45 (s, 1H), 6.74 (d, 1H, J = 16.0 Hz), 7.20-7.23 (m, 2H), 7.29-7.32 (m, 4H), 7.45-7.47 (m, 4H)

^{13}C NMR: δ 46.2, 60.0, 61.5, 77.4, 98.6, 101.3, 124.0, 124.2, 126.1, 126.9, 128.2, 129.2, 137.1, 137.5, 144.5, 145.0, 146.6

IR: 3563 cm^{-1}

EI-MS (m/z, %): 386 (M^+-H_2O, 23), 222 (82), 183 (97), 105 (100)

HRMS: Calc. for $C_{25}H_{22}O_4$: 386.1519; Found: 386.1531

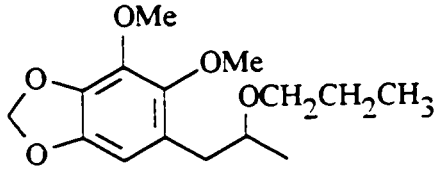

52

A vigorously stirred suspension of mercuric acetate (1.08 g, 3.39 mmol) in 1-propanol (8 mL) was treated with a solution of dillapiol **7** (616 mg, 2.77mmol) in THF (8 mL) at 0 °C over a period of 20 min. The reaction mixture was allowed to warm to RT and stirred for 5 h. After this time, the mixture was treated with an alkaline solution of $NaBH_4$ (1.12 g KOH/4 mL H_2O + 0.29 g $NaBH_4$). The liberated mercury was filtered and the filtrate was extracted with $CHCl_3$ (3 x 20 mL). The combined organic extracts were dried over Na_2SO_4, filtered, and evaporated to dryness Purification by flash chromatography (CH_2Cl_2) afforded ether **52** as a yellow liquid (130 mg, 17%). The spectral data for this compound are in accordance with those cited in the literature[16].

^{1}H NMR: δ 0.86 (t, 3H, J = 7.4 Hz), 1.09 (d, 3H, J = 6.2 Hz), 1.50-1.58 (m, 2H), 2.51 (dd, 1H, J = 13.4, 6.9 Hz), 2.81 (dd, 1H, J = 13.4, 6.1 Hz), 3.31-3.34 (m, 1H), 3.39-3.42 (m, 1H), 3.53-3.54 (m, 1H), 3.74 (s, 3H), 3.99 (s, 3H), 5.86 (s, 2H), 6.38 (s, 1H)

^{13}C NMR: δ 10.6, 19.7, 23.3, 36.9, 59.9, 61.1, 70.5, 76.0, 101.0, 103.7, 125.3, 135.9, 137.5, 144.3, 144.7

EI-MS (m/z, %): 282 (M^+, 15), 45 (100)

HRMS: Calc. for $C_{15}H_{22}O_5$: 282.1468; Found: 282.1452

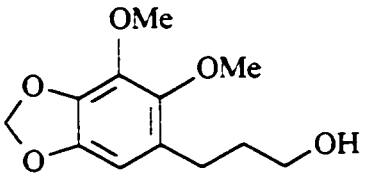

53

Borane methyl sulfide (450 μL, 4.50 mmol) was added to a cooled (0 °C) solution of dillapiol 7 (1.90 g, 8.55 mmol) in CH_2Cl_2 (10 mL). The resulting reaction mixture was allowed to warm to RT and stirred for 90 min. After this time, EtOH (5 mL) was added and the pH adjusted to 8 with 3N NaOH. The mixture was then cooled to 0 °C and treated with 30% H_2O_2 (1 mL). The organic phase was separated and the aqueous phase extracted with CH_2Cl_2 (3 x 10 mL). The combined organic extracts were dried over $MgSO_4$, filtered, and evaporated to dryness. Purification by flash chromatography (1:1 Hex:EtOAc) afforded **53** as a yellow oil (0.53 g, 26%).

^{1}H NMR: δ 1.67-1.73 (m, 2H), 2.54 (t, 2H, J = 7.4 Hz), 2.74 (s, 1H), 3.50 (t, 2H, J = 6.2 Hz), 3.69 (s, 3H), 3.93 (s, 3H), 5.79 (s, 2H), 6.27 (s, 1H)

^{13}C NMR: δ 25.7, 33.5, 59.8, 61.3, 61.4, 101.0, 102.5, 127.5, 135.6, 137.4, 144.2, 144.7

IR: 3617 cm^{-1}

EI-MS (m/z, %): 240 (M^+, 42), 208 (100), 195 (56)

HRMS: Calc. for $C_{12}H_{16}O_5$: 240.0998; Found: 240.0998

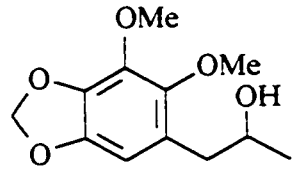

54

Alcohol **54** was obtained as a second product from the reaction described for **53**. Purification of the crude residue by flash chromatography (1:1 Hex:EtOAc) provided **54** as a yellow oil (30 mg, 2%).

^{1}H NMR: δ 1.19 (d, 3H, J = 6.2 Hz), 2.13 (d, 1H, J = 3.1 Hz), 2.61 (dd, 1H, J = 13.6, 7.9 Hz), 2.68 (dd, 1H, J = 13.6, 4.3 Hz), 3.76 (s, 3H), 3.95-3.99 (m, 1H), 4.00 (s, 3H), 5.87 (s, 2H), 6.34 (s, 1H)

^{13}C NMR: δ 23.1, 40.0, 59.9, 61.1, 68.6, 101.2, 103.6, 124.5, 136.3, 137.7, 144.7, 144.7

IR: 3502 cm^{-1}

EI-MS (m/z, %): 240 (M^+, 44), 195 (100), 181 (67)

HRMS: Calc. for $C_{12}H_{16}O_5$: 240.0998; Found: 240.0995

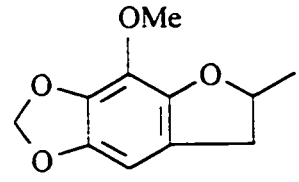

55

To a solution of dillapiol 7 (0.28 g, 1.26 mmol) in CH_2Cl_2 (5 mL) were added p-toluenesulfonic acid (0.27 g, 1.42 mmol) and NaI (0.21 g, 1.40 mmol). After 72 h at reflux, water (5 mL) was added, the organic phase was separated and subsequently washed with 5% $NaHCO_3$ (3 x 5 mL). The organic layer was dried over Na_2SO_4, filtered and concentrated affording, after flash chromatography (5:1 Hex:EtOAc), **55** as a colorless oil (80 mg, 30%). The physical and spectroscopic data for this compound are in accordance with those cited in the literature[15].

^{1}H NMR: δ 1.44 (d, 3H, J = 6.2 Hz), 2.71 (ddd, 1H, J = 14.9, 8.1, 1.0 Hz), 3.17 (ddd, 1H, J = 14.9, 8.7, 0.7 Hz), 4.00 (s, 3H, 4.88–4.92 (m, 1H), 5.82 (d, 1H, J=1.4 Hz), 5.83 (d, 1H, J = 1.4 Hz), 6.32 (d, 1H, 0.8 Hz)

^{13}C NMR: δ 21.6, 37.7, 59.9, 80.8, 98.7, 101.1, 119.1, 129.8, 136.2, 142.5, 144.9

EI-MS (m/z, %): 208 (M^+, 100)

HRMS: Calc. for $C_{11}H_{12}O_4$: 208.0736; Found: 208.0727

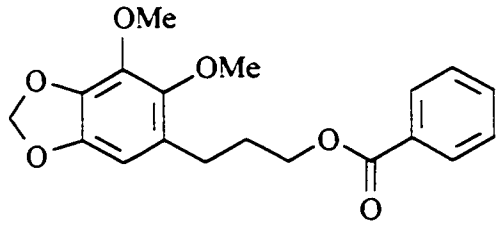

56

To a solution of alcohol **54** (154 mg, 0.64 mmol) in dry pyridine (1 mL) was added benzoyl chloride (0.16 mL, 1.36 mmol). The resulting reaction mixture was stirred at RT for 24 h after which time water (5 mL) was added. After stirring the mixture for an additional hour at RT, the aqueous phase was extracted with Et_2O (3 x 10 mL). The combined extracts were then washed successively with a 5% HCl solution and a 5% $NaHCO_3$ solution, dried over $MgSO_4$, filtered and evaporated to dryness. Purification by flash chromatography (1:1 Hex:EtOAc) afforded **56** as a colorless oil (140 mg, 64%).

^{1}NMR: δ 2.00-2.02 (m, 2H), 2.68 (t, 2H, J = 7.3 Hz), 3.75 (s, 3H), 3.98 (s, 3H), 4.32 (t, 2H, J = 6.4 Hz), 5.84 (s, 2H), 6.35 (s, 1H), 7.40-7.43 (m, 2H), 7.51-7.54 (m, 1H), 8.01-8.02 (m, 2H)

^{13}C NMR: δ 26.6, 29.8, 59.9, 61.2, 64.5, 101.1, 102.6, 127.2, 128.3, 129.5, 130.5, 132.8, 135.9, 137.7, 144.5, 144.6, 166.6

IR: 1715 cm^{-1}

EI-MS (m/z, %): 344 (M^+, 92), 222 (76), 195 (63), 177 (85), 105 (100), 77 (93)

HRMS: Calc. for $C_{19}H_{20}H_6$: 344.1260; Found: 344.1281

5.2 Dillapiol from Natural Sources

5.2.1 Dill seed oil

To a 500 mL rb flask were added 10 g of crushed dill seed (Indian or Canadian) and 250 mL of water. After collecting 50 mL of distillate by steam distillation, the mixture was extracted with hexane (3 x 50 mL), dried over Na_2SO_4 and concentrated under reduced pressure. Analysis of the oily residue (200 mg) by ^1H NMR revealed two major compounds present in a 7:1 ratio, namely carvone and dillapiol. Subsequent analysis of this mixture by GC revealed that the oil was comprised of approximately 2% dillapiol.

5.2.2 *Piper aduncum*

To a 500 mL rb flask were added 100g of either leaves, seeds or wood chips/sawdust and 250 mL of water. After steam distilling 150 mL of the mixture, each distillate was extracted with hexane (2 x 25 mL) and ethyl acetate (2 x 25 mL). The combined organic extracts were then dried over Na_2SO_4, filtered and concentrated. Finally, the crude mixtures were analyzed by ^1H NMR.

Table 5.1: Distribution of Dillapiol among the Various Parts of *Piper Aduncum*

Source	Solvent	Weight of extract (mg)	Approx. diilapiol content (mg)
Leaves	Hexane	10	trace
	Ethyl acetate	10	none
Seeds	Hexane	360	300
	Ethyl acetate	70	30
Wood chips/ sawdust	Hexane	40	30
	Ethyl acetate	20	15

5.3 Effect of Dillapiol and its Derivatives on the Accumulation of ^{3}H-vinblastine in Resistant and Sensitive Cell Lines

The drug accumulation study was carried out by Dr Claude Bourret-Bernard[62] (University of Ottawa) at the Loeb Medical Research Institute. A simplified description of the experimental procedure is given below.

5.3.1 Cell lines

Cultured NIH cells, established from NIH Swiss mouse fibroblast cultures, were used as were their multidrug resistant counterparts, G185, which were transfected with a human MDR1 gene. The Chinese hamster ovarian cell lines AUXB1, the parental, and B30, its MDR line selected for resistance against colchicine, were also used in this study.

Cells were grown in plastic flasks in a humidified atmosphere at 37 °C, 5% CO_2. Resistance levels were maintained with a weekly addition of colchicine to the cultures, 0.06 μg/mL in G185 and 30 μg/mL in B30.

5.3.2 Determination of resistance levels

A screening of the dose toxic to the four cell lines (NIH, G185, AUXB1 and B30) was achieved with lignan final concentrations in the assay from 0.25 ng/mL to 25000 ng/mL. Adherent cells in the culture flask were detached with a solution of trypsin, centrifuged at 1000 rpm for 15 min and resuspended in medium at a final concentration of 500 cells/mL. One mL of the cell suspension was distributed in each well of a 24-well plate already containing 1 mL of the lignan, or other allelochemical, at the appropriate concentration (at least 6 concentrations). Control wells contained cells and the solvent

(0.1% EtOH or DMSO) used to solubilize the drug. Cells were incubated for 8 d at 37 °C, 0.5% CO_2. The media were discarded and cell colonies stained with 0.25% methylene blue for 15 min. The concentration beyond which cell growth ceased was used for the determination of the toxicity of the compounds.

5.3.3 Drug accumulation and transport: Uptake of ^{3}H-vinblastine

Trypsinized cells were washed and resuspended in PBS-glucose (10 mM), at a concentration of 1.5 x 10^{6} cells/mL. At specific intervals (1, 15, 30, 60 and 90 min) after mixing the 1 mL cell suspension with 2 µL ^{3}H-vinblastine/mL, with or without the potential resistance modifying compounds, 300 µL of the mixture was layered onto 250 µL of a silicone oil and mineral oil mixture (4:1, v:v), and immediately centrifuged 10 sec at 14000 rpm. The aqueous phase was removed, the upper portion of the tube rinsed with 500 µL PBS, the oil removed and the pellet digested overnight in 500 µL of a 0.1 N NaOH solution. After this time, 5 mL of scintillation liquid was added to the pellet and the tritium activity was counted.

5.4 Fate of ^{14}C-radiolabeled Dillapiol in the Sprague-Dawley Rat

The toxicokinetic study of dillapiol was also carried out by Dr Claude Bourret-Bernard[96] (University of Ottawa). A simplified description of the experimental procedure is given below. The synthesis of ^{14}C-radiolabeled dillapiol was done by Dr T. Durst (Department of Chemistry, University of Ottawa) and Dr. J.T. Arnason (Department of Biology, University of Ottawa), with the collaboration of S. Majerus (University of Ottawa) and Dr Claude Bourret-Bernard.

5.4.1 Synthesis of ^{14}C-radiolabeled dillapiol

To a stirred solution of phenol **26** (100 mg, 0.48 mmol) in acetone (20 mL) were added 1 eq. of a mixture of ^{14}MeI (1.8 mg) and unlabeled MeI (x mg) and 1 eq. of K_2CO_3 (66.3 mg). The resulting mixture was vigorously stirred at RT for 72 h, after which time the solvent was evaporated. The product was purified by silica gel plate chromatography.

5.4.2 Distribution and excretion of ^{14}C-dillapiol

Male Sprague-Dawley rats weighing 250-300g were administered a single dose I.V. of 0.5 mg/kg of ^{14}C-radiolabeled dillapiol. At predetermined times (6h, 12h, 24h, 2d, 3d, 5d and 7d), 3 rats were sacrificed and various tissues analyzed for ^{14}C radioactivity (blood, liver, kidney, gut (caecum), brain, urine and feces).

In a separate experiment, one rat was administered 10x the former dosage (5 mg/kg) of ^{14}C-dillapiol, also by intravenous. After 7 d, the rat was sacrificed and the organs analyzed for any abnormalities.

5.5 Investigation of the Synergistic Activity of Dillapiol and its Derivatives on *Aedes atropalpus* Coq. Larvae

The study regarding the potential synergistic activity of dillapiol and its derivatives was carried out by undergraduate student Catherine Podeszfinski[69] (University of Ottawa) and Anne-Sophie Belzile under the supervision of Dr J.T Arnason (Department of Biology, University of Ottawa).

5.5.1 Insect rearing

All experiments were performed with *Aedes atropalpus* Coq. (Dipterae:Culicidae) larvae. Adults were reared in wire screen cages in a 18:6 (L:D) photoperiod and fed with a 20% sucrose solution. Temperature was maintained at 26 °C with a relative humidity of 80%. The larvae were kept under the same conditions in plastic trays filled with dechlorinated tap water. They were fed daily with TetraMin® fish food. Eggs were recovered in a Petri dish filled with tap water and kept to maintain the culture.

5.5.2 Toxicity tests

Groups of 20 larvae of 3rd and 4th instar were place in glass vials containing 5 mL of deionized tap water. To each vial was added a 5:1 mixture of dillapiol or derivative:α-T such that α-T concentrations were 160, 120, 80, 60, 40, 20, 10 and 5 ppb. Each treatment was duplicated but the data obtained were pooled before the final analysis. Three sets of controls were set-up. The first set consisted of vials containing only α-T at concentrations identical to those noted above. The two other control groups consisted of either dillapiol or a derivative, and water. The compounds were put alone in the solution at a concentration of 800 ppb corresponding to the highest concentration used in the different treatments. The larvae were then irradiated with 20 W Westinghouse BLB tubes for 4 h at a wavelength between 300–400 nm. Larvae were kept in the dark for another 20 h before assessing mortality. Probit analysis was then used to determine the lethal concentration of α-T (LC_{50}) against the mosquito larvae for each derivative.

5.6 Quantitative Structure-Activity Relationships of Dillapiol Derivatives

This study, an investigation of the relationship between the lipophilicity of dillapiol and its derivatives on the toxicity of α-T, was undertaken by undergraduate student Catherine Podeszfinski[69] under the supervision of Dr J.T. Arnason (Department of Biology, University of Ottawa).

5.6.1 Determination of the partition coefficients by reverse-phase HPLC

To determine whether the toxicity of dillapiol and its derivatives was related to lipophilicity, the octanol/water partition coefficient of each compound was determined using the method established by Ellgehausen and coworkers[71]. Four standard compounds with known partition coefficients[71] were eluted through a LiChrosorb RP-18 column at a flow rate of 1 mL/min using EtOH:water (65:35) as eluant. The capacity factor K' was defined as

$$K' = (t_R - t_0)/t_0 \qquad (4)$$

where t_R represents the retention time of the compound and t_0 is the retention time of the non-sorbed solvent in which the compounds were dissolved (methanol). A linear regression was performed on the plot of the logarithm of the octanol/water partition coefficient (log P) versus the logarithm of the capacity factor (log K') of those four

standards. The partition coefficient of dillapiol and its derivatives was then calculated according to the equation that was established from the four standards, equation 1.

$$\text{Log } P = 2.327 \text{ (Log } K) + 2.689 \qquad (r^2 = 0.958) \qquad (1)$$

5.6.2 Retention of α-T in the larvae

Groups of fifteen 4th instar larvae were placed in glass vials along with 40 mL of dechlorinated tap water. To each vial was added 20 µL of a 5:1 dillapiol:α-T mixture to a give an α-T final concentration of 0.0125 ppm. Each treatment was done in quadruplicate. Larvae were then rinsed with distilled water and put in 2 mL of hexane to solubilize the α-T present in the tissues. Samples were sonicated for 30 sec and then filtered before passing them through a reverse-phase C18, Ultratechsp50Ds column using a 70:30 mixture of acetonitrile and water, respectively. A standard curve for pure α-T diluted in methanol was obtained using four concentrations (10, 2.5, 1 and 0.5 ppm). The peak area, the retention time of α-T, was 14.66 min and the peak area was highly correlated with the concentration of α-T ($r^2 = 0.979$). This allowed the determination of the amount of α-T remaining in the insects for dillapiol and its derivatives.

REFERENCES

1. Brattsten, L.B.; Holyoke, C.W.; Leeper, J.R.; Raffa, K.F. *Science* **1986**, 231, 1255.

2. Georghiou, G.P. In: M.B., Green; H.M. LeBaron; W.K. Moberg (eds.) Managing Resistance to Agrochemicals: from Fundamental Research to Practical Strategies, **1990**, vol. ACS series 421. ACS, Washington DC, 18–41.

3. Moberg, W.K. In: M.B. Green; H.M. LeBaron; W.K. Moberg (eds.) Managing Resistance to Agrochemicals; from Fundamental Research to Practical Strategies, **1990**, vol. ACS series 421. ACS, Washington DC, 18–41.

4. Raffa, K.F.; Priester, T.M. *J. Agric. Entomol.* **1985**, 2, 27.

5. Arnason, J.T.; Bernard, C.B.; Philogene, J.R.; Lam, J.; Waddell, T. *Phytochemistry* **1989**, 28, 1373.

6. Casida, J.E. *J. Agr. Food Chem.* **1970**, 12, 753.

7. MacRae, W.D.; Towers, G.H. *Phytochemistry* **1984**, 23, 1.

8 Lichtenstein, E.P.; Liang, T.T.; Schultz, R.K.; Schnoes, H.K.; Carter, G.T. *J. Agr. Food Chem.* **1974**, 22, 658.

9. Mukerjee, S.K.; Saxena, V.S.; Tomar, S.S. *J. Agric. Food Chem.* **1979**, 27, 1209.

10. Harmatha, J.; Nawrot, J. *Biochem. Syst. Ecol.* **1984**, 12, 95.

11. Harmatha, J. Nawrot, J. In: F. Sehnal; A. Zabza; D.L. Delinger (eds.) Endocrinal Frontiers in Physiological Insect Ecology, **1988**, Wraclaw Technical University Press, Wraclaw.

12. Downum, K.R. *ACS Symposium Series* **1986**, 296, 206.

13. Koul, O. *Indian Rev. Life Sci.* **1982**, 2, 97.

14. Schoonhoven, L.M. *Ent. Exp. & Appl.* **1982**, 31, 57.

15. Vigneron, J.P. *Ann. Zool. Ecol. Anim.* **1978**, 10, 663.

16. Tomar, S.S.; Maheshwari, M.L.; Mukerjee, S.K. *J. Agric. Food Chem.* **1979**, 27, 547.

17. Nawrot, J.; Koul, Ol; Isman, M.B.; Harmatha, J. *J. Appl. Ent.* **1991**, 112, 194.

18. Neal, J.J. *J. Chem. Ecol.* **1989**, 15, 309.

19. Atal, C.K.; Dhar, K.L.; Singh, J. *Lloydia* **1975**, 38, 256.

20. Gbewonyo, W.S.K.; Candy, D.J.; Anderson, M. *Pestic. Sci.* **1993**, 37, 57.

21. Schultes, R.E.; Raffauf, R.F. In: R.R. Schultes, R.F. Raffauf (eds.) The Healing Forest: Medicinal and Toxic Plants of the Northwest Amazonia, **1990**, Historical, Ethno. & Economic Botany Series. Dioscoride Press, Portland, Oregon.

22. Bernard, C.B.; Arnason, J.T.; Philogene, B.J.R.; Lam, J.; Waddell, T. *Phytochemistry* **1989**, 28, 1373.

23. Bernard, C.B.; Philogene, B.J.R. *J. Toxicol. Environmental Health* **1993**, 38, 199.

24. Bernard, C.B.; Krishnamurty, H.G.; Chauret, D.; Durst, T.; Philogene, B.J.R.; Sanchez-Vindas, P.; Hasbun, C.; Poveda, L.; San Roman, L.; Arnason, J.T. *J. Chem. Ecol.* **1995**, 21, 801.

25. Tomar, S.S.; Saxena, V.S.; Maheshwari, M.L.; Sarup, P.; Mukerjee, S.K. *Indian J. Entomol.* **1978**, 40, 113.

26. Bradley, G.; Juranka, P.F.; Ling, V. *Biochim. Biophys. Acta* **1988**, 948, 87.

27. Endicott, J.A.; Ling, V. *Ann. Rev. Biochem.* **1989**, 58, 137.

28. Gottesman, M.M.; Pastan, I. *Ann. Rev. Biochem.* **1993**, 62, 385.

29. Safa, A.R.; Glover, C.J.; Meyers, M.B.; Biedler, J.L.; Felsted, R.L. *J. Biol. Chem.* **1986**, 261, 6137.

30. Juliano, R.L.; Ling, V. *Biochim. Biophys. Acta* **1976**, 455, 152.

31. Riordan, J.R.; Ling, V. *J. Biol. Chem.* **1979**, 254, 12701.

32. Ling, V.; Thompson, L.H. *J. Cell Physiol.* **1973**, 83, 103.

33. Roninson, I.B.; Chin, J.E.; Choi, K.; Gros, P.; Housman, D.E., et al. *Proc. Natl. Acad. Sci.* **1986**, 83, 4538.

34. Kane, S.; Gottesman, M.M. *Cancer Cells* **1989**, 1, 33.

35. Gottesman, M.M.; Pastan, I. *J. Biol. Chem.* **1988**, 263, 12163.

36. Murray, C.L.; Quaglia, M.; Arnason, J.T.; Morris, C.E. *J. Neurobiol.* **1994**, 25, 23.

37. Schinkel, A.H.; Borst, P. *Semin. Cancer Biol.* **1991**, 2, 213.

38. Gottesman, M.M.; Currier, S.; Bruggemann, E.; Lelong, I.; Stein, W.; Pastan, I. In: M. Caplan (ed.) Cell Biology and Membrane Transport Processes, **1994**, vol. 41, Academic Press, New York, 3-15.

39. Ye, Z.; Van Dyke, K. *Drug and Chemical Toxicol.* **1994**, 17, 149.

40. Teeter, L.D.; Atsumi, S.; Sen, S.; Kuo T. *J. Cell Biol.* **1986**, 103, 1159.

41. Mukerjee, S.K.; Walia, S.; Saxena, V.S.; Tomar, S.S. *Agric. Biol. Chem.* **1982**, 46, 1277.

42. Baker, W.; Jukes, E.H.T.; Subrahmanyam, C.A. *J. Chem. Soc.* **1934**, 1681.

43. Dallacker, F. *Chem. Ber.* **1969**, 102, 2663.

44. Cannon, J.R.; Ghisalherti, E.L.; Lojanapiwatna, V. *J. Sci. Soc. Thailand* **1980**, 6, 59.

45. March, J. Advanced Organic Chemistry, Reactions, Mechanisms and Structure, 2nd Edition, **1977**, McGraw-Hill.

46. Grubbs, R.H.; Fujimura, O.; Fu, G.C. *J. Org. Chem.* **1994**, 59, 4029.

47 Casiraghi, G.; Casnati, G.; Puglia, G.; Sartori, G.; Terenghi, G. *J.C.S. Perkin I.* **1980**, 1862.

48. Kurz, M.E.; Johnson, G.J. *J. Org. Chem.* **1971**, 36:21, 3184.

49. Vesely, J.A.; Schmerling, L. *J. Org. Chem.* **1970**, 35:12, 4028.

50. Hart, H.; Buehler, C.A. *J. Org. Chem.* **1964**, 29, 2397.

51. McClure, J.D.; Williams, P.H. *J. Org. Chem.* **1962**, 27, 24.

52. Derbyshire, D.H.; Waters, W.A. *Nature* **1950**, 165, 401.

53. Capdevielle, P.; Maumy, M. *Tetrahedron Letters* **1982**, 23:15, 1577.

54. Brackman, W.; Havinga, E. *Rec. Trav. Chim.* **1955**, 74, 937.

55. (a) Tsuji, J.; Takayanagi, H. *J. Am. Chem. Soc.* **1974**, 96, 7359. (b) Tsuji, J.; Takayanagi, H. *Tetrahedron Letters* **1976**, 1365. (c) Tsuji, J.; Takayanagi, H. *Tetrahedron* **1978**, 34, 641.

56. Swerdloff, M.D.; Rogic, M.M. *J. Am. Chem. Soc.* **1981**, 103, 5795.

57. Weller, D.D.; Stirchak, E.P. *J. Org. Chem.* **1983**, 48, 4873.

58. Pearson, D.E.; Wysong, R.D.; Breder, C.V. *J. Tenn. Acad. Sci.* **1967**, 32, 2358.

59. Dukker, L.J. Ph.D. Thesis **1964**, University of Leiden, Leiden, Holland.

60. Morrison, R.T.; Boyd, R.N. Organic Chemistry, 5th Edition, **1987**, Allyn and Bacon Inc. Toronto, 1011.

61. Kobsa, H. *J. Org. Chem.* **1962**, 27, 2293.

62. Bernard, C.B. Ph.D. Thesis **1995**, University of Ottawa, Ottawa, Ontario.

63. Loe, D.W.; Sharom, F.J. *Cancer* **1993**, 68, 342.

64. Arsenault, A.L.; Ling, V.; Kartner, N. *Biochim. Biophys. Acta* **1988**, 938, 315.

65. Kessel, D. *Biochem. Pharmacol.* **1988**, 37, 4253.

66. Bernard, C.B. Ongoing Research, University of Ottawa, Ottawa, Ontario.

67. Arnason, J.T.; Swain, T.; Wat, C.K.; Graham, E.A.; Partington, S.; Towers, H.N.; Lam, J. *Biochemical Systematics and Ecology* **1981**, 9, 63.

68. Spikes, J.D.; Straight, R.C. In: J.R. Heitz; K.R. Downum (eds.) Light Activated Pesticides, **1987**, ACS Symposium Serie 339.

69. Podeszfinski, C. Undergraduate Thesis **1996**, University of Ottawa, Ottawa, Ontario.

70. Marles, R.; Compadre, R.L.; Compadre, C.M.; Soucy-Breau, C.; Redmond, R.W.; Duval, F.; Mehta, B.; Morand, P.; Scaiano, J.C.; Arnason, J.T. *Pesticide Biochemistry and Physiology* **1991**, 41, 89.

71. Ellgehausen, H.; D'Hont, C.; Fuerer, R. *Pesticide Science* **1981**, 12, 219.

IMAGE EVALUATION
TEST TARGET (QA-3)

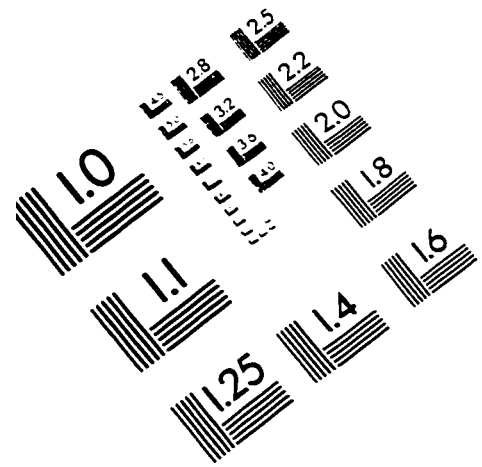

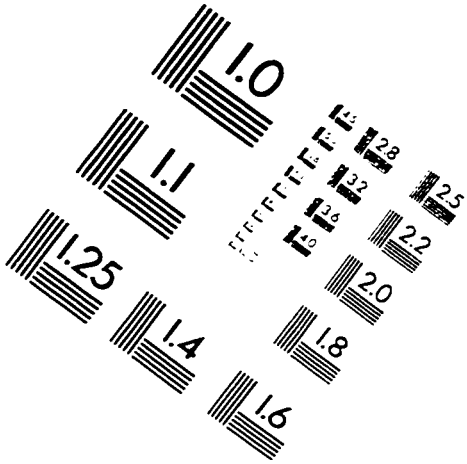

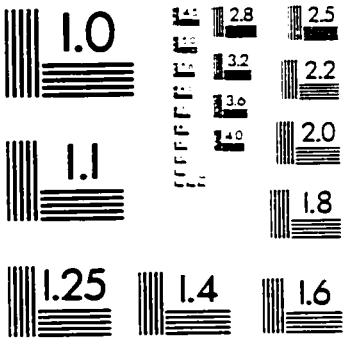

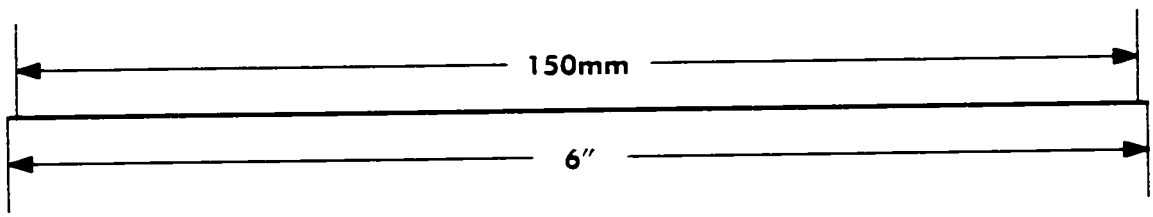

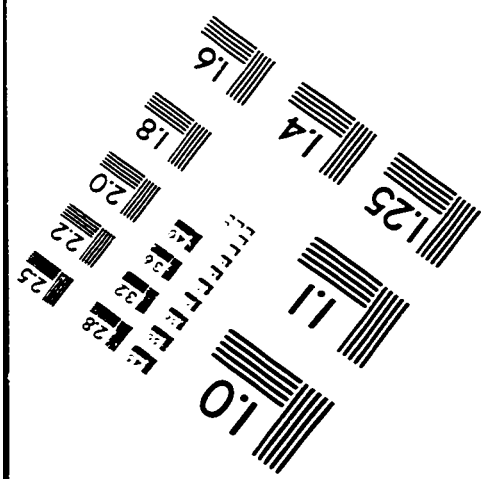

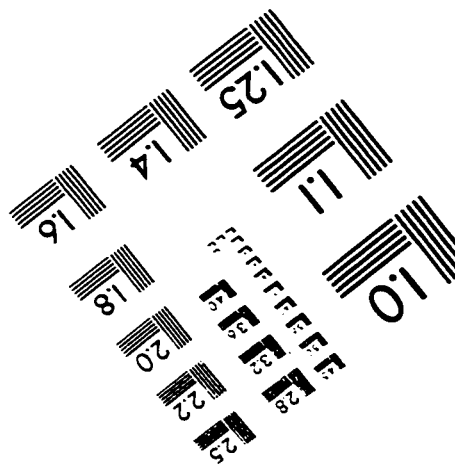

APPLIED IMAGE, Inc
1653 East Main Street
Rochester, NY 14609 USA
Phone: 716/482-0300
Fax: 716/288-5989